ANALYSIS AND DESIGN OF A HYPERSONIC SCRAMJET ENGINE WITH A STARTING MACH NUMBER OF 4.00

by

KRISTEN NICOLE ROBERTS

Presented to the Faculty of the Graduate School of

The University of Texas at Arlington in Partial Fulfillment

of the Requirements

for the Degree of

MASTER OF SCIENCE IN AEROSPACE ENGINEERING

THE UNIVERSITY OF TEXAS AT ARLINGTON

August 2008

ACKNOWLEDGEMENTS

I wish to first thank my research advisor, Dr. Donald Wilson, for his guidance throughout the duration of this project. He provided a wealth of expertise from a diverse background of research, application of theory, and technical hands-on experience in addition to providing me encouragement throughout my research and my time at UTA. Additionally, I would like to thank Dr. Wilson, Dr. Roger Goolsby, Dr. Bernd Chudoba, and the Department of Mechanical and Aerospace Engineering for the financial support provided to me, as it was a great help towards the cost of my studies.

I would like to thank Dr. Frank Lu for serving on my committee, as well as providing reference books, industry contacts, and technical expertise towards the completion of this project. I wish to thank Dr. Kent Lawrence for serving on my committee and for being an excellent professor to serve as a Graduate Teaching Assistant to for many semesters. His interest in my research and encouragement of its completion is much appreciated.

I want to thank Dr. Bob Mullins of Bell Helicopter for his advice and insight in the planning stages of this project. I would also like to thank Dr. Bernd Chudoba for teaching me about conceptual design, his support and guidance in the AIAA conference papers I authored, and for the experience I gained in working on the contract work in the Aerospace Vehicle Design lab at UTA. Additionally, I would like to thank Paul

Czysz for adding to my education through his wealth of experience and insight in hypersonic vehicle design.

I wish to thank Bryan and Brad Mixon for all the laughs, technical help and advice, and the many sci-fi Fridays. I would like to thank Philip Panicker and the other members of the Aerodynamics Research Center for providing resources and contacts as necessary. I want to thank the fellow students with whom I worked in the AVD Lab, Dr. Xiao Huang, Gary Coleman, Amit Oza, and Nauman Mhaskar, for helping to make my time at UTA more enjoyable. I would like to also thank Mr. Rick Wild and the other engineers at the FAA in OKC as well as Mr. Russ Davoren for their support and encouragement during my Bachelor's and Master's degrees.

I must gratefully acknowledge the constant support, love, and encouragement my family has provided to me, without which I would not be the person I am today. My mom is a constant source of inspiration and warmth, helping me to keep perspective; my dad set the foundation for the engineering spirit in me that seeks to constantly learn and the work ethic to make it happen; my brother has been a readily available no-nonsense source for advice and support. My late grandma Betty Reasoner and my grandpa Calvin Reasoner, my aunt and uncle Vicki and Steve Andrews, and my uncle Scott Kordis have been constant supporters of my work in many ways.

And, lastly, to not acknowledge my lifelong friends would be to ignore my second family. I wish to thank Janell, Courtney, MaxAnne, Erin, Jandy, Charlotte, Andrea, Carissa, Melissa, Lacy, and Jennifer for their friendship, encouragement,

advice, love, and support. Also, thank you to Jennifer and Sarah for the roundtable discussions and your friendship!

And a special thanks to my dog Wilbur Wright, for staying up all those long nights with me!

July 18, 2008

ABSTRACT

ANALYSIS AND DESIGN OF A HYPERSONIC SCRAMJET ENGINE

WITH A STARTING MACH NUMBER OF 4.00

Kristen Nicole Roberts, MS

The University of Texas at Arlington, 2008

Supervising Professor: Dr. Donald Wilson

When pressures and temperatures become so high in supersonic flight that it is no longer efficient to slow the oncoming flow to subsonic speeds for combustion, a scramjet (supersonic combustion ramjet) is used in place of a ramjet. Currently, the transition to supersonic combustion generally occurs at a freestream Mach number around 5.0 to 6.0. This research details analysis completed towards extending scramjet operability to lower Mach numbers, while maintaining performance at higher Mach numbers within the same flowpath as detailed in the Air Force solicitation AF073-058. The specific goal is to determine whether the scramjet starting Mach number can be lowered to Mach 3.50 and, if not, what the constraints are that prohibit it and what the lowest possible starting Mach number for a scramjet is with today's technology. This analysis has produced many significant insights into the current and required

capabilities for both fuel and overall engine design in lowering the starting Mach number; these results are presented here. The analysis has shown that a scramjet with a starting Mach number of 3.50 is not currently possible with the fuels researched unless fuel additives or another addition to the system are used. However, a scramjet with a starting Mach number of 4.00 is possible with today's existing technology. This paper has designed the engine flowpath for this case; its specifications and resulting performance are also detailed here.

TABLE OF CONTENTS

LIST OF ILLUSTRATIONS

LIST OF TABLES

LIST OF SYMBOLS AND ABBREVIATIONS

M	Mach Number
M_0	Freestream Mach Number
M_2	Isolator Entry Mach Number
M_3	Burner Entry Mach Number
M_4	Burner Exit Mach Number
M_{10}	Expansion System Exit and Engine Exit Mach Number
T_3/T_0	Ratio of Burner Entry Temperature to Freestream Temperature
φ	Ratio of Burner Entry Temperature to Freestream Temperature (Equivalent to T_3/T_0)
γ	Ratio of Specific Heats
γ_c	Ratio of Specific Heats for Compression
γ_b	Ratio of Specific Heats for Burner
γ_e	Ratio of Specific Heats for Expansion
f	Fuel-to-Air Ratio
f_{st}	Stoichiometric Fuel-to-Air Ratio
PDE	Pulsed Detonation Engine
ϕ	Equivalence Ratio
T_{t0}	Stagnation Temperature of Freestream Air
C_p	Specific Heat
C_{p0}	Specific Heat of Freestream Air
C_{pc}	Specific Heat for Engine Compression
C_{pb}	Specific Heat for Engine Burner (Combustor)
C_{pe}	Specific Heat for Engine Expansion (Exit)
V_2	Axial Velocity at Isolator Entrance
V_3	Axial Velocity at Burner Entrance

V_4	Axial Velocity at Burner Exit
V_{10}	Axial Velocity at Expansion System Exit and Engine Exit
p_2	Static Pressure at Isolator Entrance
p_3	Static Pressure at Burner Entrance
p_4	Static Pressure at Burner Exit
p_{10}	Static Pressure at Expansion System Exit and Engine Exit
S	Specific Fuel Consumption
T_2	Static Temperature at Isolator Entrance
T_3	Static Temperature at Burner Entrance
T_4	Static Temperature at Burner Exit
T_{10}	Static Temperature at Expansion System Exit and Engine Exit
n_o	Overall Efficiency
n_{th}	Thermal Efficiency
n_p	Propulsive Efficiency
n_c	Inlet Compression System Efficiency
n_b	Burner Efficiency
n_e	Expansion System Efficiency
n_{KE}	Kinetic Energy Efficiency
I_{sp}	Specific Impulse
$F/\dot{m}_0$	Specific Thrust
x	Axial Location
x_i	Axial Location of Fuel Injection
y	Distance Perpendicular from the Axial Direction
h	Distance Perpendicular from the Axial Direction, Equivalent to y
z	Distance Perpendicular from the x-y Plane
d	Distance Perpendicular from the x-y Plane, Equivalent to z
R	Perfect Gas Constant
R_b	Perfect Gas Constant in Burner

$\frac{V_{fx}}{V_3}$	Ratio of Fuel Injection Axial Velocity To Combustor Entrance Velocity
$\frac{V_f}{V_3}$	Ratio of Fuel Injection Total Velocity to Combustor Entrance Velocity
$C_f \cdot \frac{A_w}{A_3}$	Burner Effective Drag Coefficient
$C_{pb}(T - T^0) = h$	Employs a Reference Temperature To Estimate The Absolute Static Enthalpy h
h_f	Absolute Sensible Enthalpy of Fuel Entering Combustor (Neglected in Calculations because $h_f << h_{PR}$)
h_{PR}	Heat Of Reaction
T_i/T_0	Ratio of Static Temperature at Station i to Freestream Static Temperature
p_i/p_0	Ratio of Static Pressure at Station i to Freestream Static Pressure
A_i/A_0	Ratio of Area at Station i to Inlet Area
P_{ti}/P_{t0}	Ratio of Total Pressure at Station i to Freestream Total Temperature
$(s_i\text{-}s_0)/C_p$	Dimensionless Entropy Increase Between Station i and the Inlet
θ/H	Ratio of Boundary Layer Momentum Thickness to Duct Height
H	Height
θ	Empirical Constant Based on Mode of Fuel Injection and Fuel-Air Mixing
μ_i	Mach angle at a Mach number of i
IT	Ignition Temperature
π_c	Total Pressure Ratio

Φ	Stream Thrust Function
g	Gravity
T^o	Reference Temperature
K	Dimensionless Kinetic Energy
H	Dimensionless Static Enthalpy
Sa_i	Stream Thrust Function at Station i
SERN	Single Expansion Ramp Nozzle

CHAPTER 1

INTRODUCTION

This chapter will provide a basic introduction to scramjet technology by presenting the definition, historical timeline, possible applications, and the current status of scramjet engines.

1.1 Definition of a Scramjet Engine

In order to provide the definition of a scramjet engine, the definition of a ramjet engine is first necessary, as a scramjet engine is a direct descendant of a ramjet engine.

Ramjet engines have no moving parts, instead operating on compression to slow freestream supersonic air to subsonic speeds, thereby increasing temperature and pressure, and then combusting the compressed air with fuel. Lastly, a nozzle accelerates the exhaust to supersonic speeds, resulting in thrust. Figure 1 below shows a two-dimensional schematic of a ramjet engine.

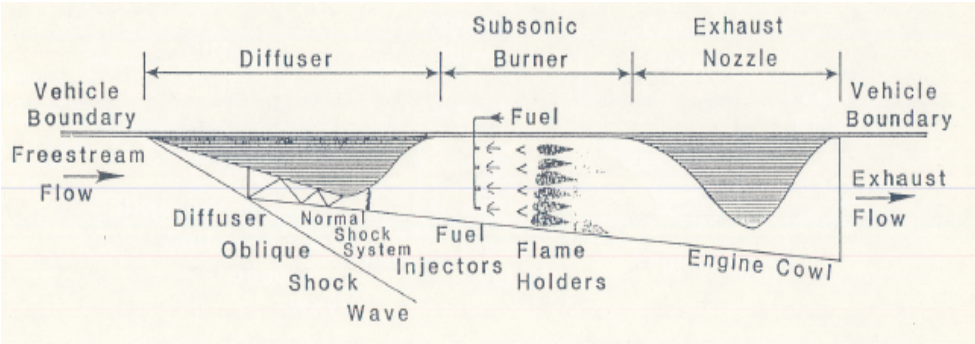

Figure 1.1: Two-dimensional Schematic of a Ramjet Engine [1]

Due to the deceleration of the freestream air, the pressure, temperature and density of the flow entering the burner are "considerably higher than in the freestream" [1]. At flight Mach numbers of around Mach 6, these increases make it inefficient to continue to slow the flow to subsonic speeds. Thus, if the flow is no longer slowed to subsonic speeds, but rather only slowed to acceptable supersonic speeds, the ramjet is then termed a 'supersonic combustion ramjet,' resulting in the acronym *scramjet*. Figure 2 below shows a two-dimensional schematic of a scramjet engine.

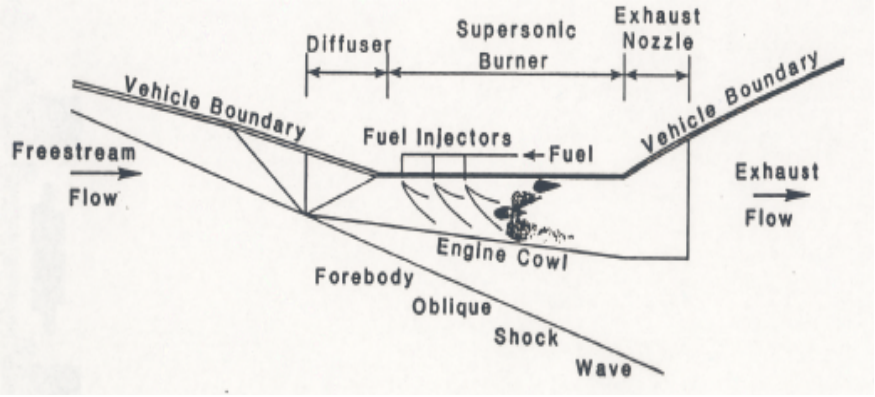

Figure 1.2: Two-dimensional Schematic of a Scramjet Engine [1]

Though the concept of ramjet and scramjet engines may sound like something out of science fiction, scramjet engines have been under development for at least forty years. The following subsection will give a brief chronological history of the scramjet engine.

1.2 Scramjet Engine Historical Timeline

It is the intention of this section to provide a brief introduction to the historical timeline of the scramjet, so as to provide a knowledge base for the current project. There have been many authors that have provided more thorough historical accounts of

both the ramjet and scramjet [1, 2, 3]; this section only seeks to list the highlights of the scramjet's development here.

As mentioned previously, the scramjet is a direct descendent of the ramjet. Therefore, in an attempt to provide a brief historical timeline of the modern-day scramjet, we must first begin with the invention of the ramjet. The first patent for a subsonic ramjet device, specifically for what is now known as an ejector ramjet, was issued to Lake in the United States in 1909 [3]. Simultaneously, René Lorin of France was working on ejector ramjets, publishing the first treatise on subsonic ramjets in 1913 [1,3]. According to Fry [3], the ramjet engine reached a relative peak of interest during the 1950s in terms of the number of operational systems being deployed, with a subsequent international resurgence of attention beginning in the 1980s.

Development on the scramjet, on the other hand, did not begin until the mid 1950s through early 1960s [1,3,4]. The basis for its development came about due to an interest in "burning fuels in external streams to either reduce the base drag of supersonic projectiles or to produce lift and/or thrust on supersonic and hypersonic airfoils in the early 1950s" [3]. Additionally, the findings of the 1960 study by Dugger on the relative performance of a kerosene-fueled conventional ramjet engine (CRJ) and a scramjet engine showed that the scramjet's performance would exceed the performance of the CRJ in the speed range of Mach 6 to 8 [2]. The first scramjet demonstration also took place in 1960 by Ferri [3]. Following this demonstration, many major scramjet development programs were started in the United States, the most extensive of these being the NASA Hypersonic Research Engine [3] or Hypersonic Ramjet Experiment [1,

3] (HRE) program in 1964. The core goal for the HRE project was to test a "complete, regeneratively cooled, flight weight scramjet on the X-15A-2 rocket research airplane" [1, 2, 3]. Unfortunately, this program was not able to be flight tested as the cost to repair the X-15 A-2 was too high and the entire X-15 program was cancelled in 1968 [1]. (Note: The damage referred to here occurred during the first non-burning test flight when the shock wave from the inlet spike impinged on the lower ventral fin, causing extensive damage—one of the first incidents of shock-shock interaction heating, which became a major research area in itself [1].) However, many other projects continued towards developing the scramjet. Fry [3] has compiled an impressive summary of the scramjet's evolution beginning with its conception in 1955 through 2004 and can be found below in Tables 1.1 and 1.2.

Table 1.1: Worldwide Scramjet Evolution, 1955-1990 [3]

Era	Country/service	Engine/vehicle	Engine type	Dates, year	Cruise Mach no.	Cruise altitude, ft	Powered range, n mile	Launcher	Total length, in.	Diameter, in.	Total weight, lbm	State of development
1955–1975	U.S. Navy	External burn[b]	ERJ	1957–1962	5–7	——	——	——	——	——	——	Combustion tests
	Russia	Chetinkov research	ERJ	1957–1960	5–7	——	——	——	——	——	——	Component tests
	U.S. Air Force	Marquardt SJ	DMSJ	1960–1970	3–5	——	——	——	88	10 × 15	——	Cooled engine tests
	U.S. Air Force	GASL SJ[a]	SJ	1961–1968	3–12	——	——	——	40	31 in^2	——	Cooled engine tests
	U.S. Navy	SCRAM[b]	LFSJ	1962–1977	7.5	100,000	350	Rail	288	26.2	5,470	Free-jet test
	U.S. Air Force	IFTV[c]	H_2/SJ	1965–1967	5–6	56,000	——	——	——	——	——	Component tests
	U.S. Air Force–NASA	HRE[a]	H_2/SJ	1966–1974	4–7	——	——	——	87	18	——	Flowpath tests
	NASA	AIM[b]	H_2/SJ	1970–1984	4–7	——	——	——	87	18	——	Cooled engine tests
	France	ESOPE[b]	DMSJ	1973–1974	5–7	——	——	——	87	18	——	Component tests
1975–1990	U.S. Navy	WADM/HyWADM[b]	DCR	1977–1986	4–6	80,000–100,000	500–900	VLS	256	21	3,750	Component tests
	Russia	Various research	SJ/DCR	1980–1991	5–7	80,000–100,000	——	——	——	——	——	Combustion tests
	NASA	NASP[b]	MCSJ	1986–1994	0–26	0–orbit	Orbital	Runway	——	——	500,000	Free-jet test (M7)
	Germany	Sänger II[b]	ATRJ	1988–1994	4	0–orbit	Orbital	Runway	3976	550	800,000	Concept vehicle

[a]System discussed and shown. [b]System discussed. [c]IFTV incremental flight test vehicle.

Fry [3] has a useful system—for which he cites McClinton et al. [10]—for dividing up the generations of scramjet development, namely: Beginnings (1960-1973), Airframe Integration (1973-1986), NASP (1986-1994), and Resurgence (1995-Today) [3]. Table 1.1 displays the Beginnings generation through the NASP generation; Table 1.2 displays mainly what Fry describes as the Resurgence generation.

Table 1.2: Worldwide Scramjet Evolution, 1990-2004 [3]

Era	Country/service	Engine/vehicle	Engine type	Dates, year	Cruise Mach no.	Cruise altitude, ft	Powered range, n mile	Launcher	Total length, in.	Diameter, in.	Total weight, lbm	State of development
1990–2003	United Kingdom	HOTOL[c]	SJ	1990–1994	2–8	——	——	——	——	——	——	Combustion tests
	Japan	PATRES/ATREX[b]	TRBCC	1990–	0–12	100,000	——	——	87	30	——	Component tests
	Japan	NAL-KPL research[b]	SJ	1991–	4–12	50,000-100,000	——	——	83	8×10	——	Component tests
	Russia	Kholod[a]	DCR	1991–1998	3.5–5.4	50,000–115,000	——	SA-5	36	24	——	Flight tests
	Russia/France	Kholod[a]	DCR	1991–1995	3.5–5.4	50,000–115,000	——	SA-5	36	24	——	Flight tests
	Russia/United States	Kholod[a]	DCR	1994–1998	3.5–7	50,000–115,000	——	SA-5	36	24	——	Flight tests
	France	CHAMIOS[b]	SJ	1992–2000	6.5	——	——	——	——	8×10	——	Component tests
	France	Monomat	DMSJ	1992–2000	4–7.5	——	——	——	——	4×4	——	Component tests
	France	PREPA[a]	DMSJ	1992–1999	2–12	0–130,000	Orbital	Ground	2560	Waverider	1×10^6	Component tests
	Russia	ORYOL/MIKAKS	SJ	1993–	0–12	0–130,000	Orbital	Ground	——	——	——	Component tests
	France/Russia	WRR[b]	DMSJ	1993–	3–12	0–130,000	——	Ground	——	Waverider	60,000	Component tests
	Russia	GELA Phase II[a]	RJ/SJ	1995–	3–5+	295,000	——	Tu-22M	——	——	——	Flight tests
	Russia	AJAX[b]	SJ	1995–	0–12	0–130,000	——	——	——	——	——	Concept
	U.S. Air Force	HyTech[a]	SJ	1995–	7–10	50,000–130,000	——	——	87	9×12	——	Component tests
	United States	GTX[d]	RBCC[e]	1995–	0–14	50,000–130,000	——	——	——	——	——	Component tests
	U.S. Navy	Counterforce	DCR	1995–	4–8	80,000–100,000	——	Air/VLS	256	21	3,750	Component tests
	NASA	X-43A/Hyper-X[a]	H2/SJ	1995–	7–10	100,000	200	Pegasus	148	60(span)	3,000	Flight tests
	France/Germany	JAPHAR[a]	DMSJ	1997–2002	5–7.6	80,000	——	——	90	4×4	——	Component tests
	United States	ARRMD[b]	DCR	1997–2001	3–8	80,000	450–800	Rail/Air	168–256	21	2,200–3,770	Component tests
	Russia	IGLA[a]	SJ	1999–	5–14	82,000–164,000	——	SS-25	197	——	——	Flight tests
	NASA	X-43C[b]	DMSJ	1999–	5–7	100,000	——	Pegasus	——	10.5 wide	——	Component tests
	Unites States	IHPTET[b]	ATR	1999–	0–5	0–90,000	——	——	——	15–40	——	Component tests
	United States	RTA[b]	TBCC	1999–	0–5	0–90,000	——	——	——	15–40	——	Component tests
	France	Promethee[b]	DMSJ	1999–2002	2–8	0–130,000	——	——	238	——	3,400	Component tests
	India	AVATAR-M[b]	SJ	1999–	0–14	0-orbit	Orbital	Ground	——	——	18–25 ton	Combustion tests
	United Kingdom	HOTOL Phase II	SJ	2000–	2–8	——	——	——	——	——	——	Component tests
	France	PIAP[b]	DMSJ	2000–	2–8	0–110,000	——	——	53	8×2	——	Component tests
	United States	MARIAH	MHD/SJ	2001–	15	——	——	——	——	——	——	Combustion tests
	Australia	HyShot[b]	SJ	2001–2002	7.6	75,000–120,000	200	Terrior Orion	55	14	——	Flight tests
	United States	Gun launch technology	SJ	2001–	——	——	——	Ground	——	——	——	Flight tests
	United States	ISTAR[b]	RBCC[e]	2002–2003	2.4–7	0-orbit	Orbital	Ground	400	Waverider	20,000	Component tests
	United States	X-43B[b]	RB/TBCC	2002–2003	0–10	100,000	200	Air	500	Waverider	24,000	Component tests
	Russia	Mig-31 HFL[b]	SJ/DCR	2002–	2–10	50,000–130,000	——	Mig–31	——	——	——	Planned flight tests
	United States	HyFly[a]	DCR	2002–	3–6.5	85,000–95000	600	F-4	225	19	2,360	Flight tests planned
	United States	SED[a]	SJ	2003–	4.5–7	80,000	——	——	——	9 wide	——	Planned flight tests
	France	LEA[a]	SJ/DCR	2003–2012	4–8	80,000	——	Air	——	——	——	Flight tests planned
	United States	RCCFD[b]	TBCC	2003–	0.7–7	0–orbit	Orbital	Ground	400	Waverider	20,000	Flight tests planned

[a]System discussed and shown. [b]System discussed. [c]Horizontal takoff and landing (HOTOL). [d]NASA Glenn Rc hydrogen fueled/cooled (GTX). [e]Reference vehicle designation (RBCC).

Table 1.2 leaves off in 2004, just prior to the X-43A setting the Guinness World Record for a jet-powered aircraft with a Mach number of 9.6 in November of that year [5]. Though the X-43A set a new speed record, it was not the first flight test of a scramjet. That title is occupied by the University of Queensland in Australia for the HyShot program in July 2002 [6].

In summary, the major propulsion systems of the modern era have a direct correlation between the year of their first flight and their current prevalence of application: Turbojet-1939, Ramjet-1940, High-Performance Large Liquid-Fueled Rocket Engine-1943, Practical Man-Rated Reusable Throttleable Rocket Engine-1960, and the Scramjet-2002 [3]. However, despite the fact that no operational and readily available scramjet engine currently exists, this is not due to a lack of potential applications which would benefit greatly from the use of the scramjet.

1.3 Applications for Scramjet Engines

There is a range of possible applications for scramjet engines, including missile propulsion, hypersonic cruiser propulsion, and part of a staged space access propulsion system [3, 8]. Figure 1.3 below displays the approximate performance range in terms of engine specific impulse and Mach number for various types of propulsion systems [3]. It can be seen that at Mach numbers higher than approximately 6-7, the only available propulsion systems are rockets and scramjets. Compared to rockets, scramjets have much higher specific impulse levels; therefore, it is clear why it is advantageous to develop the scramjet, if for this reason only. Contrary to rockets, scramjets do not require that an oxidizer be carried on board the aircraft as it is an airbreathing engine, collecting oxygen from the atmosphere [3]. This decreases the required weight of the overall propulsion system and fuel, resulting in a higher allowable payload weight or increased range. There are other reasons that the development of the scramjet is advantageous as well. Airbreathing engines produce higher engine efficiency, have a longer powered range, possess the ability for thrust modulation to ensure efficient operation, have higher maneuverability, and are completely reusable [3].

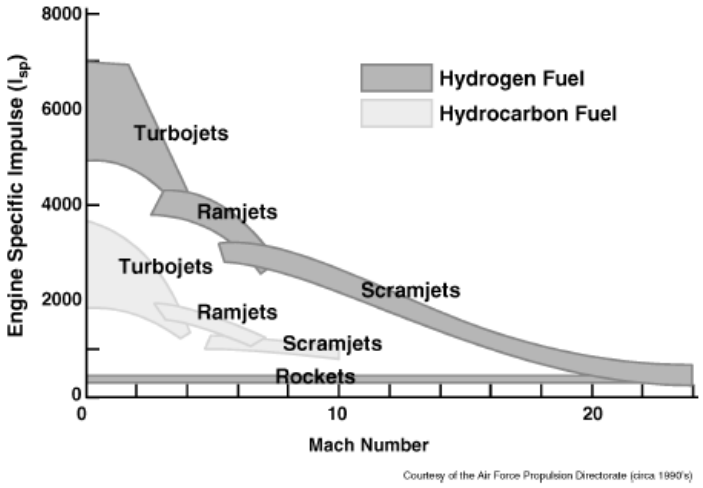

Figure 1.3: Specific Impulse Versus Mach Number for Various Engine Types [3]

Figure 1.4 displays a qualitative chart of the propulsion options based on the flight Mach number [3]. The curve represents the approximate altitude required to operate at a given flight Mach number as well as the needed propulsion system. Also shown on this chart is a relative boundary between the two primary fuel options for scramjets: hydrocarbons and hydrogen. Though Waltrup [7] concludes that the upper limit for hydrocarbons is between Mach 9 and 10 as opposed to Fry's diagram displaying approximately 8, the general consensus is that hydrogen fuel should be used for airbreathing flight faster than Mach 8-10, due to its "higher cooling capacity" and its "faster reactions" [3]. Though hydrogen can perform at higher speeds above the hydrocarbon upper limit, Curran states that with current capabilities the hydrogen-fueled scramjet will only offer "acceptable performance to about Mach 15" [2].

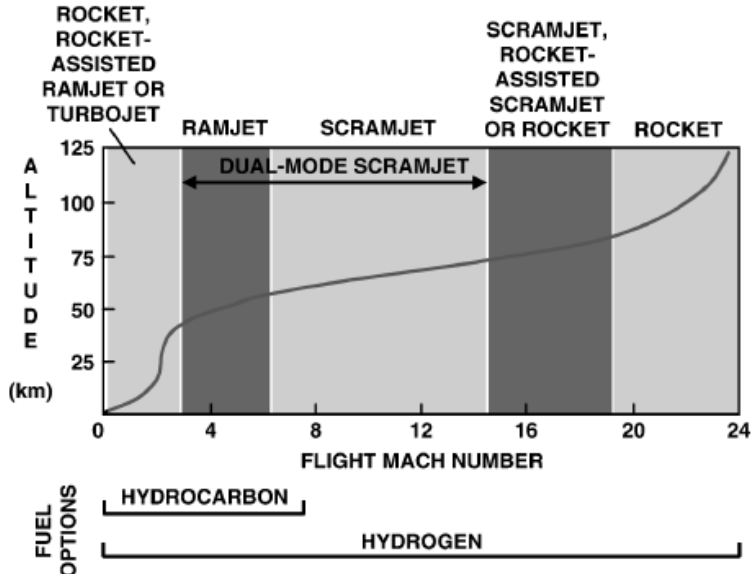

Figure 1.4: Propulsion System Options as a Function of Mach Number [3]

As for the space access application for scramjet technology, Townend argues, specifically, that there are many advantages in applying the scramjet as the propulsion system for the second stage of a two-stage-to-orbit (TSTO), hydrocarbon-fueled aerospace plane [8]. He explains that it would provide for a small TSTO vehicle as well as a small single-stage-to-orbit (SSTO) vehicle or military hypersonic cruiser that uses a hydrocarbon-fueled scramjet [8].

Fry explains that the rationale for hypersonic missile capability lies in the fact that a Mach 6-8 missile increases the possible range within a given flight time, or similarly, decreases the flight time required for a given range [3].

In summary, the goal of scramjet development is to give hypersonic vehicles a more efficient alternative to rockets. The vehicle that could most quickly benefit from current scramjet research is the cruise missile; however, a hypersonic cruiser aircraft that is an alternative to traditional turbojet transportation for civilian or military

application could also be a not-too-distant possibility. Scramjets could also be used in conjunction with rockets for space launchers [8], thereby requiring less on-board oxidizer for transport to space.

1.4 Current Scramjet Engine Technology Challenges

Figure 1.5 below is a good summary of the current challenges in the development of the scramjet engine. There are three main areas that these problems lay in, namely Air Inlet, Combustor, and Structures and Materials. Problems within these areas vary from inlet starting problems to the inherent difficulty of the ignition of the fuel in a supersonic flow, as the possibility of failure exists anywhere from the fuel not igniting to the possibility that the ignition could take place outside of the combustor due to the extraordinary velocity of the air in the engine. Additionally, structures that can withstand the extreme temperatures experienced during hypersonic flight combined with the additional temperatures experienced during combustion are necessary.

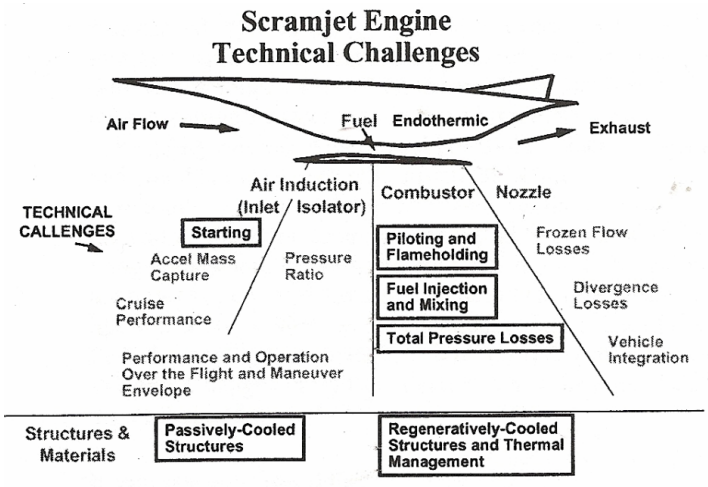

Figure 1.5: Technical Challenges of Scramjet Engine Development [9]

In addition to the current technical challenges of scramjet development, there is another area of scramjet development which deserves attention. Despite the wide range of applications possible with scramjet technology, the vehicle must first be propelled to a high enough Mach number for the scramjet to start. This requires, depending on the needed application, one or two additional propulsion systems to propel the vehicle to the needed scramjet start velocity. Current scramjet designs target the start of supersonic combustion to be between Mach 5 and 6 [1, 3, 8]. In order to minimize the weight and complexity of having multiple propulsion systems, a dual-mode ramjet/scramjet is often proposed.

However, if the necessary scramjet starting Mach number is reduced, a reduction in the number of required additional propulsion systems is possible, as the gap is bridged between the maximum possible velocity of the low speed engine(s) and the scramjet start velocity. This would have direct advantages from the resulting reduction in overall vehicle weight, the lower mass fraction required for the propulsion system (thereby resulting in more available payload weight), and fewer systems that must work in succession reliably, thereby increasing overall vehicle safety. The focus of this project is to address this issue of reducing the starting Mach number.

CHAPTER 2

PROBLEM DESCRIPTION AND BACKGROUND

This chapter will provide the problem description as well as the background theory and equations necessary to address the problem at hand.

2.1 Problem Description and Scope of Current Work

Air Force Solicitation AF073-058 states that a critical path issue in scramjet development is for scramjet operability to be extended to lower Mach numbers. Specifically, the solicitation states that scramjet start should be reduced to "Mach 3.50 while maintaining performance at higher Mach numbers within the same flowpath" with minimal variable geometry features and the use of hydrocarbon fuel [11].

According to Fry [3], a turbojet engine can provide for thrust from takeoff to a speed of Mach 3 or 4. Therefore, if a scramjet were designed with a starting Mach number of about 3.50, presumably only two propulsion systems would be needed for the entire mission, whether that is up to Mach 8-10 for a hydrocarbon-powered scramjet or up to Mach 15-20 for a hydrogen-powered scramjet. The advantage of this technology is clear due to the reasons discussed in the previous chapter—the resulting reduction in overall vehicle weight, lower mass fraction required for the propulsion system, and fewer systems that must work in succession reliably, thereby increasing overall vehicle safety.

The remainder of this chapter details the necessary background information and several possible methods for lowering the scramjet starting Mach number to 3.50. The method best suited for the current project is then selected.

2.2 Scramjets: Options for Lowering the Starting Mach Number

As previously discussed, there is a need for the starting Mach number of the scramjet to be reduced. There have been a few projects which sought, at least in part, to lower the scramjet starting Mach number, the most extensive being HyTech. The main objective of that program is to "enable sustained hypersonic flight for missile or aircraft applications and to develop and demonstrate Mach 4-8 hydrocarbon-fueled, actively cooled scramjet engine technology" [3]. The program has been successful in demonstrating Mach 4.5 and 6.5 ground testing [3, 12].

The project described in this paper, however, seeks to lower the starting Mach number to 3.50 and to determine the main factors influencing this ability. There are a number of possible ways to lower the starting Mach number of the scramjet. The methods discussed in the literature are listed and briefly explained here in turn.

2.2.1. Variable Geometry

In a variable geometry scramjet, the flowpath is changed according to the freestream Mach number to ensure high performance values throughout a wide range of Mach numbers. An example of a program which employed this technique is the HRE program which developed a flight-weight hydrogen-fueled scramjet designed to operate from Mach 4 to 7 using variable geometry [3]. Though this technique ensures high

performance, it is highly complex and instills a high level of inherent risk, as it relies on a large number of moving parts which require large actuation forces.

2.2.2. Hypersonic Dual-Combustor Ramjet (DCR)

The DCR engine was developed by James Keirsey of Johns Hopkins University/Applied Physics Laboratory in the early 1970s. The concept of this type of scramjet engine is that a portion of the captured air in the engine is "diverted to a small, embedded subsonic dump combustor into which all of the fuel is injected" [3]. The fuel and air are then mixed to a sufficient level in the subsonic combustor, which, essentially, acts as a "hot, fuel-rich gas generator for the main supersonic combustor" [3].

2.2.3. Manipulation of "Pure" Scramjet Engine Key Design Parameters

There are a few key parameters of the "pure" scramjet engine—that is, a scramjet with one combustor and a non-variable flowpath—that are able to be varied and manipulated to perhaps lower the starting Mach number of a scramjet. For instance, as the cycle static temperature ratio (T_3/T_0) increases, the Mach number of the flow entering the burner (M_3) decreases [1]. Thus, T_3/T_0 directly affects the freestream Mach number (M_0) at which the flow entering the burner (M_3) becomes supersonic. Due to this, it is possible that the manipulation of T_3/T_0 would yield a lower freestream Mach number at which supersonic combustion can occur. Additionally, the key design parameters of fuel selection and fuel-to-air ratio (f) for the scramjet may have an impact on the starting scramjet Mach number.

The SBIR solicitation by the Air Force [11] specifically stated that minimal variable geometry features should be used; therefore, exploring the use of variable geometry as a solution to the problem is not an option. Though the concept of the DCR engine may prove effective at lowering the starting Mach number of the scramjet, determining whether the starting Mach number of a "pure" scramjet can be accomplished should be the first task. Therefore, of these three possible avenues for investigation, the manipulation of the pure scramjet's key design parameters is the best approach for the current project.

2.3 Scramjet Reference Station Designations

Before setting out in the analysis, it is first necessary to establish the reference station designations of the scramjet engine. Using Heiser and Pratt's designations [1], Figure 2.1 and Table 2.1 show the designation system used throughout this paper.

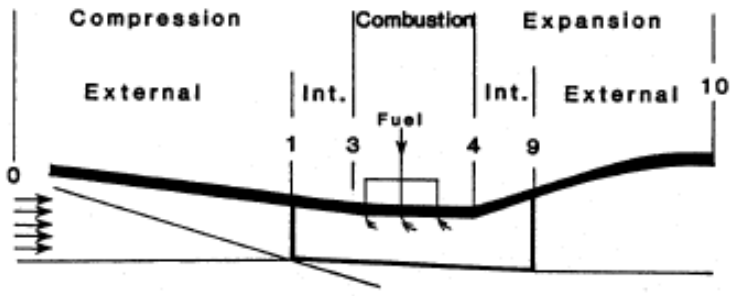

Figure 2.1: Scramjet Reference Station Designations [1]

Table 2.1 below shows the corresponding engine location descriptions for each reference station identified in Figure 2.1.

Table 2.1: Engine Locations for Scramjet Reference Station Designations [1]

Reference Station	Engine Location
0	Undisturbed or freestream conditions
	External compression begins
1	External compression ends
	Internal compression begins
	Inlet or diffuser entry
3	Inlet or diffuser exit
	Internal compression ends
	Burner or combustor entry
4	Burner or combustor exit
	Internal expansion begins
	Nozzle entry
9	Internal expansion ends
	Nozzle exit
	External expansion begins
10	External expansion ends

Identifying the reference station designations is the first step required towards completing the theory and analysis necessary for this project.

2.4 Chapter Summary

In summary, the current problem to be investigated is whether the scramjet starting Mach number can be lowered to Mach 3.50 and, if so, how it can be accomplished. Various options were discussed as to how the Mach number could be lowered and the variation of key scramjet design parameters was chosen as the best, most applicable method. The reference station designations for a scramjet engine were specified.

The remainder of the paper will detail the analysis process towards achieving the project objective and the results found from the investigation. Chapter 3 will detail the theory and analysis of the key design parameters for lowering the scramjet starting Mach number. The effects that the ratio of combustor entry temperature to freestream temperature (T_3/T_0), fuel selection, and fuel-to-air ratio variation have on lowering the starting Mach number of scramjets are explored respectively during the Chapter 3

analysis. Once these topics have been addressed, Chapter 4 will detail the theory and design of the required engine flowpath to achieve scramjet start at the lowest possible Mach number calculated from the Chapter 3 analysis. Chapter 5 details the calculations of the on- and off-design performance of the resulting scramjet designed in Chapter 4, and, finally, the overall Conclusions and Recommendations of the project are provided in Chapter 6.

CHAPTER 3

ANALYSIS OF KEY DESIGN PARAMETERS TO REDUCE SCRAMJET STARTING MACH NUMBER

This chapter will detail the theory and equations necessary as well as the analysis completed towards developing a scramjet with a lower starting Mach number of Mach 3.50. Section 3.1 details the theory and equations, whereas Sections 3.2, 3.3, and 3.4 will explain the analysis completed based on the information in Section 3.1. Section 3.5 will provide a chapter summary and conclusion. The goals of this chapter are as follows: determine what impact the driving design parameters for a scramjet have in lowering the starting Mach number and assess whether a starting Mach number of 3.50 is currently possible or feasible in the future.

Table 3.1 lists the one-dimensional stream thrust performance analysis inputs and how they are determined. As seen in the table, the vast majority of the inputs are set by the freestream Mach number, are properties that remain constant for air, earth, etc., or are assumed based on reasonable values within a typical range. The values for the constant and assumed inputs can be seen in Table 3.2 below. These values are used throughout the paper for all analysis calculations as needed unless otherwise noted. All assumed values were chosen based on recommendations from [1]. Additionally, all constants were determined based on information in [1].

Table 3.1: Performance Analysis Inputs and Corresponding Determination Methods

Performance Analysis Inputs	*How Determined*
M_o, V_o, T_o, p_o	Set by Mach Number
C_{pc}, R, C_{pb}, C_{pe}, h_f, g_o	Constant
V_{fx}/V_3, V_f/V_3, $C_f(A_w/A_3)$, n_c, n_b, n_e, T^o, p_{10}/p_0, γ_c, γ_e, γ_b	Assumed
T_3/T_0, f, h_{pr}	Variation

Table 3.2: Stream Thrust Inputs: Values for Constant and Assumed Values

Constants [1]		
C_{pc}	1090.00	J/kgK
R	289.3	$(m/s)^2/K$
C_{pb}	1510.00	J/kgK
C_{pe}	1510.00	J/kgK
h_f	0.00	
g_0	9.81	m/s^2
Assumed Values [1]		
V_{fx}/V_3	0.50	
V_f/V_3	0.50	
$C_f{*}A_w/A_3$	0.10	
η_c	0.90	
η_b	0.90	
η_e	0.90	
T^0	222.00	K
p_{10}/p_0	1.40	
γ_c	1.362	
γ_e	1.238	
γ_b	1.238	

For one-dimensional flow analysis, there are only three inputs that are able to be varied to alter performance results. These are the cycle static temperature ratio (T_3/T_0), the fuel selected, and the fuel-to-air ratio (*f*). Therefore, these three variables will be discussed and analyzed in this chapter.

3.1 Theory and Equations

This section will provide the necessary theory to complete the analysis of the key design parameters that may aid in lowering the scramjet starting Mach number.

3.1.1. Preliminary Calculation of Cycle Static Temperature Ratio T_3/T_0 Necessary for Starting Mach Number of 3.50

Due to the large design impact of T_3/T_0, this subsection will present the theory and governing equations that the preliminary investigation of this parameter requires.

The largest factor in changing the freestream Mach number at which supersonic combustion begins is the cycle static temperature ratio, T_3/T_0. As T_3/T_0 increases for a given freestream Mach number (M_0), the Mach number of the flow entering the combustor decreases [1]. Thus, T_3/T_0 directly affects the M_0 at which the flow entering the burner (M_3) becomes supersonic. So, with a range of freestream Mach numbers, the necessary T_3/T_0 can be determined based on M_0 and the ratio of specific heats at compression (γ_c) where M_3=1 by the following equation [1]:

$$M_3 = \sqrt{\frac{2}{\gamma_c - 1}\left\{\frac{T_o}{T_3}\left(1 + \frac{\gamma_c - 1}{2} M_o^{\,2}\right) - 1\right\}} \tag{3.1}$$

This preliminary calculation serves an adequate way to get an estimate of the required T_3/T_0 value to lower the starting Mach number of the scramjet. The following subsection will detail methods which will more accurately weigh all of the design parameters' influences.

3.1.2. Hypersonic Airbreathing Engine Performance Analysis Methods

In order to accurately assess whether a scramjet starting Mach number of 3.50 is possible or worthwhile, performance analysis must be completed to determine whether the necessary T_3/T_0 is achievable. Additionally, performance analysis is needed to parametrically vary the engine parameters of fuel-to-air ratio and fuel properties to determine whether a scramjet with a starting Mach number of 3.50 is possible.

For this analysis to be completed, a one-dimensional flow approach will be used. As Heiser and Pratt explain, "Although the one-dimensional approach can never be perfectly correct, the alternatives are both hopelessly complex and completely unwieldy for reaching a basic understanding built upon fundamental principles" [1]. For the current project, a complex analysis is not needed. The one-dimensional flow approach assumes that the fluid properties remain constant across the flow and thus only depend on the axial dimension coordinate [1]. This serves as an excellent method for the current project, as the flow within a scramjet engine is confined within the definite boundaries of the engine flowpath, making a two- or three-dimensional analysis unnecessary for achieving an understanding of the flow [1].

Heiser and Pratt [1] have compiled an excellent resource for understanding and applying one-dimensional flow analysis. There are three main approaches to this analysis, varying in depth, complexity, and accuracy. These three methods are described here, in order of increasing depth and accuracy.

1. *Thermodynamic Closed Cycle Analysis*

   This analysis method is based on classical thermodynamics and is often referred to as Brayton cycle analysis [1]. Thermodynamic Closed Cycle Analysis is accomplished through working through the classical thermodynamic cycle and is characterized by the rules that the working medium must:

   - Be treated as a "pure substance" [1].
   - "Experience a series of equilibrium processes that return it to its original state" [1].

   The second rule is accomplished through the four processes depicted on a Brayton cycle T-s diagram [1].

2. *First Law Analysis*

   The second method for calculating hypersonic airbreathing performance analysis is through "analyzing the behavior of the flow across each of the successive thermodynamic processes by means of simple but physically tenable models of the behavior of air" [1]. This method was originally conceived by C.H. Builder [1, 13]. The main purpose of this method is to provide an evaluation of the static enthalpy at each engine reference station [1]. The organization of this method is identical to the Thermodynamic Closed Cycle Analysis described above, but the goal of this method is to "find closed form solutions for the performance of real ramjets and scramjets" and then

use these solutions to "expose important trends and sensitivities without recourse to elaborate thermochemical calculations" [1]. The following assumptions are required:

- Equilibrium air behaves as a calorically perfect gas across each process of the Brayton cycle [1].
- There exist reasonable empirical models to "describe the adiabatic compression, constant-pressure combustion, and adiabatic expansion processes" [1]. They will be described by process efficiencies that will be assumed to be constant [1]. An inherent measure of risk is introduced when using this method [1].

3. *Stream Thrust Analysis*

   This method requires more initial information and uses the entire set of control volume conservation equations [1]. It leans heavily on momentum relationships and offers a different approach than the energy methods previously discussed [1]. This method accounts for phenomena that the previous two methods are unable to account for.

Of the three possibilities for use in evaluating scramjet engine performance, the Stream Thrust Analysis method has the greatest depth. It is able to account for several phenomena that considerably influence performance, namely: "the mass, momentum, and kinetic energy fluxes contributed by the fuel, the geometry of the burner, and exhaust flows that are not matched to the ambient pressure" [1]. Due to these benefits,

the Stream Thrust Analysis method will be employed here, as it accounts for the most engine parameters and influences compared to other one-dimensional flow analysis methods. The following section will describe this method in more detail as well as provide the equations for it.

3.1.3. Stream Thrust Analysis Method for Hypersonic Airbreathing Engine Performance Analysis

Before diving into the equations necessary for this analysis, it is first necessary to define the control volume under consideration. Figure 3.1 shows the defined control volume for a scramjet. In this definition, the outside surface of the engine lines up with the dividing streamlines that constitute the internal and external flow boundaries [1].

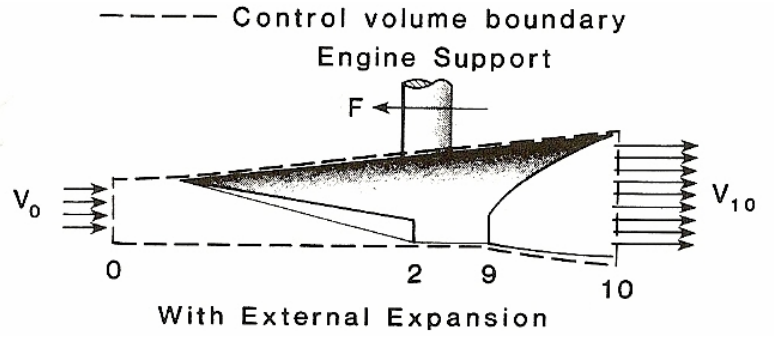

Figure 3.1: Scramjet Control Volume Definition [1]

As noted in Section 3.1.2, this one-dimensional flow analysis method assumes that all of the flow through the engine is aligned in the axial direction, and therefore, that the throughflow area is perpendicular to the axial [1]. Also, it is assumed that the perfect gas constant (R) is constant across the engine, as the molecular weight of air does not vary enough across the engine to make a significant difference in the calculations [1]. Heiser and Pratt note that the perfect gas law was used "repeatedly to

eliminate density from the equations" and that p_{10}/p_0 is treated as an independent parameter in the equations for this analysis [1].

It is best to break the engine down into separate functional parts, as "significantly different physical phenomena are at work in each"; therefore, this analysis operates with the following component breakdown [1]:

1. **Compression Component (Reference Stations 0 to 3):** Includes compression surfaces (internal and external), isolator, intake, etc. up to the combustor entrance.
2. **Combustion Component (Reference Stations 3 to 4):** Consists of the combustor and all parts that make combustion happen including fuel injectors, etc. that lie within the combustor.
3. **Expansion Component (Reference Stations 4 to 10):** Includes all expansion surfaces after the combustor exit up to the engine exit.

With the component breakdown established, it is now possible to step through the equation set of this analysis method. Please observe the symbolic definitions and abbreviations located immediately preceding the Introduction of this thesis. All equations listed below are taken directly from Reference 1.

Compression Component (Reference Stations 0 to 3)

1. Stream thrust function at freestream conditions

$$Sa_0 = V_0\left(1+\frac{RT_0}{V_0^{\,2}}\right) \tag{3.2}$$

2. Combustor entrance temperature

$$T_3 = \varphi T_0 \tag{3.3}$$

3. Combustor entrance velocity

$$V_3 = \sqrt{V_0^{\,2} - 2C_{pc}T_0(\varphi - 1)} \tag{3.4}$$

4. Stream thrust function at combustor entrance

$$Sa_3 = V_3\left(1 + \frac{RT_3}{V_3^{\,2}}\right) \tag{3.5}$$

5. Ratio of combustor entrance pressure to freestream pressure

$$\frac{p_3}{p_0} = \left\{\frac{\varphi}{\varphi(1-\eta_c)+\eta_c}\right\}^{C_{pc}/R} \tag{3.6}$$

6. Ratio of combustor entrance area to freestream entrance area

$$\frac{A_3}{A_0} = \varphi \cdot \frac{p_0}{p_3} \cdot \frac{V_0}{V_3} \tag{3.7}$$

Combustion Component (Reference Stations 3 to 4)

There are two methods for calculating the combustion properties, depending on the type of combustor designed: constant-pressure or constant-area combustion. The constant-pressure combustor is able to achieve results closest to ideal, since it is designed to conserve pressure, therefore generating less total pressure loss which in turn gives the engine a higher overall efficiency. Therefore, this is the combustor that will be used in the current project and the combustor type to which the proceeding equations apply.

However, there are some considerations to be made before these equations are listed. An absolutely constant-pressure burner is not feasible in terms of current manufacturing capabilities [1], so the application of an isolator which prevents inlet unstart should be used. Additionally, the burner walls will need to be more or less straight with a small variation in area in the axial direction [1]. A constant ratio of the area at the combustor exit to entrance will be instilled; that is, variable geometry will not be used. The combination of a small variation in axial area combined with the use of an isolator helps to achieve nearly equal pressures from the burner entry to the burner exit [1]. The following equations apply to the constant-pressure combustor case. Please note that as this is a constant-pressure burner design $p_4/p_0=p_3/p_0$ is assumed.

1. Combustor exit velocity

$$V_4 = V_3\left\{\frac{1+f\cdot\frac{V_{fx}}{V_3}}{1+f}-\frac{C_f\cdot\frac{A_w}{A_3}}{2(1+f)}\right\} \tag{3.8}$$

2. Combustor exit temperature

$$T_4 = \frac{T_3}{1+f}\left\{1+\frac{1}{C_{pb}T_3}\left[\eta_b f h_{PR} + f h_f + f C_{pb} T^o + \left(1+f\cdot\frac{V_f{}^2}{V_3{}^2}\right)\frac{V_3{}^2}{2}\right]\right\} - \frac{V_4{}^2}{2C_{pb}} \tag{3.9}$$

3. Ratio of area at combustor exit to combustor entrance

$$\frac{A_4}{A_3} = (1+f)\cdot\frac{T_4}{T_3}\cdot\frac{V_3}{V_4} \tag{3.10}$$

4. Stream thrust function at combustor exit conditions

$$Sa_4 = V_4\left(1+\frac{RT_4}{V_4^2}\right) \tag{3.11}$$

Expansion Component (Reference Stations 4 to 10)

1. Temperature at engine exit

$$T_{10} = T_4\left\{1-\eta_e\left[1-\left(\frac{p_{10}}{p_0}\cdot\frac{p_0}{p_4}\right)^{R/C_{pe}}\right]\right\} \tag{3.12}$$

2. Velocity at engine exit

$$V_{10} = \sqrt{V_4^2 + 2C_{pe}(T_4 - T_{10})} \tag{3.13}$$

3. Stream thrust function at engine exit conditions

$$Sa_{10} = V_{10}\left(1+\frac{RT_{10}}{V_{10}^2}\right) \tag{3.14}$$

4. Ratio of area at engine exit to area at freestream entrance

$$\frac{A_{10}}{A_0} = (1+f)\cdot\frac{p_0}{p_{10}}\cdot\frac{T_{10}}{T_0}\cdot\frac{V_0}{V_{10}} \tag{3.15}$$

Overall Engine Performance Measures (Across Stations 0 to 10)

With the analysis equations defined for the three engine components, it is now possible to establish the equations necessary to evaluate the overall engine performance. These equations are shown below, and also taken from Reference 1.

1. Specific thrust

$$\frac{F}{\dot{m}_0} = (1+f)Sa_{10} - Sa_0 - \frac{R_0T_0}{V_0}\left(\frac{A_{10}}{A_0}-1\right) \tag{3.16}$$

2. Specific fuel consumption

$$S = \frac{f}{F \big/ \dot{m}_0} \tag{3.17}$$

3. Specific impulse

$$I_{sp} = \left(\frac{h_{PR}}{g_0 V_0} \right) \eta_0 \tag{3.18}$$

4. Overall efficiency

$$\eta_0 = \frac{V_0}{h_{PR} S} \tag{3.19}$$

5. Thermal efficiency

$$\eta_{th} = \frac{\left[(1+f) \frac{V_{10}^2}{2} \right] - \frac{V_0^2}{2}}{f h_{PR}} \tag{3.20}$$

6. Propulsive efficiency

$$\eta_p = \frac{\eta_0}{\eta_{th}} \tag{3.21}$$

7. Mach number

$$M = \frac{V}{\sqrt{\gamma R T}} \tag{3.22}$$

In summary, three methods of one-dimensional analysis of scramjet engine performance were discussed. The stream thrust analysis method has been chosen as the method of choice for this project, as it is the most in-depth one-dimensional flow analysis available. The equations of this method were also presented.

3.2 Analysis: Variation of Cycle Static Temperature Ratio

This section will detail the analysis of the key design parameter cycle static temperature ratio T_3/T_0, as it may aid in lowering the scramjet starting Mach number. This analysis is based on the equations shown in Section 3.1.

3.2.1. Influence: Impact on Lowering the Starting Scramjet Mach Number

The cycle static temperature ratio (T_3/T_0) has a powerful impact on the starting Mach number of a scramjet. As Equation 3.1 shows, T_3/T_0, the ratio of specific heats during compression (γ_c), and the freestream Mach number (M_0) are the only variables which determine the burner entry Mach number (M_3). The specific heat ratio can be considered constant in the compression component. With the requirement that $M_3>1$ to ensure supersonic combustion, lowering M_0 can apparently be achieved by lowering T_3/T_0. Therefore, T_3/T_0 has perhaps the greatest impact on whether it is possible to lower the scramjet starting Mach number.

Thus, it is necessary to determine what the required value of T_3/T_0 is to achieve a starting scramjet Mach number of 3.50. Using Equation 3.1 with a range of freestream Mach numbers, and $\gamma_c=1.36$ [1], the necessary T_3/T_0 for each freestream starting Mach number can be determined where $M_3\geq1$. The result can be seen in Figure 3.2.

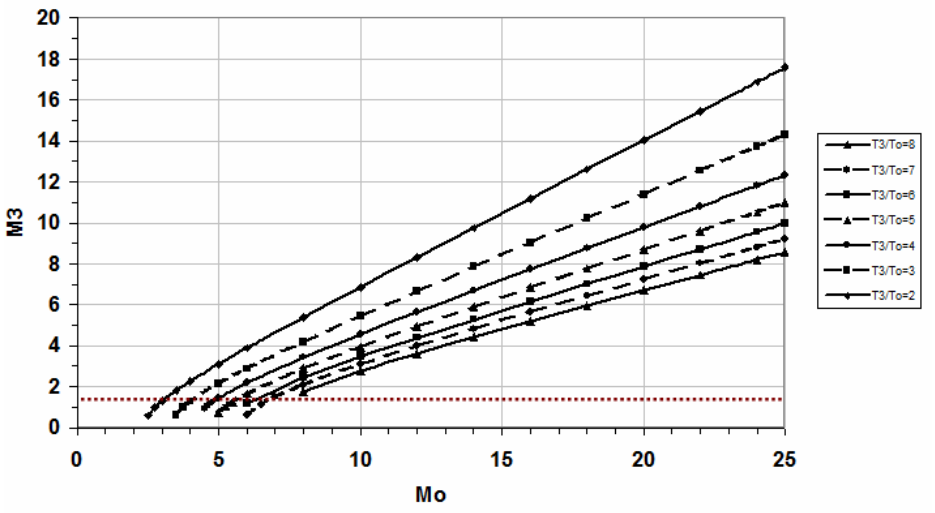

Figure 3.2: M_3 as a Function of M_0 and Cycle Static Temperature Ratio

As seen in Figure 3.2, the T_3/T_0 at which supersonic flow is achieved at the entrance to the combustor around Mach 3.5 is between 2 and 3. Specifically, solving Equation 3.1 with M_0=3.50, γ_c=1.36, and providing M_3 with a 10% margin by equating it to 1.10, gives a T_3/T_0 of 2.63. Figure 3.3 shows for the target starting Mach number of 3.50 that the required T_3/T_0 is approximately 2.75 solely based on M_0 and γ_c where $M_3 \geq 1$.

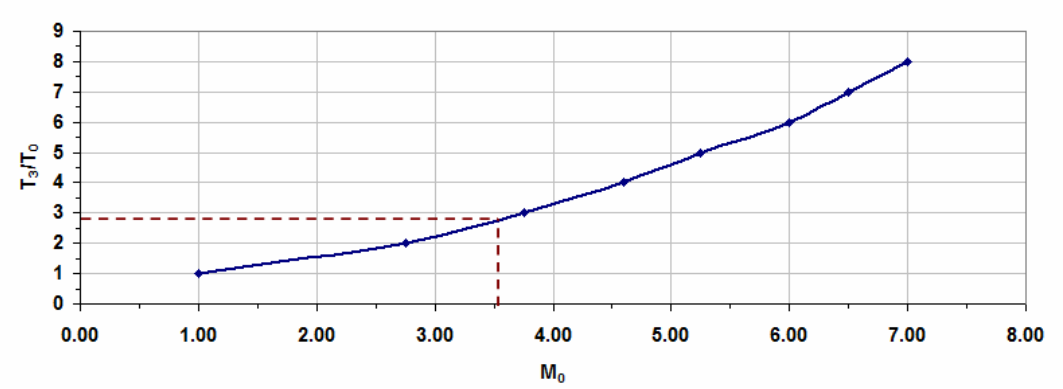

Figure 3.3: M_0 as a Function of Cycle Static Temperature Ratio

Therefore, preliminary calculations show that a T_3/T_0 approximately equal to 2.75 would allow for a scramjet starting Mach number of 3.50.

3.2.2. Assessment: Feasibility of Mach 3.50 Starting Scramjet Today or in the Future

The above discussion concluded that $T_3/T_0 \approx 2.75$ for a scramjet to start at Mach 3.50. Before any research or calculations could be done to determine how this can be accomplished, it is first necessary to determine whether a $T_3/T_0=2.75$ is not only feasible practically, but also whether it is reasonable in terms of performance.

In order to determine this, a constant dynamic pressure (q) trajectory is applied and is used to determine the corresponding performance for a scramjet at a starting Mach number of 3.50 with a T_3/T_0 of 2.75. Figure 3.3 below shows the trajectory used for this analysis. It was determined by using a constant q value of 47,880 N/m^2 in the Trajectory program of the Heiser and Pratt software "HAP" (Hypersonic Airbreathing Propulsion) [1]. The Trajectory program uses standard atmosphere properties, the freestream Mach number, and the value of dynamic pressure input to calculate a constant-q trajectory and provides the corresponding velocity, altitude, temperature, and pressure for the freestream Mach number entered. Thus, for a range of Mach numbers, in this case Mach 3.50 to 10, the overall trajectory path can be plotted as seen in Figure 3.4 below.

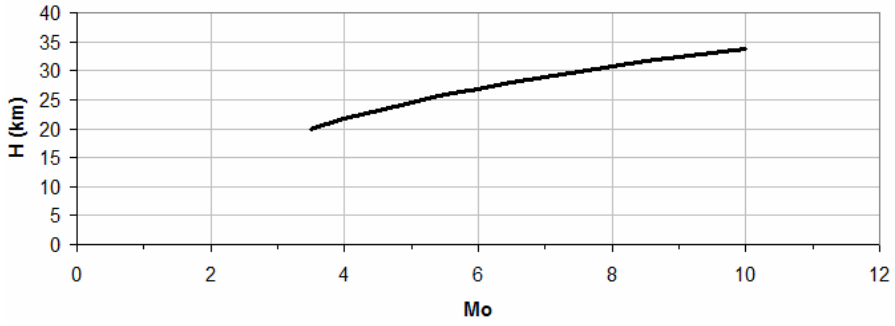

Figure 3.4: Constant Dynamic Pressure (q_0=47,880 N/m^2) Trajectory for Scramjet

Table 3.3: Flow Properties for Each Mach Number on a Constant Dynamic Pressure (q_0=47,880 N/m^2) Trajectory

q_o	47880.26	N/m^2			
η_c	0.9				
γ_c	1.362				
M	Vo (m/s)	H (m)	H (km)	To (K)	po (Pa)
3.5	1032.74	19936.97	19.94	216.65	5582
4	1184.56	21646.90	21.65	218.22	4275
4.5	1337.23	23167.85	23.17	219.73	3377
5	1490.40	24539.45	24.54	221.09	2736
5.5	1644.02	25786.08	25.79	222.33	2260
6	1798.05	26929.08	26.93	223.47	1900
6.5	1952.46	27989.78	27.99	224.52	1619
7	2107.21	28974.29	28.97	225.49	1397
7.5	2262.29	29894.78	29.89	226.41	1217
8	2417.68	30760.42	30.76	227.26	1069
10	3061.05	33790.13	33.79	233.16	684

The information obtained from the trajectory (V_0, T_0, p_0) as well as M_0=3.50, T_3/T_0=2.75, a standard fuel-to-air ratio (f) of 0.04 [1], a standard fuel heat of reaction (h_{PR}) of 87806.5 kJ/kg [1] (which falls between hydrogen and methane's heats of reaction), and the constants and assumed values shown in Table 3.2 can then be entered into the series of equations shown in Equations 3.2 through 3.22 for a constant-pressure combustor to determine a reasonable estimate of the performance of a scramjet with a starting Mach number of 3.50. The results of doing this can be seen in Table 3.4 below, as determined from a Microsoft Excel spreadsheet that was built for this purpose. A figure displaying the setup of the spreadsheet can be seen in Appendix A.

Table 3.4: Preliminary Performance Results for Scramjet with Starting Mach Number of 3.50 with an f=0.04 and h_{PR}=87806.5 kJ/kg

M	Vo (m/s)	To (K)	F/mo (N-s/kgA)	S (kgF/s-N)	Isp (s)	no	nth	np	M3	M4	M10	T3 (K)	T4 (K)	T10 (K)
3.5	1032.74	216.65	907.50	4.41E-05	2313.41	0.27	0.32	0.83	1.01	0.47	2.36	595.84	2609.56	1612.09
4	1184.56	218.22	839.27	4.77E-05	2139.47	0.28	0.32	0.88	1.55	0.73	2.46	600.10	2624.76	1621.48
4.5	1337.23	219.73	778.18	5.14E-05	1938.73	0.30	0.32	0.93	2.00	0.93	2.57	604.26	2641.51	1631.82
5	1490.40	221.09	723.54	5.53E-05	1844.45	0.31	0.31	0.98	2.40	1.12	2.69	608.00	2659.50	1642.94
5.5	1644.02	222.33	674.58	5.93E-05	1719.65	0.32	0.31	1.02	2.78	1.30	2.81	611.41	2678.82	1654.87
6	1798.05	223.47	630.61	6.34E-05	1607.54	0.32	0.31	1.06	3.14	1.46	2.94	614.54	2699.52	1667.66
6.5	1952.46	224.52	590.99	6.76E-05	1506.56	0.33	0.30	1.09	3.49	1.62	3.08	617.43	2721.65	1681.33
7	2107.21	225.49	555.20	7.21E-05	1415.31	0.33	0.30	1.13	3.83	1.78	3.21	620.10	2745.22	1695.89
7.5	2262.29	226.41	522.75	7.65E-05	1332.60	0.34	0.29	1.16	4.17	1.93	3.35	622.63	2770.33	1711.41
8	2417.68	227.26	493.24	8.11E-05	1257.37	0.34	0.29	1.19	4.50	2.08	3.49	624.96	2796.94	1727.84
8.5	2573.34	228.07	466.31	8.58E-05	1188.73	0.34	0.28	1.23	4.83	2.22	3.63	627.19	2825.11	1745.25
9	2731.26	229.17	441.35	9.06E-05	1125.10	0.34	0.27	1.26	5.15	2.37	3.78	630.22	2856.06	1764.37
9.5	2895.80	231.21	417.55	9.58E-05	1064.41	0.34	0.27	1.30	5.48	2.51	3.92	635.83	2892.34	1786.78
10	3061.05	233.16	395.66	1.01E-04	1008.61	0.35	0.26	1.34	5.80	2.65	4.07	641.19	2930.36	1810.27

The performance values for specific impulse and specific thrust are reasonable, and the combustor entrance temperature (T_3) is below the maximum allowed value range of 1440-1670 K [1] to prevent oxygen dissociation. Additionally, the combustor entrance pressure (p_3) is within the allowable range of 0.5 atm to 10 atm (50.66 to 1013.25 kPa) up to Mach 6 [1]. The lower limit of this range is to support combustion and the upper limit is constrained by the structural and weight limits of the vehicle. Although these results show reasonable performance values, there is one area that is of concern as it means that supersonic combustion did not occur throughout the combustor: M_4. As Table 3.4 shows, the generic scramjet (designed only with T_3/T_0, a generic h_{PR} and f, with a constant q trajectory) analyzed here does not maintain supersonic combustion throughout the combustor with M_3 and M_4>1 until a freestream Mach number of 5.00. This is made even clearer by Figure 3.5 which plots the combustor Mach numbers versus the freestream Mach numbers. The red dashed line shows the lowest limit for supersonic combustion to occur, with no margin.

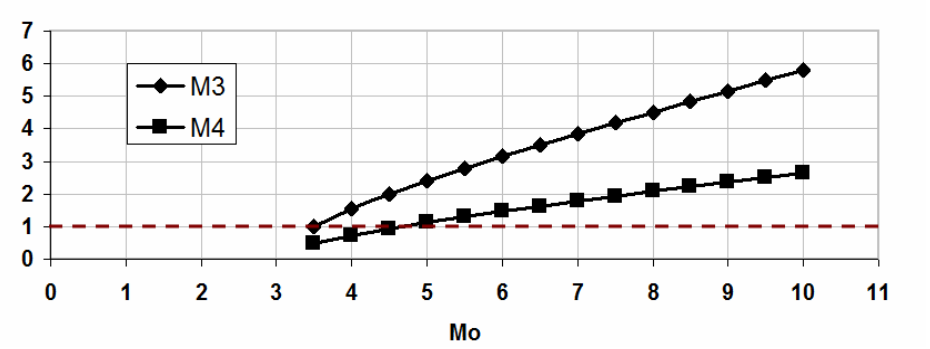

Figure 3.5: Preliminary Combustor Mach Numbers for Scramjet with Starting M_0=3.50

Therefore, it is necessary to determine if a different T_3/T_0 would produce supersonic combustion throughout the entire burner. M_3 and M_4 have been determined for a range of T_3/T_0 values so as to ascertain whether supersonic combustion can be maintained throughout the burner at a lowered starting Mach number. All other values remained the same as the previous calculation. Table 3.5 below shows these results.

Table 3.5: T_3/T_0 Required for Each Lowered Starting Mach Number

Mo	T3/To	M3	M4
3.5	1.25	2.98	1.00
3.75	1.50	2.78	1.01
4	1.75	2.64	1.02
4.25	2.00	2.54	1.04
4.5	2.50	2.22	1.00

According to this analysis, the maximum T_3/T_0 for a generic scramjet with a starting Mach number of 3.50 to maintain supersonic combustion throughout the combustor is 1.25. Using a T_3/T_0 of 1.25 with the other variables remaining the same, the performance results can be seen in Table 3.6 below.

Table 3.6: Performance Results for $T_3/T_0 = 1.25$ at $M_0=3.50$

M_0	3.5	n_p	2.28
V_0 (m/s)	1032.75	M_3	2.98
T_0 (K)	216.67	M_4	1.00
$F/\dot{m}_0$ (N-s/kgA)	316.80	M_{10}	1.30
S (kgF/s-N)	1.26E-04	T_3 (K)	270.84
I_{sp} (s)	807.60	T_4 (K)	2320.94
n_o	0.09	T_{10} (K)	2162.55
n_{th}	0.04		

3.2.3. Conclusion: Design Implications on a Lowered Starting Mach Number Scramjet

According to the calculations of this section, with generic values chosen for the fuel properties and the fuel-to-air ratio, the maximum T_3/T_0 for a scramjet with a starting Mach number of 3.50 to maintain supersonic combustion is 1.25 (with no available margin), which hardly requires any compression at all.

Although a T_3/T_0 value exists for lowering the starting scramjet Mach number to 3.50, the overall performance values shown in Table 3.6 are quite low. Though scramjet overall efficiencies are commonly around 50%, and are often as low as 30%, the overall efficiency here is only 9%. This is a very low efficiency and one that severely impedes any possible benefits for starting the scramjet at $M_0=3.50$. Also, the values of specific impulse and specific thrust are significantly reduced with a value of T_3/T_0 this low. Therefore, this section has shown that further investigation of the remaining design parameters is needed to aid in lowering the scramjet starting Mach number, so that the T_3/T_0 value may be selected at a higher value closer to the value of 2.75 determined in subsection 3.2.1.

3.3 Analysis: Fuel Selection

This section will detail the analysis completed of the impact of fuel selection on lowering the scramjet starting Mach number, culminating in the final decision of which fuel is best suited for the current project.

3.3.1. Influence: Impact on Lowering the Starting Scramjet Mach Number

Fuel selection plays a very important role not only in engine design, but also on the impact that the propulsion system has on the vehicle and mission design. For example, the less dense the fuel, the more volume will be required, leaving less volume for other things such as crew compartments and payload areas, among other penalties. In seeking to lower the scramjet starting Mach number, it is therefore imperative that the fuel is carefully selected to ensure not only that the goal is met for the current project, but also that the fuel selection will not inhibit the resulting engine's application potential.

A list of fuels to be analyzed has been completed, resulting from research into commonly applied fuels for scramjets as well as fuels used in other applications that may be of use here. The fuels to be analyzed can be seen in Table 3.7 below. In order to analyze these selected fuels against each other to determine their impact on the starting Mach number, it is necessary to first establish a characteristic that will help to distinguish between them. The purpose of fuel in a propulsion system is, in the most basic sense, to convert the chemical energy stored in the fuel to thermal energy which can produce thrust [1]. It is therefore beneficial to distinguish between the various fuels on a chemical level. The characteristic which will enable this is the heat of reaction of

the fuel, h_{PR}. This value represents the energy made available by the chemical reactions in a fictitious combustion process at constant pressure with no heat or work interactions [1]. This energy is then defined as the "heat that must be removed from the final combustion products in order to return them to the same temperature as the initial reactants (at the same pressure)" [1]. This heat is then expressed on a per mass basis, resulting in the characteristic of h_{PR} [1]. The fuels which will be analyzed in Section 3.3.2 can be seen in descending order of h_{PR} below in Table 3.7, compiled from References 1, 14, and 32.

Table 3.7: Heats of Reaction of Fuels for Analysis [1, 14, 32]

Fuel Type	hPR (kJ/kg Fuel)
Hydrogen	119954.00
Methane	50010.00
Ethane	47484.00
Hexane	45100.00
Octane	44786.00
JP-7	43903.25
JP-10	42100.00

With this characteristic established, it is now possible to consider the possible fuels. The two types of fuels most generally applied to scramjet designs are hydrogen and hydrocarbon fuels. Hydrogen fuels are often favored for flight above Mach 8-10 whereas hydrocarbon fuels are favored for Mach number ranges below 8 [17]. There are many advantages and disadvantages to both types of fuels which should be considered. These have been compiled here from numerous references [9, 15, 16, 17] in Tables 3.8 and 3.9 below.

Table 3.8: Hydrogen Fuel Advantages and Disadvantages

	Advantage	Disadvantage
Hydrogen Fuel	Rapid burning [15]	Very low density [15, 17]
	High mass-specific energy content [15, 17]	Boil-off problems [15]
	Shortest ignition delay [9]	Requires largest vehicle size [8]

Table 3.9: Hydrocarbon Fuel Advantages and Disadvantages

	Advantage	Disadvantage
Hydrocarbon Fuels	Storable [15]	Slow burning [15]
	Handling is familiar [9, 15, 16]	Long ignition delay time [16]
	11 times the storage density of hydrogen [15]	Require quick vaporization before mixing [16]
	3.5 times more energy content per volume than hydrogen [15]	Exposing to high temperatures can result in coking [9, 17]
	Some offer smaller vehicles, logistic simplicity [8]	
	Safer to handle than hydrogen [9]	
	Realistic ground testing in existing facilities is possible [9]	

There has been research that seeks to reduce the disadvantages for both types of fuels. One example of this type of research is searching for additives to decrease the ignition delay and increase reactivity of hydrocarbon fuels (for examples, see References 9 and 18).

Another property that should be considered is the ignition temperature of each fuel to be analyzed. The ignition temperature (IT) of a fuel is the temperature at which the fuel will self-ignite in air without a flame source or spark. The IT of the various fuels is very important for the current project, as a scramjet with a starting Mach number of 3.50 will have relatively low air temperatures, therefore requiring the fuel to be able to ignite at those temperatures [9]. The IT of the fuels which will be analyzed can be seen in Table 3.10, as compiled from References 33, 34, and 35.

Table 3.10: Ignition Temperatures of Fuels for Analysis at 1 atm [33, 34, 35]

Fuel Type	IT (K)
Hydrogen	845.15
Methane	810.15
Ethane	745.15
JP-10	518.15
JP-7	514.15
Hexane	498.15
Octane	479.15

Research into fuel properties alone is quite informative, but further analysis is required to determine whether fuel selection will enable a lower starting scramjet Mach number and, if so, what the best fuel for this goal is. The next section seeks to accomplish this.

3.3.2. Assessment: Feasibility of Mach 3.50 Starting Scramjet Today or in the Future

Section 3.2 determined that investigation of the other key design parameters—fuel selection and fuel-to-air ratio—is needed to aid in lowering the starting scramjet Mach number, as the performance values associated with a T_3/T_0 of 1.25 or lower are not practical. Therefore, this section will detail the analysis necessary to determine whether fuel selection will enable a higher T_3/T_0 value that will result in better performance.

Equations 3.2 through 3.22 are necessary for this determination to be made. However, instead of the default values for fuel used in Section 3.2, the heat of reaction and the stoichiometric fuel-to-air ratio of each of the fuels to be analyzed will be applied in order to determine whether fuel selection impacts the starting Mach number by an amount significant enough to enable scramjet start at a freestream Mach number of 3.50. The constants and assumed values shown in Table 3.2 will be used here as well.

Therefore, in order to complete this analysis, the stoichiometric fuel-to-air ratio and the heats of reaction of the various fuels need to be established. Table 3.7 shows the values for the heats of reaction h_{PR}. The stoichiometric fuel-to-air ratio (f_{st}) is calculated for each of the fuels by Equation 3.23 below from Reference 1.

$$f_{st} = \frac{36x + 3y}{103(4x + y)} \quad \textit{where the fuel is represented in the form of } C_xH_y \tag{3.23}$$

Table 3.11 shows the results from calculating f_{st} by Equation 3.23 for each of the fuels studied in this analysis.

Table 3.11: Stoichiometric Fuel-to-Air Ratios for Fuels for Analysis

Fuel Type	Chemical Formula	f_{st}
Hydrogen	H_2	0.0291
Methane	CH_4	0.0583
Ethane	C_2H_6	0.0624
Hexane	C_6H_{14}	0.0659
Octane	C_8H_{18}	0.0664
JP-7	$C_{12}H_{25}$	0.0674
JP-10	$C_{10}H_{16}$	0.0707

With the h_{PR} and f_{st} established, the one-dimensional flow analysis equations shown in Equations 3.2 through 3.22 have been run repeatedly for a range of freestream Mach numbers to determine the maximum T_3/T_0 possible with supersonic flow maintained throughout the burner, that is, where M_3 and M_4 are both greater than 1. The advantage of using a range of freestream Mach numbers is that if the fuel is not able to maintain supersonic combustion at a T_3/T_0 for Mach 3.50 with practical performance, it will be possible to determine the minimum freestream Mach number at which the fuel can do so.

The ignition temperatures listed in Table 3.10 must be taken into account to determine the T_3/T_0 required for each fuel to ignite in the airflow at each freestream Mach number. Therefore, the results for the maximum possible T_3/T_0 for each fuel were then compared to the necessary T_3/T_0 to ignite each fuel for each freestream Mach number. The analysis was completed starting with an M_0 of 3.50 and continuing upwards until ignition could be accomplished. Once ignition was reached, the analysis was not continued for higher Mach numbers, as the goal of this project is to reduce the starting Mach number to 3.50, or, if this can not be accomplished, a Mach number that is at least lower than the typical starting Mach number range of Mach 5.0-6.0. A margin was included in these calculations to allow for error by adding 5% to the necessary T_3/T_0 and subtracting 5% from the possible T_3/T_0. The results of this analysis are shown below in order of descending starting Mach number in Figures 3.6-3.12.

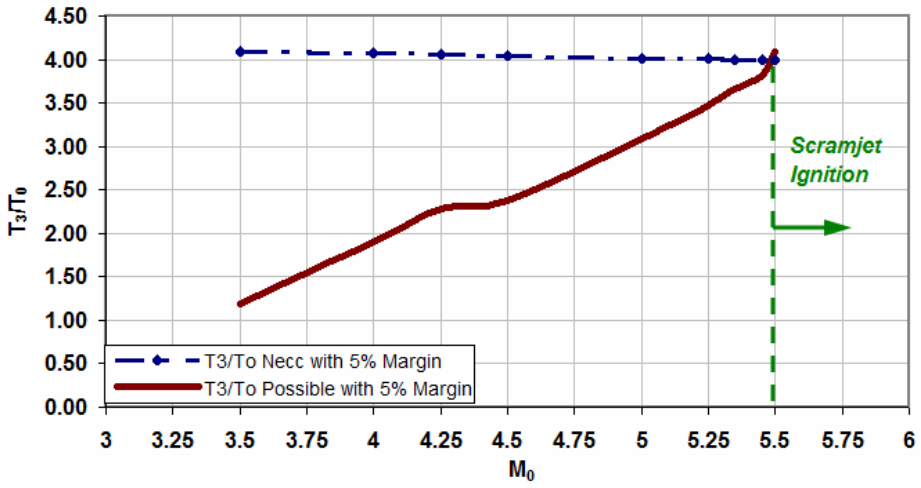

Figure 3.6: Lowest Possible Starting Mach Number for Hydrogen Ignition

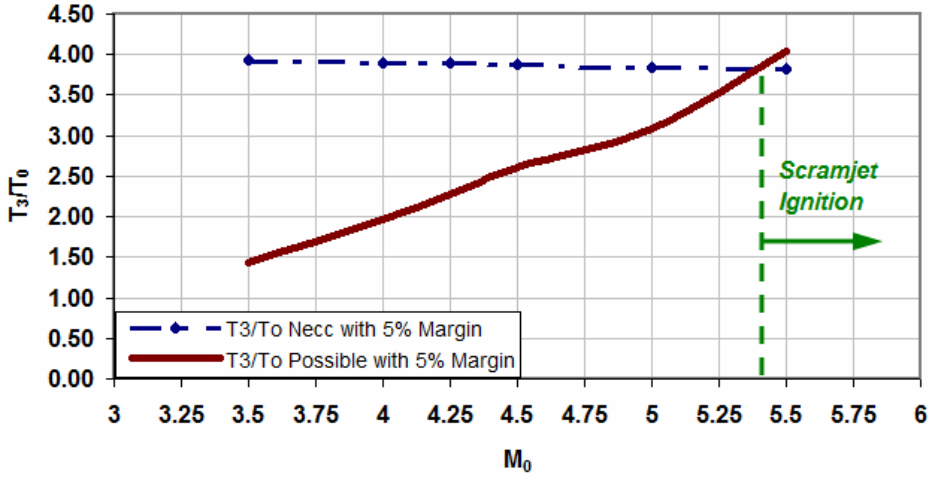

Figure 3.7: Lowest Possible Starting Mach Number for Methane Ignition

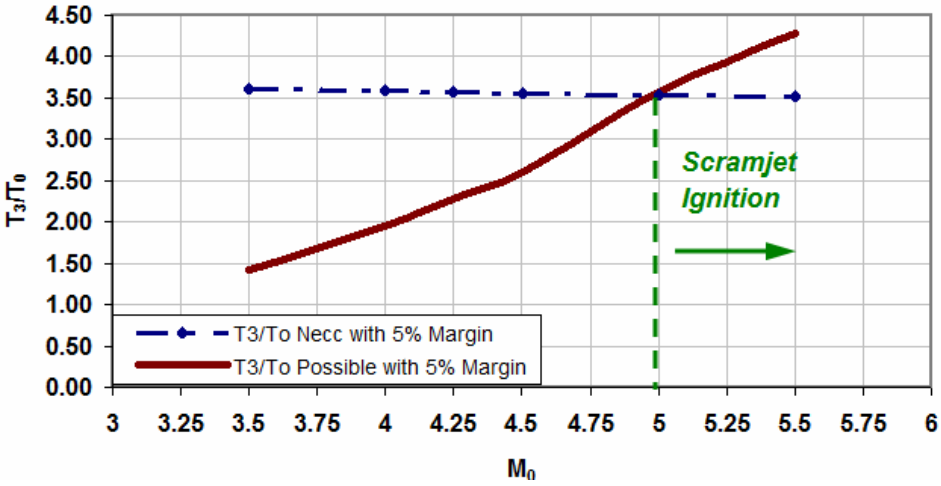

Figure 3.8: Lowest Possible Starting Mach Number for Ethane Ignition

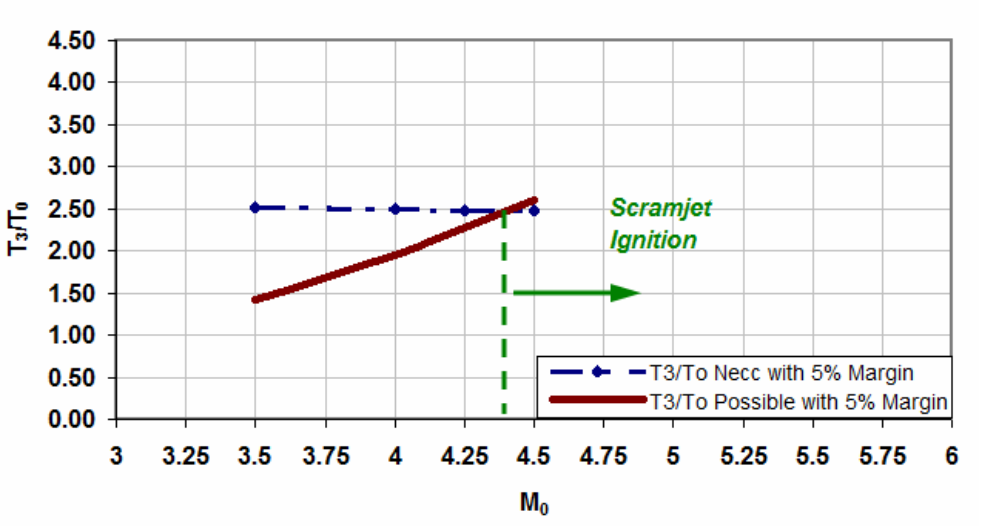

Figure 3.9: Lowest Possible Starting Mach Number for JP-10 Ignition

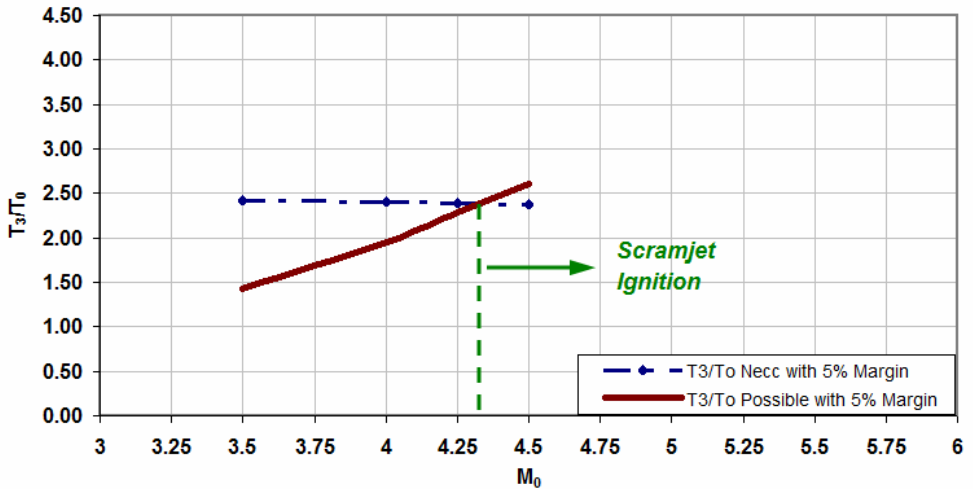

Figure 3.10: Lowest Possible Starting Mach Number for Hexane Ignition

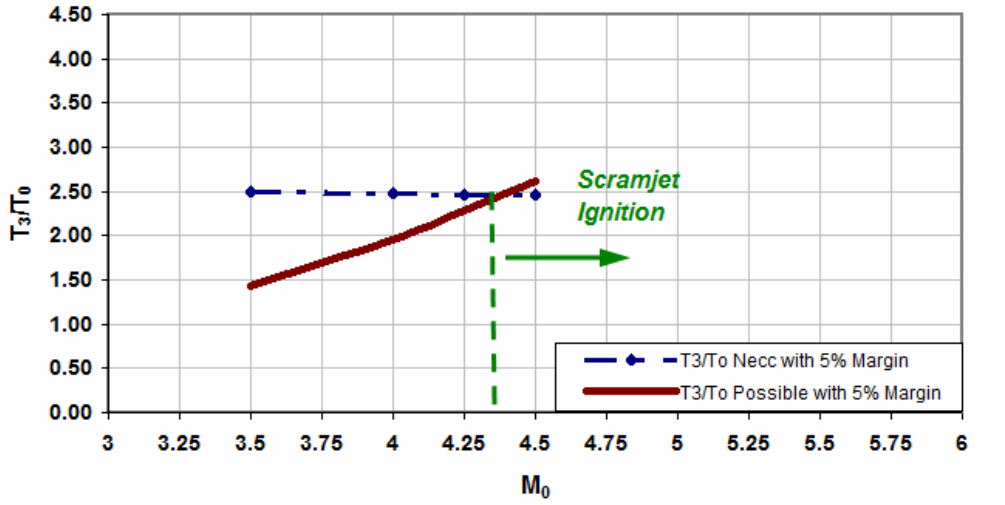

Figure 3.11: Lowest Possible Starting Mach Number for JP-7 Ignition

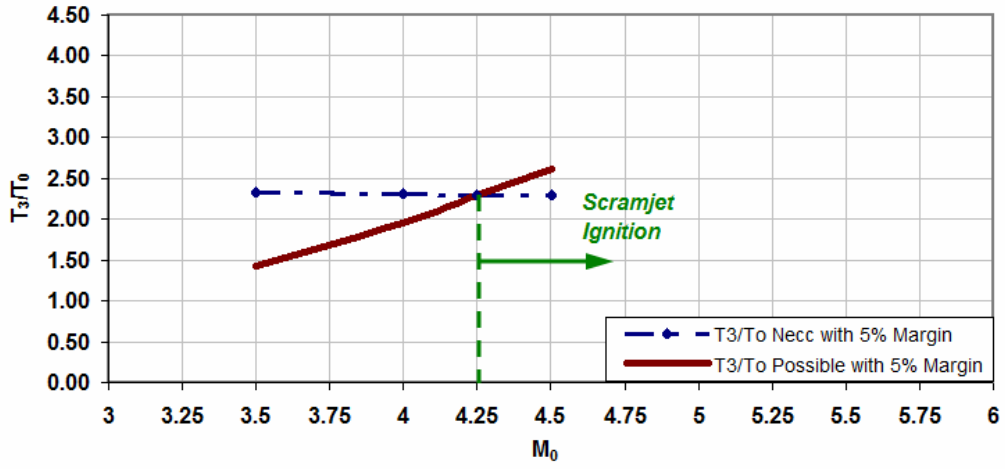

Figure 3.12: Lowest Possible Starting Mach Number for Octane Ignition

A summary table of the results from the previous seven figures is provided in Table 3.12. Methane is mentioned often as a fuel for a hypersonic cruiser with Mach 6+ cruising speed and hydrogen, as previously discussed, is applicable for Mach 8-10+ applications due of its high energy content. However, neither hydrogen nor methane is a

feasible fuel for the current project, as their lowest starting Mach numbers are 5.50 and 5.35, respectively, therefore providing no ability to lower the starting Mach number. Ethane is not applicable as a feasible fuel either, since its lowest starting Mach number at f_{st} is 5.0. JP-10 is used in missiles and some PDE designs. Though it reduces the starting Mach number at f_{st} to 4.35, it is not the best choice available for this application as there are other fuels which are able to reduce it even further.

JP-7 was developed for the SR-71 [19] and is used for military applications today. It reduces the starting Mach number at f_{st} to 4.3, and is a candidate fuel due to its wide availability and engine cooling capabilities. Hexane is similar in starting Mach number to JP-7, reducing it to 4.3 as well. However, hexane is not a necessary choice for further pursuit, as its results are similar to JP-7 and is not used as widely. Octane is a widely available fuel and succeeds in reducing the starting Mach number the furthest to 4.25; therefore it is also a candidate fuel for this project.

Table 3.12: Summary of Lowest Starting Mach Numbers and Corresponding T_3/T_0 for Analyzed Fuels

Fuel Type	IT (K)	Lowest Starting M_0	T_3/T_0
Hydrogen	845.15	5.50	4.00
Methane	810.15	5.35	3.75
Ethane	745.15	5.00	3.50
JP-10	518.15	4.35	2.50
JP-7	514.15	4.30	2.50
Hexane	498.15	4.30	2.40
Octane	479.15	4.25	2.25

When analyzing the resulting starting Mach numbers displayed in Table 3.12, it is evident that there is a trend between the ignition temperature of the fuels and the

resulting scramjet starting Mach number. Thus, these values are plotted in Figure 3.13 below. A trend which is nearly linear emerges, making it possible to determine the approximate minimum freestream starting Mach number possible for a fuel when given only its ignition temperature—a useful ability for a preliminary design check. The equation which approximates this is:

$$M_{0,starting} \cong 0.0034IT + 2.6096 \tag{3.24}$$

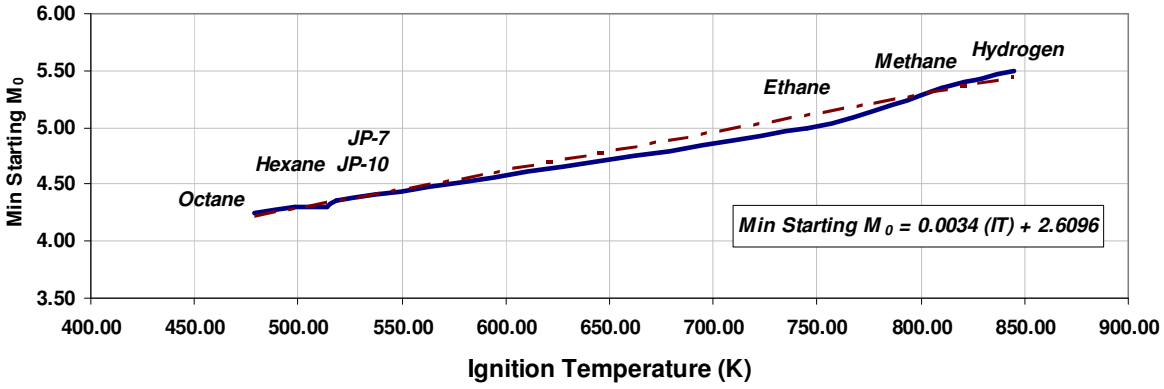

Figure 3.13: Lowest Possible Scramjet Starting Mach Number versus Ignition Temperature at Stoichiometric Fuel-to-Air Ratios for Several Fuels

Turning back to the problem at hand, the fuels which performed the best at stoichiometric fuel-to-air ratios and were the most applicable overall are JP-7 and octane. However, neither fuel reduces the starting Mach number to 3.50. There is still another key design parameter to explore—varying the fuel-to-air ratio. Before trying to further reduce the starting Mach number further though, a decision should first be made as to which fuel is better suited for the current project. The following points are important in this decision:

- Octane and JP-7 returned similar results: starting Mach numbers of 4.25 and 4.30, respectively.
- In the SR-71 engine, JP-7 was used in the engine hydraulic system in addition to being the propellant. [19]
- In high Mach number flight in the SR-71, JP-7 served as "a heat sink for the various aircraft and engine accessories which would otherwise overheat at the high temperatures encountered" [19].
- JP-7 contains A-50, which aided in disguising the radar signature of the exhaust plume of SR-71 [19].

In considering the above points, and due to its past military applications, JP-7 stands out as the best fuel for the current project.

3.3.3. Conclusion: Design Implications on a Lowered Starting Mach Number Scramjet

In summary, this section has analyzed the impact that fuel selection has on the starting Mach number of a scramjet. The analysis has discovered that a nearly linear trend between the minimum possible freestream starting Mach number and the ignition temperature of a fuel exists; therefore, the impact of fuel selection on lowering the starting Mach number of a scramjet is high. The lower the ignition temperature of a fuel, the more the starting Mach number can be reduced. Secondarily, the higher the heat of reaction of a fuel, the better the overall performance of the engine will be.

The result of the analysis in this section is that JP-7 has been selected as the best fuel for the current project and can reduce the starting Mach number to 4.30 for a

scramjet with the JP-7 stoichiometric fuel-to-air ratio. The resulting performance of the scramjet engine with the parameters defined thus far can be seen in Table 3.13 below.

Table 3.13: Performance Results with JP-7 Fuel at Stoichiometric *f* and T_3/T_0 of 2.50

Input		
M_0	4.3	
V_0	1276.1	m/s
T_0	219.15	K
T_3/T_0	2.50	
f	0.0674	
h_{pr}	43903.25	kJ/kg Fuel
Engine Performance Measures		
F/m_o	682.16	N-s/kgA
S	9.88E-05	kg F/s-N
I_{sp}	1031.70	s
n_o	0.29	
n_{th}	0.29	
n_p	1.02	
T_3	547.88	K
T_4	2210.82	K
T_{10}	1432.66	K
M_3	2.06	
M_4	1.00	
M_{10}	2.47	

As can be seen in this table as a result of selecting JP-7 as the fuel, the performance values have increased considerably over the values obtained with generic fuel values—the overall efficiency (η_o) is now 29% versus the 9% obtained in Section 3.2. The overall goal of this section was accomplished as well, as the T_3/T_0 value at which supersonic combustion can be maintained was increased to 2.50 from 1.25 with the application of JP-7 fuel. However, the goal of the project has not yet been accomplished, as the desired starting Mach number of 3.50 has not been achieved; the lowest possible starting Mach number stands at 4.30 after fuel selection. Fortunately, there is another key design parameter that may be able to aide in achieving the goal—the fuel-to-air ratio.

3.4 Analysis: Variation of Fuel-to-Air Ratio

3.4.1. Influence: Impact on Lowering the Starting Scramjet Mach Number

Section 3.3 determined that investigation the final key design parameter—fuel-to-air ratio—is needed to aid in lowering the starting scramjet Mach number, as the selection of fuel did not succeed in lowering the starting Mach number of a scramjet to Mach 3.50, but rather, only to Mach 4.30. Therefore, this section will detail the analysis necessary to determine whether the variation of the fuel-to-air ratio (f) from stoichiometric will enable the reduction of the starting Mach number to 3.50 while maintaining supersonic combustion.

As discussed in the previous section, the stoichiometric fuel-to-air ratio f_{st} is defined by Equation 3.23. The stoichiometric f is the fuel-to-air ratio which "usually results in the greatest liberation of sensible energy from the breaking of molecular bonds" [1]. In the variation of f, when f is smaller than the f_{st}, the available oxygen is not fully used and when f is larger than the f_{st}, fuel is wasted as not all of it can be burned [1]. Therefore, f_{st} is the ideal upper limit for the fuel-to-air ratio [1]. So, by varying f, combustion is not necessarily ideal. However, the goal of this project is not to produce ideal combustion (though it is always beneficial), but rather to lower the freestream Mach number at which the scramjet can start.

In order to know the limits for the variation of f, the equivalence ratio is used. Defined by Equation 3.25 below, the equivalence ratio is the ratio of the fuel-to-air ratio used to the stoichiometric fuel-to-air ratio [1].

$$\phi \equiv \frac{f}{f_{st}} \tag{3.25}$$

Heiser and Pratt state that a general guideline for the equivalence ratio is from 0.2 to 2 for "combustion to occur within a useful timescale" [1]. Therefore, the fuel-to-air ratio has been varied across this range for JP-7 fuel. This analysis and its results will be shown in the following subsection.

3.4.2. Assessment: Feasibility of Mach 3.50 Starting Scramjet Today or in the Future

The variation of the fuel-to-air ratio *f* across the recommended equivalence ratio range produces the results shown below in Table 3.14 for JP-7 fuel.

Table 3.14: Fuel-to-Air Ratios Used for Analysis with JP-7 Fuel and Corresponding Equivalence Ratios

Equiv Ratio	f
1.78	0.12
1.63	0.11
1.48	0.10
1.34	0.09
1.19	0.08
1.04	0.07
0.89	0.06
0.74	0.05
0.59	0.04
0.45	0.03
0.30	0.02

In order to determine whether the variation of the fuel-to-air ratio helps reduce the scramjet starting Mach number, the JP-7 fuel property of h_{PR} was applied to Equations 3.2 through 3.22 with a range of freestream Mach numbers from 3.50 to 4.50 and the range of fuel-to-air ratios listed above. Since the limiting factor is the ignition temperature of the fuel, and the T_3/T_0 has been low due to the lower Mach number goal, the maximum possible T_3/T_0 for supersonic combustion to be maintained at each *f* was determined and recorded. Then, from these results, the minimum possible T_3/T_0 which

could ignite the JP-7 fuel was found, as this is obviously necessary for supersonic combustion to even begin. Figures 3.14 through 3.16 below show the results for Mach numbers 3.50, 4.00, and 4.50. Again, a 10% margin was implemented by making the criterion for supersonic flow throughout the combustor be that the Mach numbers at stations 3 and 4 have to be greater than or equal to Mach 1.10.

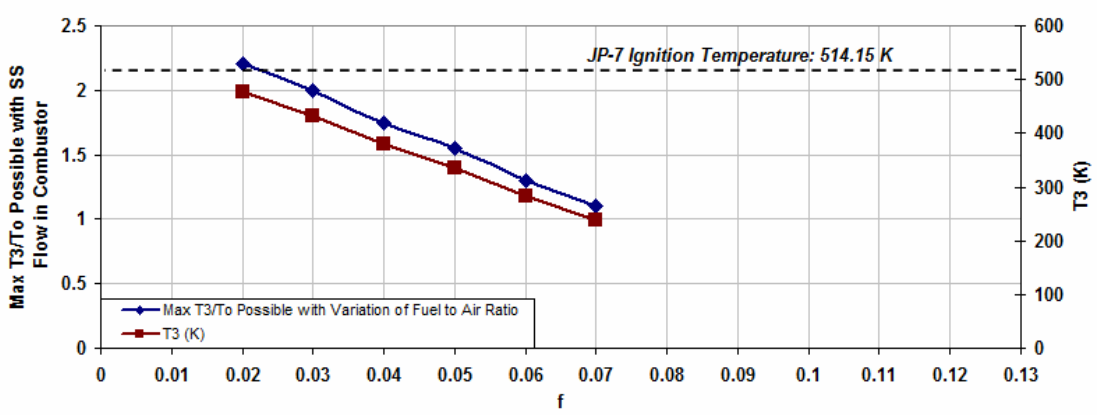

Figure 3.14: Max T_3/T_0 Possible with Supersonic Flow in Combustor versus Fuel-to-Air Ratio for JP-7 Fuel at Mach 3.5

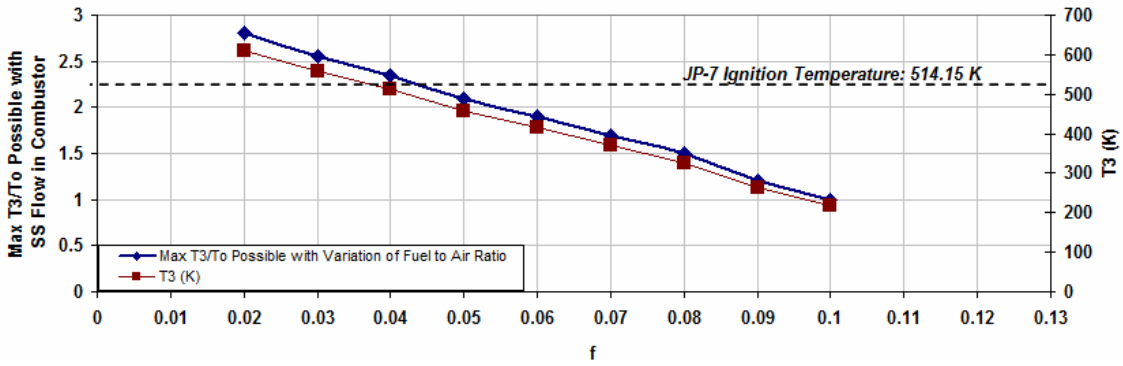

Figure 3.15: Max T_3/T_0 Possible with Supersonic Flow in Combustor versus Fuel-to-Air Ratio for JP-7 Fuel at Mach 4.0

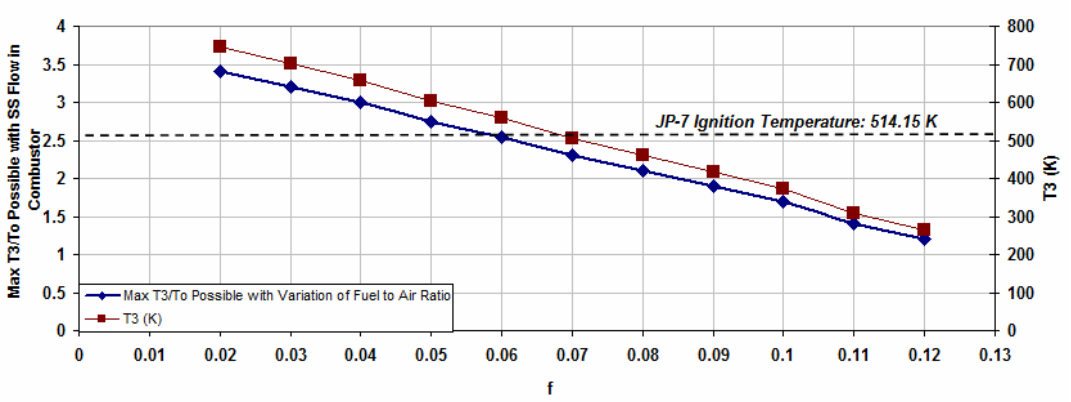

Figure 3.16: Max T_3/T_0 Possible with Supersonic Flow in Combustor versus Fuel-to-Air Ratio for JP-7 Fuel at Mach 4.5

From these figures, it is possible to tell the minimum achievable starting Mach number of a scramjet with JP-7 fuel and no ignition system or fuel additives. As can be seen in Figure 3.14, a starting Mach number of 3.50 is not achievable, as the ignition temperature required by JP-7 is not reached at the lowest fuel-to-air ratio possible within the equivalence ratio range. However, a starting Mach number of 4.00 is possible, as shown in Figure 3.15. Compiling the data from Figures 3.14-3.16 and including the lower limit of the required T_3/T_0 for JP-7 fuel to ignite, the design space for a scramjet with JP-7 fuel, plotted against the variation of *f*, is shown in Figure 3.17. A linear trendline has been added in the plot, which, upon testing, proves to be highly accurate compared to the one-dimensional flow results. This equation approximates the maximum value of *f* that can be used with JP-7 fuel while maintaining supersonic combustion and ensuring JP-7 ignition when given a desired starting freestream Mach number. It is:

$$f \cong 0.0543M_0 - 0.185 \tag{3.26}$$

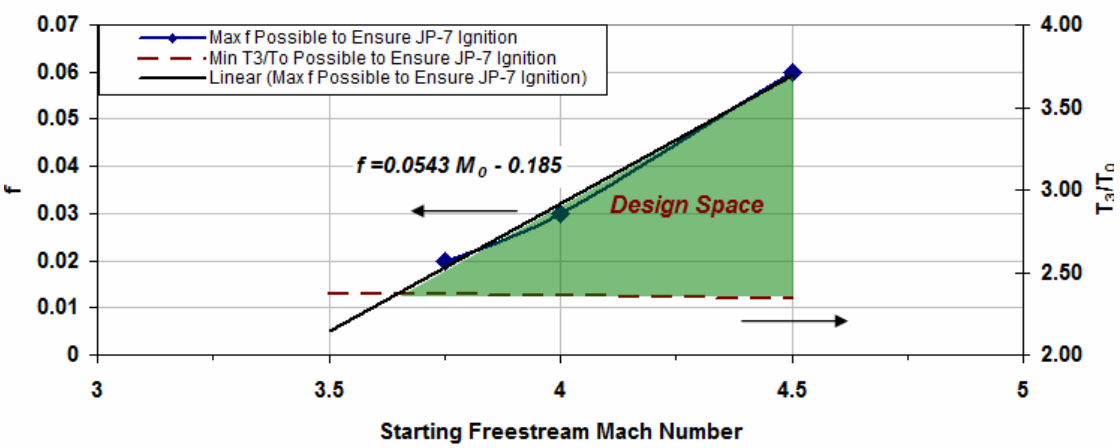

Figure 3.17: Design Space : Fuel-to-Air Ratio versus Starting Mach Number for JP-7 Fuel; Bounded by Minimum T_3/T_0 Necessary for JP-7 Ignition

It is evident in Figure 3.17 that the available design space does not extend down to Mach 3.50. Using Equation 3.26 above, assuming the trend continues linearly, the required fuel-to-air ratio for a scramjet to maintain supersonic combustion at Mach 3.50 would be 0.005. However, if this is entered into the one-dimensional stream thrust equations used for analysis, the combustor entrance temperature (T_3) is still just shy of the required ignition temperature for JP-7 fuel. Therefore, without fuel additives or another way of lowering the ignition temperature of JP-7, a scramjet with a starting Mach number of 3.50 is not possible, according to this one-dimensional flow analysis.

Therefore, as a starting Mach number of 3.50 cannot be accomplished, it is prudent to turn attention to what can. The design space suggests that the lowest possible starting Mach number lies approximately between Mach 3.50 and 3.75. By utilizing the stream thrust analysis equations iteratively, the minimum possible starting freestream Mach number for a scramjet using JP-7 fuel and no additives maintaining supersonic flow is found to be 3.65. Equation 3.26 yields a similar result with M_0=3.68.

However, at this lowest limit of the design space, there is relatively no room for error. To ensure that the engine does not transition to subsonic combustion, causing a normal shock wave to form in the combustor thereby choking the engine, and to ensure that JP-7 is actually ignited inside of the confines of the combustor, the starting freestream Mach number of the scramjet will be taken to be 4.00. Additionally, this starting Mach number has the ability to operate with a fuel-to-air ratio of 0.03, which is above the normally stated minimum lean value limit of 0.02 to maintain combustion.

3.4.3. Conclusion: Design Implications on a Lowered Starting Mach Number Scramjet

The analysis completed in this section has shown that the fuel-to-air ratio has a significant impact on the starting Mach number of a scramjet. By varying the fuel-to-air ratio with JP-7 fuel, the starting Mach number of a scramjet can be lowered from 4.30 to 3.68.

In summary, reducing the fuel-to-air ratio below the stoichiometric value allows for further reduction in starting Mach number beyond that achieved by the optimal selection of T_3/T_0 and fuel selection previously discussed in this chapter. However, it should be restated that there is a risk introduced when running an engine near the lean limit for combustion. It is also necessary to state that as the desired starting freestream Mach number is increased, the highest possible value for fuel-to-air ratio that can be used is also increased.

Additionally, the analysis completed in this section has shown that an approximately linear trend exists for the maximum value of *f* that can be used with JP-7

fuel while maintaining supersonic combustion and ensuring ignition for a given starting freestream Mach number.

Fuel-to-air ratio variation analysis was also completed for the several fuels that are often considered for scramjet applications for comparison purposes. The resulting design space for each of these fuels can be seen in Figure 3.18. It is evident from this figure that methane and hydrogen are not able to start at a freestream Mach number lower than 5.00. Also, it appears that octane, though performing slightly better than JP-7 in the fuel selection study at lowering the starting Mach number, cannot achieve a starting M_0=3.50 either, without additives. The individual design space plots for octane, methane, and hydrogen with a variation in fuel-to-air ratio can be found in Appendix B.

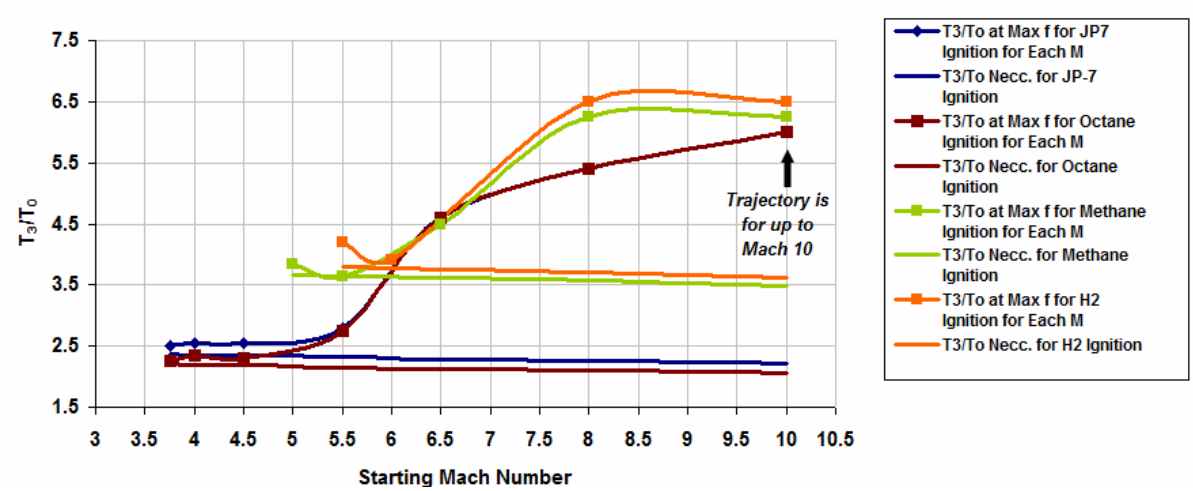

Figure 3.18: Design Space : T_3/T_0 versus Starting Mach Number for Various Fuels with Variation of Fuel-to-Air Ratio

The curve in Figure 3.19 below represents the starting Mach number at each fuel's stoichiometric fuel-to-air ratio; all of the analyzed fuels are included. The figure also shows the lowest possible starting M_0 for each fuel across each fuel's allowable equivalence ratio range for *f* in the form of deviation bars on the curve.

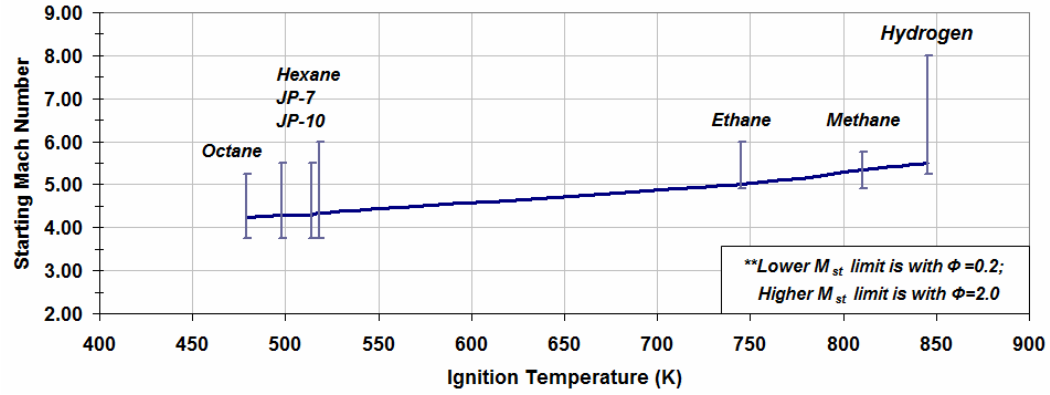

Figure 3.19: Starting Mach Number as a Function of Ignition Temperature and Fuel-to-Air Ratio

Figure 3.20 below further emphasizes the point. For the lean fuel-to-air ratio of 0.02, Equations 3.2 through 3.22 were repeatedly run for a range of T_3/T_0 at Mach 3.50. For each T_3/T_0, the maximum heat of reaction possible to keep the flow supersonic in the combustor was determined. The results were then plotted in Figure 3.20 below. A point for each fuel analyzed was plotted at the location where its h_{PR} and minimum T_3/T_0 for ignition intersected. It is evident from this figure that with the lowest fuel-to-air ratio possible, none of the fuels analyzed are able to start the scramjet at a freestream Mach number of 3.50.

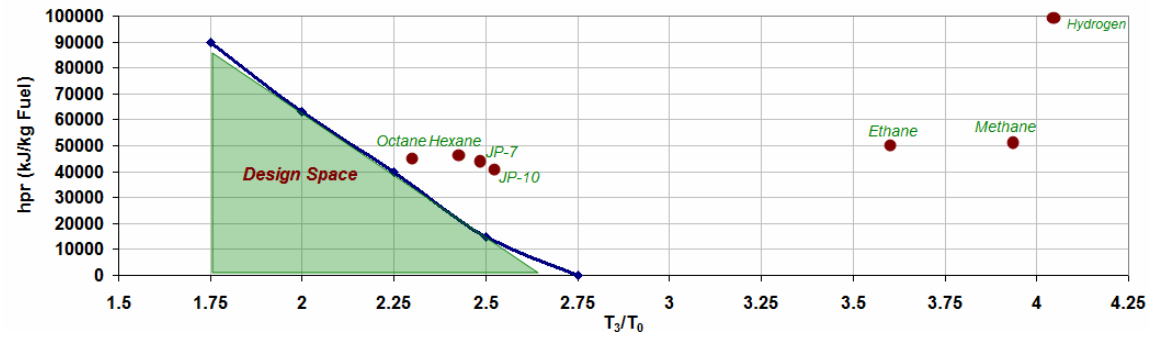

Figure 3.20: Design Space for Scramjet Start at Mach 3.50: Maximum h_{PR} to Maintain Supersonic Flow in the Combustor as a Function of T_3/T_0 with f=0.02

In conclusion, this section completed the investigation towards uncovering the lowest possible starting Mach number of a scramjet engine. With JP-7 fuel and no additives, a scramjet can start at a freestream Mach number of approximately 3.68. This is obviously not as low as the desired Mach 3.50 starting point; however, as it is often said, knowing the boundaries is half of the problem. The design of a scramjet with a starting Mach number of 4.00 is a realistic and readily applicable one, in addition to the fact that it is at least a Mach number below the lower end of the average range of starting Mach number scramjet designs, making it a worthwhile endeavor.

Although it is possible to use a value of f =0.03 at M_0=4.00, the value of 0.02 will be used in order to give more of a margin for the combustor entrance temperature to fluctuate and still ensure that ignition of JP-7 begins. A fuel-to-air ratio of 0.02 corresponds to an equivalence ratio of 0.3, which is above the minimum required equivalence ratio (0.2 to 2) for "combustion to occur within a useful timescale" [1]. Although it is near the lean limit for combustion, a value of f =0.02 allows T_3 to decrease by 19% and still ignite JP-7; however, with f =0.03, T_3 can only decrease 8% before reaching the lowest limit possible for JP-7 ignition. The final design parameters and the preliminary performance measures for the scramjet engine to be designed in Chapter 4 are shown below in Table 3.15.

Table 3.15: Final Key Design Parameters (Shown in Input Section in Table) and Preliminary Performance Measures

Input		
M_0	4	
V_0	1184.56	m/s
T_0	218.23	K
T_3/T_0	2.80	
f	0.02	
h_{pr}	43903.25	J/kg Fuel
Engine Performance Measures		
F/m_o	229.70	N-s/kgA
S	8.71E-05	kg F/s-N
I_{sp}	1170.75	s
n_o	0.31	
n_{th}	0.25	
n_p	1.24	
T_3	611.04	K
T_4	1134.52	K
T_{10}	697.11	K
M_3	1.51	
M_4	1.09	
M_{10}	2.69	

Comparing these results with those attained in Section 3.3, the overall efficiency has been raised 2%, the starting Mach number has been successfully lowered further to Mach 4.00, and the specific impulse has increased slightly. The visible drawback to lowering the fuel-to-air ratio can be seen in the large reduction in specific thrust by over 450 N-s/kgA.

3.5 Chapter Summary and Conclusions

In summary, this chapter discussed the theory necessary for one-dimensional hypersonic airbreathing engine performance analysis and detailed the equations for stream thrust analysis as the method of choice. This chapter also completed the analysis of the key design parameters—T_3/T_0, fuel selection, and the fuel-to-air ratio *f*—in detail. The goals of the chapter have been met, as it has been determined that:

- The impact of the driving design parameters for a scramjet all have a significant impact in lowering the starting Mach number;

- According to one-dimensional analysis, a scramjet with a starting Mach number of 3.50 is not feasible without fuel additives or another addition to the overall system;
- A scramjet with a starting Mach number of 4.00 is both practical and achievable currently.

Additionally, before the close of this chapter, it is worth noting that there are other possible ways of lowering the starting scramjet Mach number through additions to the system. A couple of these are listed here and briefly discussed.

- *Use of an ignition system.*

  Not preferred since it usually complicates the internal flow and increases drag. Also, it may not necessarily be helpful because it increases T_3, which, in turn, increases the starting Mach number.

- *Additives*.

  This concept was explored further, as many additives have been used in past systems such as SR-71, which used triethylborane (TEB) [19]. Silane has often been cited as a possible additive as well, in addition to many other chemicals. However, additives were not used in the analysis and design for this particular project for several reasons. It is difficult to calculate final ignition temperature of two fuels either mixed together or injected into the same airstream as this is normally

done experimentally. Also, Curran states that using "very energetic fuels or oxidizers" are "from an operational viewpoint…usually unacceptable" [2]. Additionally, discovering the starting Mach number boundaries for a scramjet engine without additives is important, as it gives a baseline for future investigations which may then reduce the starting Mach number even more. [See References 2, 9, 16, 18, 19, and 31 for more information on additives.]

With the key design parameters established, the next chapter will provide the theory necessary and the analysis completed for the design of the inlet compression system, combustor, and expansion system for a scramjet with a starting Mach number of 4.00 using JP-7 fuel.

CHAPTER 4

DESIGN OF A SCRAMJET WITH STARTING MACH NUMBER OF 4.00

The previous section concluded that a scramjet with a starting freestream Mach number of 4.00 is both currently feasible and worthwhile.

The scramjet will be designed to operate from Mach 4.00 to Mach 10, as shown in the trajectory diagram in Figure 3.4. Though Mach 3.50 would provide more of a margin, a Mach 4.00 starting scramjet is still a feasible choice, as a turbojet engine is capable of providing "thrust from takeoff up to a Mach of 3-4" [3]. Therefore, the benefits of having a lower starting Mach number scramjet would still be possible as a vehicle using this system would only require two propulsion systems, therefore reducing overall vehicle weight and complexity. Mach 10 is still used as the upper limit for the design of the flowpath as JP-7, a hydrocarbon fuel, will be used. Waltrup states that the "maximum freestream Mach number of a hydrocarbon-fueled scramjet-powered vehicle flying at 47.88 MN/m^2 trajectory would be between Mach 9 and 10" [7]. Therefore, in order to ascertain the overall vehicle performance of a Mach 4.00 starting scramjet across the entire possible performance range, Mach 10 is used as the upper limit of the flight path.

This chapter will detail the design process for the flowpath of a scramjet with a starting M_0=4.00, T_3/T_0=2.80, and f=0.02. The design process includes the design of the

compression system, isolator, combustion system, and expansion system. The theory and equations for each component's design in general are given in Section 4.1. The design process conducted for this project is detailed in Section 4.2.

4.1 Theory and Equations

This section will detail the theory and equations behind the design process conducted for each of the scramjet engine components: compression system, combustion system, and expansion system. They will be discussed in the order listed here, as designing the system in order of station components is not only intuitive, but makes the design process more straightforward.

4.1.1. Compression System and Inlet Design

The goal of the compression system in a scramjet engine is to "provide the desired cycle static temperature ratio (T_3/T_0) over the entire range of vehicle operation in a controllable and reliable manner with minimum aerodynamic losses (i.e., maximum compression efficiency or minimum entropy increase" [1]. This compression, for the one-dimensional analysis used throughout this project, relies on oblique shock waves. Normal shock wave compression is reserved for ramjets as it is able to offer "reasonable performance for $0 < M_0 < 3$," whereas for Mach numbers greater than 3, the "normal shock losses become unacceptably high and oblique shock compression becomes necessary" [1].

There are three options for the application of oblique shock waves in a scramjet, as listed and defined below [1].

1. *Internal Compression*—All oblique shock compression waves occur inside of the engine's inlet. This is difficult to design and complex flows are produced at off-design Mach numbers [1].
2. *External Compression*—All oblique shock compression waves occur outside of the engine's inlet, utilizing the vehicle's forebody. The waves generally focus on and terminate at the cowl lip [1].
3. *Mixed Internal and External Compression*—A mixture of internal and external oblique shock compression waves are used. Compared to external compression, this method has, in general, less of an entropy increase, but the overall length required for the shock system is greater [1]. This method "decouple[s] the engine cowl angle from the amount of compression and can result in a cowl that is parallel to the freestream flow" [1].

As an internal compression system is highly complex in design, the choice for this project is between an external compression system and a mixed internal and external compression system. The decision between these two options is generally based on practical integration issues. Since this project is a preliminary analysis based on one-dimensional flow and integration issues are not yet visible, mixed internal and external compression will be used as it allows for a cowl that is parallel to the freestream flow.

Before detailing the method of the compression system design, it should be noted that the compression system is important in the determination of the performance

of the overall engine, as the airflow which exits the compression system feeds directly into the burner. The following points illustrate the complexity of the compression system and provide a basis for which to start the theory.

- Compression systems seldom operate exactly at the design point; therefore, "extraneous oblique shock and expansion waves flourish" making it rare that "uniform and parallel exit flows" will ever be encountered [1]. This is especially true in vehicles with a large operating Mach number range.
- Viscous and boundary-layer effects lead to serious "two- and three-dimensional distortions of the relatively simple oblique shock and expansion wave-created flowfields" [1].
- Practical vehicle design requirements may "prevent the compression system from being either perfectly two-dimensional or axisymmetric" [1].

Therefore, due to the complex nature of flow in a compression system, CFD analysis or physical experiments are often needed [1]. However, for a preliminary study, an estimation will suffice. Therefore, the following assumptions are made for the compression system design process, as taken from Reference 1:

1. One-dimensional flow; boundary layer is represented only by its average effect on flow properties.
2. Air is represented as a calorically perfect gas.
3. Heat transfer to or from the wall will be neglected.

With these assumptions, the software tool HAP(GasTables) [1] can be used to calculate the performance of the resulting compression system. This tool accompanies the Reference 1 text and calculates the compression system's oblique shock wave configuration for the given number of oblique shock waves, the freestream Mach number, and the static cycle temperature ratio specified [1]. The output is the resulting properties at the exit of the compression system (Station 2), the required turning angle for each shock wave to turn the flow through to accomplish the overall required compression, the static pressure ratio, the adiabatic compression efficiency, and the kinetic energy efficiency [1, 20].

4.1.1.1. Inviscid Compression System Analysis

HAP(GasTables) works by calculating "special families" of hypersonic compression systems, which are "characterized by the cardinal number of oblique shock waves available to produce a specified cycle static temperature ratio at a specified Mach number" and in the cases when more than one shock wave is specified, "all oblique shock waves must provide equal amounts of geometric turning of the flow" [1]; the disadvantage is that the flow is not turned back to the axial direction. The compression sequence in this tool is assumed to begin at the leading edge of the vehicle [1].

A "special family" can be designed by using HAP(GasTables) for as many cases as necessary by inputting M_0, T_3/T_0, γ_c, and the number of desired oblique shock waves. The number of oblique shock waves has a direct impact on the compression efficiency (η_c); a good estimate of this correlation can be seen in Figure 4.1 below. It is from this figure that an educated guess can be made as to how many shock waves are necessary

based on the M_0, T_3/T_0, and the desired compression efficiency. It should be noted that the higher the number of oblique shock waves, the longer the compression system will be. Also, with more oblique shocks, more off-design complications will exist.

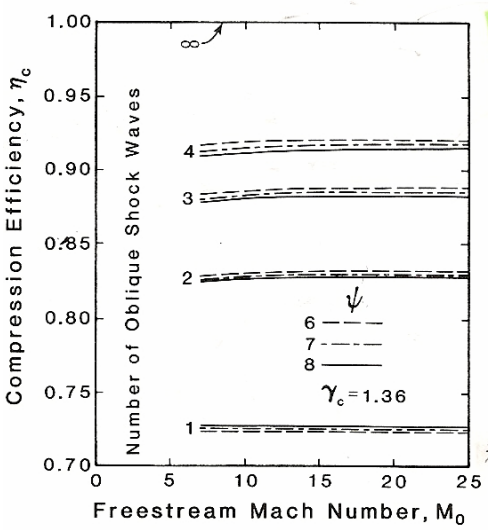

Figure 4.1: Adiabatic Compression Efficiency (η_c) Correlated to M_0 , T_3/T_0, and Number of Oblique Shock Waves [1]

With this information input into HAP(GasTables), the tool then calculates the properties of the flow (M, T/T_0, p/p_0, A/A_0, Pt/Pt_0, $(s-s_0)/C_p$) after each oblique shock wave using inviscid oblique shock theory. The compression component performance measures are calculated by the equations below, taken from Reference 1.

1. Total Pressure Ratio

$$\pi_c = \frac{p_{t3}}{p_{t0}} = \frac{p_3}{p_0}\left(\frac{1}{\varphi}\right)^{\gamma_c/(\gamma_c-1)} \tag{4.1}$$

where $\varphi = T_3/T_0$

2. Adiabatic Compression Efficiency

$$\eta_c = \frac{\varphi - \left(\frac{1}{\pi_c}\right)^{(\gamma_c - 1)/\gamma_c}}{\varphi - 1} \tag{4.2}$$

where $\varphi = T_3/T_0$

3. Kinetic Energy Efficiency

$$\eta_{KE} = 1 - \frac{2}{(\gamma_c - 1)M_0^2}\left\{\left(\frac{1}{\pi_c}\right)^{(\gamma_c - 1)/\gamma_c} - 1\right\} \tag{4.3}$$

4. Dimensionless Entropy Increase

$$\frac{s_3 - s_0}{C_{pc}} = \frac{\gamma_c - 1}{\gamma_c}\ln\frac{1}{\pi_c} \tag{4.4}$$

It is from these performance measures that the determination can be made on whether the resulting compression system of oblique shocks will suffice, or rather HAP(GasTables) should be run again until the best compression system is designed. With these equations specified, it is now possible to decipher whether friction can indeed be neglected in these calculations, as assumed previously, or whether its impact will significantly alter performance values.

4.1.1.2. Boundary Layer Friction Influence on Compression System Analysis

In the first assumption listed earlier for the compression design process, it is stated that the "boundary layer is represented only by its average effect on flow properties" [1]. However, in order to determine whether this is a fair assumption to make, the inviscid flow results should be compared to results obtained from calculations of the influence of the boundary-layer friction. Therefore, a two-step process is

implemented. In Step 1, the inviscid flow calculations as described in the previous subsection for results at Station 2 are completed for the design point. Then, Step 2 is the calculation of the same flow parameters with boundary layer friction effects included. The comparison of the two results then makes it possible to obtain an estimate of the influence of boundary layer friction.

The equations necessary to calculate the performance of the compression system with the boundary-layer friction effects included (Step 2) as well as the equations for the resulting compression system exit values are shown below, as taken from Reference 1 and adapted slightly. The assumption is made of a shock-free isolator; therefore no shock waves will exist in the isolator and the flow will not be altered between Stations 2 and 3. In other words, it is assumed that the Station 2 flow property values are equivalent to the Station 3 flow property values for this test of the influence of boundary layer friction. If a shock-free isolator is later determined to not be possible, then the analysis of the effect of boundary layer friction would be repeated. This method maintains the one-dimensional approach used throughout this project, and although the boundary-layer flowfield is inherently two- or three-dimensional, it calculates the overall effects qualitatively [1]. Figure 4.2 below displays the analytical model for the equations following it, where Station 3 in the figure is equivalent to Station 2 in the equations.

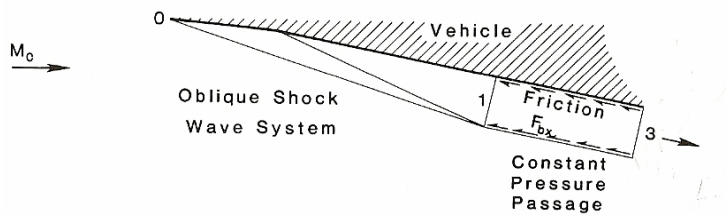

Figure 4.2: Conceptual and Analytical Model to Estimate the Boundary Layer Friction Influence [1]

1. Static Pressure Ratio: Station 1 to Freestream

$$\frac{p_1}{p_0} = \left\{ \frac{\varphi_1}{\varphi_1(1-\eta_1)+\eta_1} \right\}^{\gamma_c/(\gamma_c-1)} \tag{4.5}$$

2. Static Temperature Ratio: Station 1 to Freestream

$$\varphi_1 = \frac{T_1}{T_0} = 1 + \frac{\gamma_c - 1}{2} M_0^2 \left\{ 1 - \left[1 + \frac{C_f}{2} \cdot \frac{A_w}{A_3} \right]^2 \left[1 + \frac{2(1-\varphi)}{(\gamma_c - 1) M_0^2} \right] \right\} \tag{4.6}$$

3. Adiabatic Compression Efficiency at Station 1

$$\eta_1 = \eta_c \left(\frac{1 - \frac{1}{\varphi}}{1 - \frac{1}{\varphi_1}} \right) \tag{4.7}$$

4. Pressure at Inlet Compression System Exit (Station 2)

$$p_2 = p_0 \left(\frac{p_1}{p_0} \right) \tag{4.8}$$

5. Temperature at Inlet Compression System Exit (Station 2)

$$T_2 = T_0 \left(\frac{T_1}{T_0} \right) \tag{4.9}$$

6. Velocity at Inlet Compression System Exit (Station 2)

$$V_2 = \sqrt{V_0^2 - 2C_{pc}T_0(\varphi - 1)} \tag{4.9}$$

7. Mach Number at Inlet Compression System Exit (Station 2)

$$M_2 = \frac{V_2}{\sqrt{\gamma_c RT_2}} \tag{4.10}$$

If it is determined that the effect of boundary layer friction has less than a 5% effect on overall flow properties at Station 2, then it is safe to assume for this analysis that boundary layer friction can be neglected and the inviscid calculations of HAP(GasTables) can be used to design the compression system.

The application of the two-step process for determining the effect of boundary layer friction can be seen in Section 4.2.1. Additionally, the design of the compression system will be completed in that section. The following subsection, 4.1.2, will detail the theory and equations needed for the design of the next component in the scramjet flowpath—the combustion system.

4.1.2. Combustion System Design

Weber and McKay stated in 1958 that there are many practical problems of employing supersonic combustion [1, 21]. Though many of these been advanced since 1958, Weber and McKay's summary description of supersonic combustion applies even today: "It is necessary to capture a stream tube of supersonic air, inject fuel, achieve a fairly uniform mixture of fuel and air, and carry out the combustion process—all within a reasonable length, and preferably without causing a normal shock within the engine" [1, 21]. The inlet compression system for capturing the stream tube of supersonic air has

been accomplished by using the methods detailed in the previous section, the application and results of which can be found in Section 4.2.1. It is now possible to detail the method for the design of the combustion system which will inject fuel into the supersonic air and carry out the combustion process. The theory and equations necessary to design the burner will be detailed in this section.

In order to begin the theory behind designing a burner for a scramjet, it is first necessary to define the axial locations of the geometry that will be dealt with. Corresponding to Figure 2.1, Figure 4.3 below displays the details of the combustion system station designations.

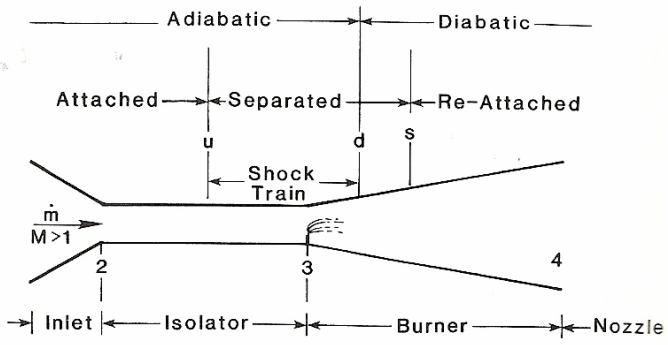

Figure 4.3: Combustion System Station Designations [1]

As depicted in Figure 4.3, Station 2 is the entrance to the isolator, Station 3 is the entrance to the burner, and Station 4 is the exit from the burner and entrance to the expansion nozzle. Stations *u* and *d* are the upstream and downstream limits of a "positive or adverse axial pressure gradient, respectively" [1]. Station *s* is the upstream limit of the "negative or favorable pressure gradient which extends through the

remainder of the burner and right on through the expansion system" [1] and is also the location of the lowest Mach number in the entire combustion system [1].

The combustion system design method includes two main components for its analysis: the isolator and the burner. The isolator is generally considered to be a part of the compression system, but it is included here in the design of the combustion system due to the important role the isolator design plays on the combustion system design. The primary function of the isolator is to prevent inlet unstart, by "providing sufficient additional adiabatic compression above its entry pressure p_2 to match or support whatever back pressure p_3 the burner may impress upon it" [1]. The isolator does not have a direct interaction with the flow in the burner unless there is flow separation caused by "thermal occlusion unrelieved by area expansion" [1], causing a back pressure on the isolator. The burner is the active component of the combustion system which injects the airflow with fuel, ensures adequate time for mixing and ignition, and passes off the resulting flow to the expansion system to generate thrust.

With the component station designations defined, it is now possible to give attention to the theory and equations necessary for designing the combustion system for a scramjet with a starting Mach number of 4.00. One-dimensional flow analysis will also be employed for the combustion system by utilizing the Design tool of the HAP(Burner) code [1, 20]. A brief description of the logic and equations contained within the software will be described here. All equations in this section are taken directly from Reference 1, in which the authors point to Shapiro [22, 29] as their key reference.

Frictionless flow with heat addition, but without mass addition, is assumed in this method [1]. The following equation is solved by a fourth-order Runge-Kutta method in HAP(Burner):

$$\frac{dM}{dx} = M\left(\frac{1+\frac{\gamma_b - 1}{2}M^2}{1-M^2}\right)\left\{-\left(\frac{1}{A}\frac{dA}{dx}\right)+\frac{\left(1+\gamma_b M^2\right)}{2}\left(\frac{1}{T_t}\frac{dT_t}{dx}\right)\right\} \tag{4.11}$$

Starting from burner entry, Equation 4.11 is numerically integrated for M(x) along the burner axis until the burner exit, assuming a change in cross-sectional area *dA* and a change in total temperature T_t due to heat addition [1]. According to Heiser and Pratt [1], there are only a few closed form, integral solutions known to exist for this equation. Therefore, numerical methods are necessary to solve it; hence the use of Runge-Kutta. In Equation 4.11, *A(x)* and $T_t(x)$ are the independent variables; the sole dependent variable is M, influenced by the coefficients of *A(x)* and $T_t(x)$ [1]. *A(x)* is defined by the needs pertaining to the engine design, which may be determined from iteration until the necessary measures are reached. $T_t(x)$ is not as easily determined, but can be "usefully represented in nondimensional form by a rational function" [1] as shown in Equation 4.12 below.

$$\tau(x) = 1 + \left(\tau_b - 1\right)\left\{\frac{\theta\chi}{1+(\theta-1)\chi}\right\}, \theta \geq 1 \tag{4.12}$$

$$\textit{where } \tau(x) \equiv T_t\left(x\right)\Big/T_{t2}$$

$$\chi \equiv \left(x - x_i\right)/\left(x_4 - x_i\right);$$

x_i=axial location where heat addition begins;
i=u when isolator is shock-free, otherwise i=d;

$$\tau_b = T_{t4} \Big/ T_{t2};$$

and θ*=empirical constant of order 1 to 10 depending on mode of fuel injection and fuel-air mixing.*

Using this equation, $T_t(x)$ can be systematically varied to determine the effect on burner performance [1].

This method works as long as M(x) remains well above the critical (sonic) value of 1 in the burner [1] and records the intermediate values of M(x) as the solution is stepped through axially, thus it is able to display M(x) along the burner axis [1]. The HAP(Burner) Design tool records the axial x location of each iteration and the corresponding values of the following variables at that location: A/A_2, T_t/T_{t2}, M, p/p_2, p/p_{t2}, A_c/A, Φ, u/u_2, T/T_2, p_t/p_{t2}, H, and K. The equations for the remaining necessary flow variables can be calculated from Equations 4.13 through 4.19 below. Again, all equations in this section are taken directly from Reference 1.

$$T(x) = T_2 \cdot \frac{T_t(x)}{T_{t2}} \left[\frac{1 + \left(\frac{\gamma_b - 1}{2} \right) M_2^2}{1 + \left(\frac{\gamma_b - 1}{2} \right) M^2(x)} \right], \theta \geq 1 \tag{4.13}$$

$$p(x) = p_2 \cdot \frac{A_2}{A_c(x)} \cdot \frac{M_2}{M(x)} \sqrt{\frac{T(x)}{T_2}} \tag{4.14}$$

$$P_t(x) = P_{t2} \cdot \frac{p(x)}{p_2} \left[\frac{T_2}{T(x)} \frac{T_t(x)}{T_{t2}} \right]^{\gamma_b/(\gamma_b - 1)} \tag{4.15}$$

$$u(x) = u_2 \cdot \frac{M(x)}{M_2} \sqrt{\frac{T(x)}{T_2}} \tag{4.16}$$

$$H(x) = \frac{T(x)}{T_{t2}} \tag{4.17}$$

$$K(x) = \left(\frac{\gamma_b - 1}{2}\right) M(x)^2 H(x) \tag{4.18}$$

$$\Phi = \left(\frac{\gamma_b - 1}{\gamma_b}\right) \frac{A}{A_c} \frac{H}{\sqrt{2K}} + \sqrt{2K} \tag{4.19}$$

As previously stated in Chapter 3, the burner for the current scramjet project will be designed for constant pressure. For a frictionless constant-pressure burner, Equations 4.20 and 4.21 below provide the axial variation of Mach number and area distribution for a given $T_t(x)$, as taken from Reference 1. The constant-pressure burner is designed for the design point case (M_0=4.00); however, the off-design cases will experience a small pressure loss in the burner as they are operating at Mach numbers higher than the design point. All symbols and abbreviations are defined in the section of the same name at the beginning of this paper.

$$M(x) = \frac{M_3}{\sqrt{\tau(x)\left(1 + \frac{\gamma_b - 1}{2} M_3^2\right) - \left(\frac{\gamma_b - 1}{2}\right) M_3^2}} \tag{4.20}$$

$$A(x) = A_3 \left[\tau(x)\left(1 + \frac{\gamma_b - 1}{2} M_3^2\right) - \left(\frac{\gamma_b - 1}{2}\right) M_3^2 \right] \tag{4.21}$$

The final portion of theory for the design of a scramjet combustion system is in the analysis pertaining to the interaction between the isolator and burner. For the constant-pressure burner, there are two possibilities for the isolator-burner interaction.

- *Scramjet with shock-free isolator.* In this case, there is no pressure feedback from the burner to the isolator, assuming frictionless flow [1]. Therefore, there is no interaction between the two components as a shock system is not needed in the isolator to equalize backpressure from the burner. This is the least complex, and therefore, optimal design.
- *Scramjet with oblique shock train.* In this system, there is a pressure feedback from the burner which is kept from propagating upstream to the inlet, thereby inlet unstart is prevented, by an oblique shock train in the isolator.

As previously stated, the above equations are employed through the use of the Design tool in the HAP(Burner) software [1]. The application of this tool to design the combustion system will be described in Section 4.2.2.

4.1.3. Expansion System Design

As Heiser and Pratt state, "The function of the expansion component is to produce thrust" [1]. The expansion system begins at Station 4 and ends at Station 10, where, ideally, $p_{10}/p_0=1$. However, scramjet expansion systems often operate underexpanded, that is $p_{10}/p_0>1$, while some operate overexpanded, where $p_{10}/p_0<1$ [1]. Operating underexpanded provides a benefit by decreasing the overall length of the expansion system, thereby decreasing the overall length of the engine.

Despite the fact that the exhaust flow is far from one-dimensional, it can still be approximated to a degree through one-dimensional analysis, as much of the flow

leaving the engine lies in the axial direction [1]. Additionally, as the goal of the current study is to lower the starting Mach number of a scramjet, the expansion system is not the primary component of interest since it is not a principal determinant of the starting freestream Mach number of the engine.

In the design of the expansion system, an ideal nozzle (p_{10}/p_0=1) is assumed for the Mach 4.00 on-design condition as well as for the off-design conditions for comparison purposes of the resulting performance characteristics. Therefore, the assumption is effectively that of a variable geometry expansion system. Such a system is not a practical one; however, as Figure 4.4 below shows, whether or not the nozzle is designed practically (that is, a non-ideal, non-variable nozzle) does not make a large difference in the overall performance for the one-dimensional case, as the curve begins to level off early in the expansion process. Heiser and Pratt state that a "partial expansion can indeed recover most of the available thrust" [1].

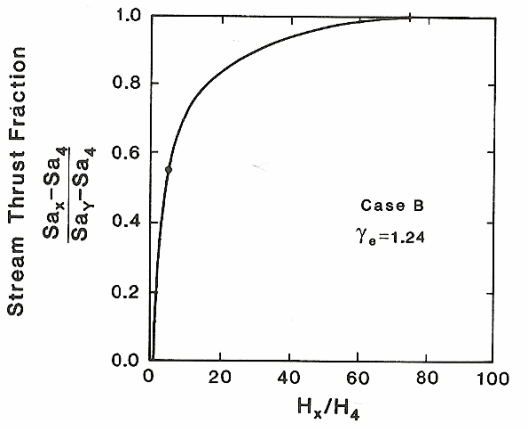

Figure 4.4: Stream Thrust Fraction as a Function of Local Height to Entry Height of the Expansion System [1]

With this assumption in place, the expansion system is calculated and thereby designed for each Mach number with the one-dimensional flow analysis equations as a Single Expansion Ramp Nozzle (SERN) [30]. These equations are used for the expansion component, with the results from HAP(Burner) for the flow parameters at Station 4 for each Mach number used as input. This procedure uses Equations 3.12-3.15 and will be described in Section 4.2.3.

4.2 Design Process

With the theory and equations detailed in the previous section, the design process for a scramjet with a starting freestream Mach number of 4.00 can now be completed. The following subsections will detail the process and resulting design for each of the scramjet components: compression system and inlet, combustion system, and expansion system.

4.2.1. Compression System and Inlet Design

This section will apply the theory discussed in Section 4.1.1. As discussed in that section, using HAP(GasTables) as the tool for calculating the compression system characteristics involves making the assumption of no boundary layer friction. However, as was also discussed in Section 4.1.1, in order to determine whether this assumption can be made without a large impact on the outcome, the calculation of the results with boundary layer friction must be compared to the inviscid results determined from HAP(GasTables) by virtue of a two-step process that compares the flow properties resulting from each method for the design case. Reference 1 states that the range for the dimensionless boundary layer skin friction quantity—$(C_f/2)(A_w/A_3)$—is approximately

0.01 to 0.05, with the "most likely value" being 0.02 [1]. Therefore, using the value of 0.02, the two-step comparison returned a maximum difference of only 2.9% across the Station 2 flow properties in comparison to the inviscid results. This is consistent with the statement made by Heiser and Pratt that "boundary-layer friction should do little to diminish overall scramjet performance for freestream Mach numbers up to about 10 or 15" [1]. Thus, the compression system calculations for the design of the scramjet with a starting Mach number of 4.00 are completed with the HAP(GasTables) inviscid oblique shock wave tool.

The input values to begin the design process of the compression system must be determined first. The values of M_0 and T_3/T_0 were determined as a result of the analysis in Chapter 3. The value of γ_c is a constant also used in Chapter 3. The number of oblique shocks is the only remaining design constraint which must be determined, and can be found by analyzing Figure 4.1. As the general rule of thumb assumption for η_c is 0.90 [1], it is evident from the figure that achieving at least this efficiency with a T_3/T_0=2.80 requires at least three oblique shock waves. HAP(GasTables) has been run for both the three and four oblique shock wave cases. These results can be seen below in Table 4.1 and 4.2, respectively.

Table 4.1: Results of Inviscid Compression System Design with Three Oblique Shocks

Input							
M_0	4						
T_3/T_0	2.8						
Number of OS	3						
γ_c	1.362						
Flow Properties to Determine Station 2 Values			Resulting Compression System Properties				
p_0	4275	Pa	delta	16.9499	deg		
T_0	218.22	K	$p_{t3}/p_{t0}=\pi_c$	0.6111			
C_{pc}	1090	J/kgK	n_c	0.9223			
V_0	1184.56	m/s	n_{ke}	0.9517			
Flow Properties After Each Oblique Shock							
O.S. Number	M	T/T_0	p/p_0	A/A_0	p_t/p_{t0}	$(s-s_0)/C_p$	
1	2.8551	1.5739	4.1260	0.4260	0.7489	0.0768	
2	2.0903	2.1755	12.2165	0.2310	0.6560	0.1120	
3	1.4706	2.8000	29.4134	0.1547	0.6111	0.1309	
Flow Properties at Compression System Exit							
		p_2	125742.285	Pa			
		T_2	611.016	K			
		V_2	739.518163	m/s			
		M_2	1.4706				

Table 4.2: Results of Inviscid Compression System Design with Four Oblique Shocks

Input							
M_0	4						
T_3/T_0	2.8						
Number of OS	4						
γ_c	1.362						
Flow Properties to Determine Station 2 Values			Resulting Compression System Properties				
p_0	4275	Pa	delta	13.3082	deg		
T_0	218.22	K	$p_{t3}/p_{t0}=\pi_c$	0.721			
C_{pc}	1090	J/kgK	n_c	0.9495			
V_0	1184.56	m/s	n_{ke}	0.9686			
Flow Properties After Each Oblique Shock							
O.S. Number	M	T/T_0	p/p_0	A/A_0	p_t/p_{t0}	$(s-s_0)/C_p$	
1	3.1063	1.4186	3.1775	0.4827	0.8526	0.0424	
2	2.4565	1.8622	8.1162	0.2738	0.7824	0.0652	
3	1.9350	2.3222	17.7187	0.1778	0.7443	0.0785	
4	1.4706	2.8000	34.6985	0.1312	0.7210	0.0870	
Flow Properties at Compression System Exit							
		p_2	148336.0875	Pa			
		T_2	611.016	K			
		V_2	739.5181631	m/s			
		M_2	1.4706				

As can be seen in the comparison of the above two tables, the four-shock system has overall better results. There is less pressure loss, as evidenced by the 0.11 increase in π_c, and in the fact that the compression efficiency is nearly 3% higher than the three-shock system. Therefore, the four-shock system will be used as the final compression

system design, with the first three shocks taking place external to the engine and the final shock occurring just inside of the engine to turn the flow upward a value of delta, to bring it closer to parallel to the axial direction. A shock cancellation surface will be required inside the engine. With this compression system design, the updated performance parameters are shown in Table 4.3.

Table 4.3: Preliminary Performance Results for M_0 = 4.00 Scramjet Following Compression System Design

Input		
M_0	4	
V_0	1184.56	m/s
T_0	218.23	K
T_3/T_0	2.80	
f	0.02	
h_{pr}	43903.25	kJ/kg Fuel
Engine Performance Measures		
F/m_o	262.98	N-s/kgA
S	7.61E-05	kg F/s-N
I_{sp}	1340.39	s
n_o	0.35	
n_{th}	0.31	
n_p	1.16	
T_3	611.04	K
T_4	1134.52	K
T_{10}	664.95	K
M_3	1.51	
M_4	1.09	
M_{10}	2.83	

The results found for Station 2 as displayed in Table 4.2 will be the required input for the combustion system design in the next subsection.

4.2.2. Combustion System Design

This section will apply the theory discussed in Section 4.1.2. As discussed in that section, the Design option of HAP(Burner) will be used as the tool for the design of the combustion system. The required inputs for this program are: the state and Mach number of air entering the combustion system (M_2, T_2, u_2, p_2, R_b, γ_c), the length and

divergence angle of a planar combustor geometry (x, A/A_2, θ/H, H) and an estimate of axial distribution of total temperature (θ, x_i, $\eta_b f h_{PR}$) [20]. The program then determines "whether or not a solution is possible for the given inputs, and if possible, calculates the axial variation of static and total properties within the combustion system, including effects of internal flow separation and choking due to thermal occlusion" [20].

The source and/or method for determining the inputs required for the program will be discussed in turn below.

- *State and Mach Number of Air Entering the Combustion System (M_2, T_2, u_2, p_2, R_b, γ_c).* The quantities required from Station 2 are determined from the compression system design in the preceding subsection. These are shown in the bottom rows of Table 4.2. The values of R for the burner and γ for the compression system are constants, and can be found in Table 4.4.
- *Length and divergence angle of a planar combustor geometry (x, A/A_2, θ/H, H).* The default values for x that are in HAP(Burner) are used. After the design is complete, the default x values are then added to the length of the compression system, thereby keeping the same axial variation in the combustion system. H is kept at the default value unless changes are needed during the process. A/A_2 and θ/H are varied systematically to determine the necessary values to keep the pressure constant in the burner and to provide for the necessary Station 3 and 4 values.

- *Estimate of axial distribution of total temperature (θ, x_i, $\eta_b f h_{PR}$).*

  The value of θ is varied systematically to determine the necessary value to keep the pressure constant in the burner and to provide for the necessary Station 3 and 4 values. The value of x_i is assumed to occur at the burner entrance, and therefore the default value of x_i is used. The value of $\eta_b f h_{PR}$ is a constant, defined by the product of the burner efficiency, fuel-to-air ratio of 0.02, and the heat of reaction of JP-7. The burner efficiency is assumed at 0.90 as Reference 1 assumes.

The values that will serve as the desired result for Stations 3 and 4 during this process can be determined from dividing the values of pressure, temperature, and velocity at Stations 3 and 4 (determined by the preliminary results of the one-dimensional flow equations) by the corresponding values of the same at Station 2. These results, as well as M_3 and M_4 can then be compared to the results produced by HAP(Burner) for the same parameters; the systematically varied parameters of A/A_2, θ, and θ/H can be adjusted accordingly until the results are roughly equivalent. The flow parameters for Stations 3 and 4 are determined from the results of applying Equations 3.2 through 3.22 in the spreadsheet built for this project with the same input as detailed in Chapter 3, except for η_c which is now 0.9495, due to the design of the compression system in the previous subsection. Table 4.4 summarizes the input values used in the HAP(Burner) code. Table 4.5 shows the desired Station 3 and 4 values which are used as the goal as the program is repeated. Note that the values of p_3/p_2 and p_4/p_2 are equal, as an ideal constant-pressure burner should have.

Table 4.4: Input Values for the HAP(Burner) Program for Combustion System Design

Flow Properties at Station 2		
M_2	1.47	
T_2	611.02	K
V_2	739.52	m/s
p_2	148.3361	kPa
R_b	289.30	J/kg-K
γ_c	1.238	
Isolator/Combustor Geometry		
x(2, 3, 3p, 4)	(0, 0.914, 0.914, 1.829)	m
A/A_2(2, 3, 3p, 4)	(1, 1, 1, 1.8-2.5)	
θ/H	Vary: 0.01-0.03	
H	0.152	m
Axial Heat Addition Parameters		
θ	Vary: 1 to 10	
x_i	0.914	m
$\eta_b fh_{PR}$	790.263	kJ/kg

Table 4.5: Station 3 and 4 Flow Parameters: Serves as Check for Desired Output from HAP(Burner)

	M	p/p_2	u/u_2	T/T_2
Station 3	1.51	1.005	1.0000	1.0000
Station 4	1.09	1.005	0.9411	1.8568

Therefore, with the inputs as listed in Table 4.4, HAP(Burner) is ran repeatedly until the values shown in Table 4.5 are met or matched as closely as possible and a shock-free isolator system is obtained, if possible. This process was done eleven times before all parameters were matched as closely as possible. The result includes a shock-free isolator. Table 4.6 below shows the final Station 3 and 4 flow parameters which are comparable to the desired results shown in Table 4.5.

Table 4.6: Final Station 3 and 4 Flow Parameters

	M	p/p_2	u/u_2	T/T_2
Station 3	1.581	1.000	1.0000	1.0000
Station 4	1.16	1.000	1.0000	1.8590

The iterations included four variations of the three-shock compression system shown in Table 4.1; the rest of the variations were done with the four-shock system which was selected in the previous subsection as the compression system of choice. The three-shock compression system was varied here to ensure that the four-shock system was indeed the best selection. It is important that the burner design code is run before deciding on a final compression system to ensure that the required burner results can be obtained with the compression system selected. The final parameters of the combustion system designed are listed in Table 4.7 below.

Table 4.7: Final Parameters of Combustion System Design at Design Point of M_0=4.00

Flow Properties of Burner		
M_3	1.58	
T_3	611.02	K
V_3	739.52	m/s
p_3	148.3064	kPa
M_4	1.16	
T_4	1135.88	K
V_4	739.52	m/s
p_4	148.2471	kPa
Isolator/Combustor Geometry		
x(2, 3, 3p, 4)	(0, 0.914, 0.914, 1.829)	m
A/A_2(2, 3, 3p, 4)	(1, 1, 1, 1.86)	
θ/H	0.03	
H	0.152	m
Axial Heat Addition Parameters		
θ	1	
x_i	0.914	m
$\eta_b f h_{PR}$	790.263	kJ/kg
Isolator-Burner Interaction		
Shock-Free Isolator		

The results found for Station 4 as displayed in Table 4.7 will be the required input for the expansion system design in the next subsection.

4.2.3. Expansion System Design

This section will apply the theory discussed in Section 4.1.3. As discussed in that section, the expansion system will be designed for each Mach number by using the

one-dimensional flow analysis equations for the expansion component with the ideal expansion assumption of p_{10}/p_0=1. A Single Expansion Ramp Nozzle (SERN) is used with an assumed expansion angle value of 20 degrees [30].

This analysis utilizes Equations 3.12-3.15, with the results from HAP(Burner) for the flow parameters at Station 4 for each Mach number used as input. The resulting performance is then determined, as before, using Equations 3.16-3.22.

The method to determine the expansion system values is to change the input sources for M_4, T_4, V_4, and p_4 in Equations 3.12-3.15 (expansion component equations) to the actual HAP(Burner) output instead of using the results of Equations 3.8-3.11 (combustor component equations) in the spreadsheet described previously which calculates the one-dimensional flow analysis. The result is output that includes the results of the design of the compression and combustion systems which is used for the design of the expansion component and in the calculation of the overall engine exit parameters. The two-dimensional schematic illustrating the resulting expansion system can be found in the next section as a part of the overall scramjet design schematic. Chapter 5 will detail the performance of the final scramjet, for both on- and off-design conditions; the expansion system output values can be seen in Table 5.2 in that chapter for the on-design case designed here.

4.3 Scramjet Engine Design with a Freestream Starting Mach Number of 4.00

This chapter has succeeded in designing the flowpath for a scramjet with a freestream starting Mach number of 4.00. The starting Mach number also serves as the

on-design case for the engine flowpath as it is the limiting operation Mach number. This section will integrate the three components of the scramjet engine.

There are three steps required to determine the planar, two-dimensional schematic of the scramjet flowpath. These are explained in turn below.

1. *Inlet Compression System Height and Length.*

Determining the height of the compression system as it varies axially is found by using two equations. Before these two equations are discussed, however, please refer to Figure 4.5 for the coordinate axes convention utilized for all ensuing equations and calculations.

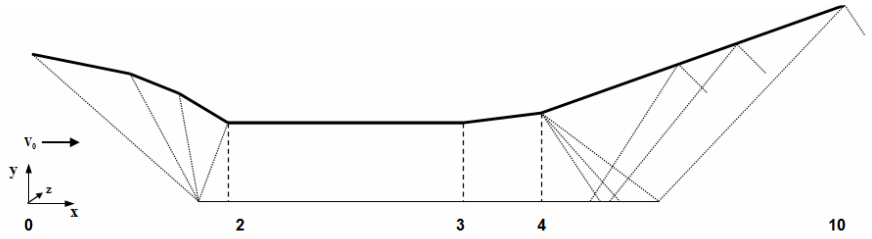

Figure 4.5: Coordinate Axes Convention for Scramjet Engine Designed

With this convention in place, it is possible now to display the equations used for calculating the height *h* along the y-axis as it varies axially, that is, along the x-axis.

$$h_n = \frac{A_n}{A_2}(h_2) \tag{4.22}$$

where n = point on the x-axis;
A = area.

Equation 4.22 is valid when the depth into the page (*d)* is constant for the length between two given station numbers. In other words, it is valid when $d_2 = d_n$ along the z-axis due to the following:

For $\frac{A_n}{A_2} = \frac{h_n d_n}{h_2 d_2}$,

when $d_2 = d_n$,

$$\frac{A_n}{A_2} = \frac{h_n}{h_2} \tag{4.23}$$

Therefore, using Equation 4.22, it is possible to calculate the height of the inlet at any given point along the compression system if the ratio of the area at that point to the area at the beginning of the isolator (A_n/A_2) is known.

In the design of the inlet compression system, an output parameter produced by HAP(GasTables) is the area ratio of the area after each oblique shock to the inlet area at Station 0 (A_n/A_0). This information can be used to generate A_n/A_2 after each oblique shock using Equation 4.24 below.

$$\frac{A_n}{A_2} = \frac{A_n / A_0}{A_2 / A_0} \tag{4.24}$$

With the value of A_n/A_2 determined, the height of the compression system as it varies axially can therefore be determined by using Equation 4.22 above and the value of h_2, which is equal to 0.152 m, a value determined during the combustor design process.

The determination of the compression system length is an approximation using simple geometry and the properties of the compression system as depicted in Figure 4.6.

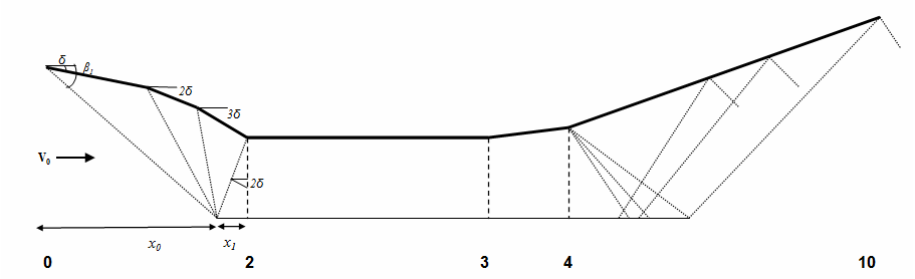

Figure 4.6: Conceptual Diagram of Four Oblique Shock System for Scramjet

The first three oblique shocks converge on the cowl lip of the engine, as seen in Figure 4.6 above. The value of x_0 as depicted in the figure provides a good estimation of the length of the first three oblique shocks at M_0=4.00 using Equation 4.25.

$$x_0 = h_0 \tan(90 - \beta_1) \tag{4.25}$$

where β_1 = wave angle of first oblique shock;

h_0 = height of engine inlet.

In order to find the best estimate of the length of the compression system, the length covered by the fourth and last oblique shock must be determined. This is done by Equation 4.26 below.

$$x_1 = \frac{h_0}{\sin \delta} \tag{4.26}$$

where δ = degrees each oblique shock turns flow through

Once x_0 and x_1 have been determined, the total estimated length of the compression system can be determined by summing these two values. The axial distance after each shock wave along the flowpath can then be determined by simple geometry, using the results for the height as described above.

Performing the necessary calculations for both the height and length of the compression system, the data in Table 4.8 is obtained.

Table 4.8: Inlet Compression System Axial Height and Length for a Design Point of Mach 4.00

i	x (m)	A/A_2	h (m)
0	0.000	7.622	1.159
0a, after OS 1	2.534	3.679	0.559
0b, after OS 2	3.017	2.087	0.317
0c, after OS 3	3.149	1.355	0.206
0d, after OS 4	3.190	1.000	0.152

Plotting the height as a function of axial location shows the two-dimensional view of the scramjet's inlet compression system.

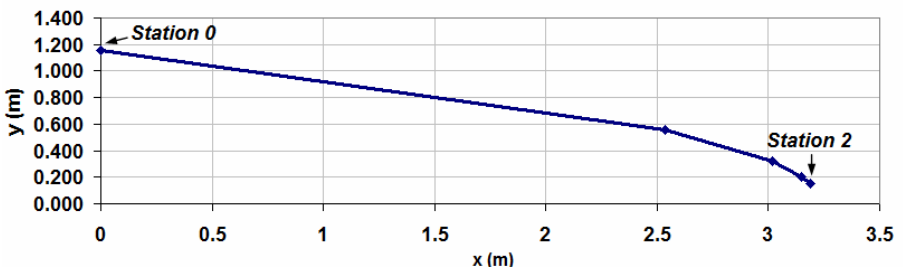

Figure 4.7: Inlet Compression System Two-Dimensional Schematic for a Design Point of Mach 4.00

2. *Combustion System Height and Length.*

The calculation of the height of the combustion system is performed using Equation 4.22 of the compression system method detailed above with the assumption contained in Equation 4.23. In the design of the combustion system, the HAP(Burner) program produced A_n/A_2 as part of the output for the designed combustion system. Therefore, as the value of A_n/A_2 is already determined, the height of the combustion system as it varies axially can therefore be determined by using Equation 4.22 above with the value of h_2=0.152m.

The coordinates defining the length of the combustion system are found by adding the total length of the compression system to the x-axis location of each iteration generated in the output of HAP(Burner) during the design of the combustor.

Performing the necessary calculations for both the height and length of the combustion system, the data in Table 4.9 is obtained.

Table 4.9: Combustion System Axial Height and Length for a Design Point of Mach 4.00

i	x (m)	A/A_2	h (m)	x(m) shifted to beginning of engine
Station 2 (Isolator)	0.000	1.000	0.152	2.678
Station 3a, u	0.914	1.000	0.152	3.592
Station 3b, u,s	0.917	1.002	0.152	3.595
Station 3c	0.919	1.005	0.153	3.597
Station 3d	0.945	1.029	0.156	3.623
Station 3e	1.059	1.136	0.173	3.737
Station 3f	1.213	1.280	0.195	3.891
Station 3g	1.367	1.425	0.217	4.045
Station 3h	1.521	1.570	0.239	4.199
Station 3i	1.675	1.715	0.261	4.353
Station 4	1.829	1.860	0.283	4.507

Plotting the height as a function of axial location with the results from the plot of the inlet compression system shows the two-dimensional view of the scramjet's inlet compression system and combustion system—from freestream conditions through Station 4.

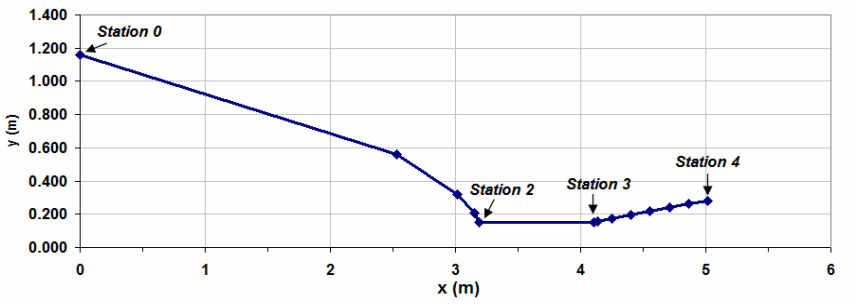

Figure 4.8: Combustion System Two-Dimensional Schematic for a Design Point of Mach 4.00

3. *Expansion System Height and Length.*

Lastly, it is necessary to determine the height and length of the expansion system designed. The expansion system is assumed to be ideal (p_{10}/p_0=1) and the application of a Single Expansion Ramp Nozzle (SERN) will be used, since the expansion system is not a primary focus for this project because it does not have a major bearing on the starting Mach number of the scramjet.

The height of the expansion system is calculated by the same method as for the inlet compression system; that is, through the use of Equation 4.22 combined with the assumption of Equation 4.23. As for the determination of A_n/A_2 which is necessary for this calculation, Equation 3.15 provides the value of A_{10}/A_0. With this value, Equation 4.24 can be used to determine A_{10}/A_2. This value can be used to determine the overall height at the exit of the nozzle. This will only provide a rough estimate of the expansion system by connecting the height of Station 4 to the height of Station 10.

Once the value of A_{10}/A_2 is determined, using Equation 4.22 and the value of h_2, which is equal to 0.152 m, the height at Station 10 can be determined. This calculation results in a value for h_{10}=2.8175 m.

As it was for the inlet compression system, the expansion system length will be an approximation. However, instead of approximating it using only simple geometry, the use of Prandtl-Meyer expansion wave theory will be implemented [29, 30].

Figure 4.9 below displays a conceptual view of the parameters used to calculate the length of the expansion system on the scramjet designed. This simplified model will only provide a rough estimate of the total length of the expansion system. This is

acceptable as the expansion system does not affect the lowered starting Mach number and the length is calculated here mainly for comparison and to give an overall perspective of the final design.

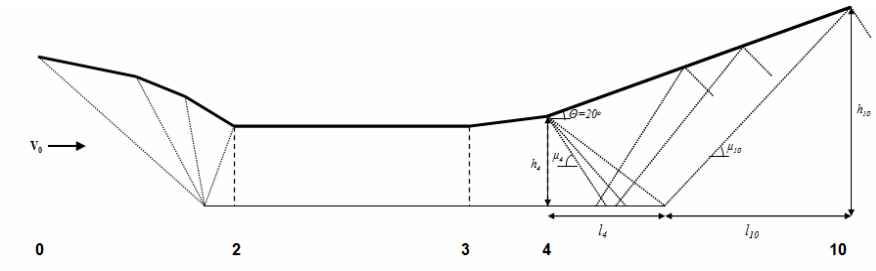

Figure 4.9: Expansion System Conceptual Diagram for Calculating Length

The first step in calculating the length of the expansion system is to use Prandtl-Meyer expansion wave theory at Station 4, as M_4 and h_4 are known. A SERN nozzle with an expansion angle of 20 degrees is used. The resulting Prandtl-Meyer function ν, Mach angle μ, and Mach number after the first expansion wave are calculated, allowing for the determination of l_4 as shown in Figure 4.9 through simple geometry. Next, ignoring the wave refraction on the bottom surface, the remaining length of the expansion system l_{10} can be determined through the same process. Finally, the sum of l_4 and l_{10} approximates the total length of the expansion system.

Performing these calculations returns a total length value for the expansion system of 8.15 m. Figure 4.10 shows the results of plotting the height as a function of axial location: the two-dimensional view of the overall scramjet designed for the design point at a starting M_0= 4.00.

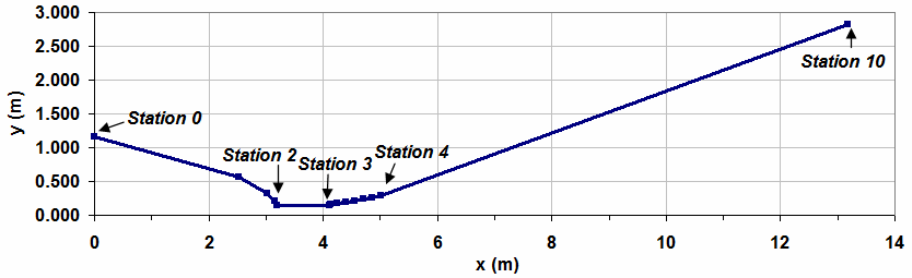

Figure 4.10: Two-Dimensional Schematic of the Overall Scramjet Designed for Mach 4.00 Start

CHAPTER 5

PERFORMANCE MEASURES OF SCRAMJET WITH STARTING FREESTREAM MACH NUMBER OF 4.00

Chapters 3 and 4 respectively defined the key design parameters and designed the three components of a scramjet with a starting Mach number of 4.00. Chapter 4 also calculated the dimensions of height and length for the three components of the scramjet, integrating these into a final two-dimensional schematic for the overall scramjet as shown in Figure 4.10.

The purpose of this chapter is to calculate the resulting performance of the scramjet at both the on- and off-design conditions. The performance results at the off-design conditions (operation at Mach numbers 5, 6, 8, and 10 to determine performance across the trajectory) will be compared to scramjets designed subsequently in this paper for on-design operation at each respective Mach number with a starting Mach number in the typical range of design at Mach 5.00. In addition, the off-design performance results for the scramjet designed in this paper will be compared to the off-design performance at Mach 6, 8, and 10 of a Mach 5.00 engine that will be designed in order to have a comparison with a scramjet designed with a higher starting Mach number. These comparisons will help to decipher the impact that transitioning to scramjet power at a lower Mach number makes on the overall performance. Sections 5.1 and 5.2 will provide the Mach 4.00 designed scramjet's on- and off-design performance respectively

as well as detail the process used for the calculations involved. Section 5.3 will provide a summary and discussion of the results.

5.1 On-Design Performance

The on-design performance of the scramjet is evaluated at M_0=4.00, the freestream Mach number at which the engine starts and for which the engine is designed. The process of calculating on-design performance begins with transferring the Mach 4.00 output from the HAP(Burner) Design tool to the spreadsheet created for this project which includes Equations 3.2-3.22 for the calculation of performance via one-dimensional flow analysis. The software produced results for the following values at each x location for which an iteration was conducted, as described in Section 4.1.2: A/A_2, T_t/T_{t2}, M, p/p_2, p/p_{t2}, A_c/A, Φ, u/u_2, T/T_2, p_t/p_{t2}, H, and K. From these values and using the flow information at Station 2 from the inlet compression system design shown in Table 4.2, the pressure, velocity, and temperature at each iteration point can be determined as well.

With the data in place, the calculation of on-design performance can begin, using Equations 3.2 through 3.22. This is done by using the data from the output for the designed combustion system as input into the one-dimensional flow analysis equations. The values output for T_3, V_3, p_3/p_0, and M_3 are inserted in place of Equations 3.3, 3.4, 3.6, and 3.22, respectively. Also, Equations 3.8 and 3.9 are replaced by the values output from the combustion results for V_4 and T_4, respectively. Therefore, with the output for the combustion system designed used in place of the one-dimensional

analysis equations, the Station 10 results include the flow parameters of the air entering the expansion system from the combustor.

Equations 3.16 through 3.21 are then applied to determine the overall performance for the on-design case. The numerical results for the entire process can be seen in Tables 5.1 through 5.3 here.

Table 5.1: On-Design Performance Inputs for Scramjet Designed for Mach 4.00 Start

INPUT		
M_0	4.00	
V_o	1184.56	m/s
T_o	218.22	K
T_3/T_0	2.8	
po	4275.00	Pa
f	0.0200	
h_{pr}	43903250.00	J/kg fuel
fh_{pr}	878065.0	J/kg
C_{p0}	1088.47	J/kgK
C_{pc}	1090.00	J/kgK
T_{to}	850.19	K
R	289.30	$(m/s)^2/K$
V_{fx}/V_3	0.500	
V_f/V_3	0.500	
$C_f^*A_w/A_3$	0.10	
Cpb	1510.0	J/kgK
Cpe	1510.0	J/kgK
η_c	0.9495	
η_b	0.90	
η_e	0.9	
h_f	0.0	
T^v	222.0	K
p_{10}/p_0	1.00	
g_0	9.8	m/s^2
γ_c	1.3620	
γ_e	1.2380	
γ_b	1.2380	

Table 5.2: On-Design Performance Calculation: Component Parameters for Scramjet Designed for Mach 4.00 Start

OUTPUT		
Compression Component (0 to 3)		
Sa_o	1237.855	
T_3	611.016	K
V_3	739.518	m/s
M_3	1.581	
Sa_3	978.548	
p_3/p_0	34.866	
p_3	148306.420	Pa
A_3/A_0	0.129	
Combustion Component (3 to 4)--Constant Pressure Combustion		
V_4	739.518	m/s
M_4	1.160	
T_4	1135.879	K
A_4/A_3	1.896	
Either Constant Pressure or Constant Area Combustion		
Sa_4	1183.875	
Expansion Component (4 to 10)		
p_4/p_0	34.678	
T_{10}	631.812	K
V_{10}	1438.461	m/s
M_{10}	3.024	
Sa_{10}	1565.530	
A_{10}/A_0	2.432	

Table 5.3: On-Design Performance Results for Scramjet Designed for Mach 4.00 Start

Engine Performance Measures		
F/m_o	282.671	N-s/kgA
S	7.075E-05	kg F/s-N
I_{sp}	1440.73	s
n_o	0.381	
n_{th}	0.403	
n_p	0.947	
T_3	611.02	
T_4	1135.88	
T_{10}	631.81	
M_3	1.58	
M_4	1.16	
M_{10}	3.02	

As the combustion system design results produced the dimensionless static enthalpy (H) and dimensionless kinetic energy (K), it is possible to produce the H-K diagram for the scramjet at the on-design condition, as shown in Figure 5.1 below. This diagram is important for evaluating scramjet engine performance, as it provides a view of the scramjet's ability to produce net thrust.

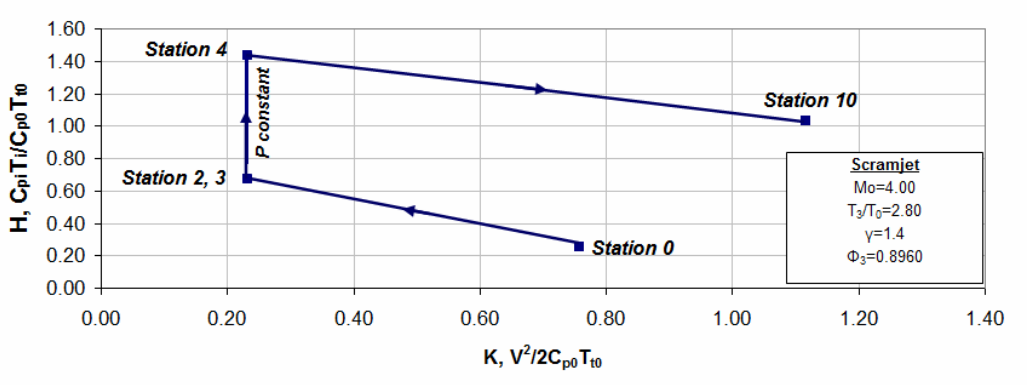

Figure 5.1: H-K Diagram for On-Design Performance Results for Scramjet Designed for Mach 4.00 Start

The H-K diagram displays the overall process occurring internally in the scramjet in terms of kinetic energy and enthalpy. Reference 1 discusses the H-K diagram for a scramjet in general which will be discussed here as it applies to the scramjet designed during this project. At Station 0, the freestream air is decelerated and compressed through the four oblique shock waves of the inlet compression system up to the isolator inlet at Station 2, resulting in a loss in K and an increase in H. Stations 2 and 3 occur at the same H and K, since the isolator is shock-free. Inside the combustor, as the air is heated to ignite the fuel, the pressure is constant for the on-design case, keeping K constant as H steadily increases from Station 3 to Station 4. This results in constant velocity throughout the burner as well. After exiting the combustor, the air is then expanded and accelerated in the expansion system from Station 4 to Station 10 to freestream conditions. The Mach number at the exit can never equal the freestream Mach number due to total pressure loss through the engine, but as long as the Mach number is large enough at the exit for K_{10} and V_{10} to exceed K_0 and V_0 respectively, net

thrust is generated [1]. It is evident in Figure 5.1 that this is indeed the case for the scramjet designed here.

5.2 Off-Design Performance

Although the determination of the on-design performance is important, perhaps equally as important is the calculation of the performance during flight when the scramjet must operate at off-design Mach numbers. After all, if an engine is only able or worthwhile to operate at one flight Mach number, there is not much application for it. As the goal of this project is to design a scramjet with a lowered starting Mach number, Mach 4.00 is the design case. The remaining Mach numbers of operation up to Mach 10 are then operating in an off-design condition.

Thus, the off-design performance at Mach numbers 5, 6, 8, and 10 will be determined and subsequently compared to the off-design performance of a scramjet designed for start and operation at Mach 5.00 (a value in the range of typical scramjet starting Mach numbers), as well as scramjets designed for on-design operation at each respective Mach number with a starting Mach number of Mach 5.00.

The procedure and results for calculating the off-design performance of the Mach 4.00 scramjet will be detailed first, in Section 5.2.1. Section 5.2.2 provides the procedure and results for designing a scramjet with a starting Mach number of 5.00 and determining its off-design performance at Mach 6, 8, and 10. The procedure and results for determining the reference engines optimized for each Mach number of 6, 8, and 10 to which off-design performance will be compared are discussed in Section 5.2.3. Finally, Section 5.2.4 will provide figures comparing all performance data, to determine

general trends and the overall impact a starting Mach number of 4.00 has on scramjet performance.

5.2.1. Determination of Off-Design Performance for Scramjet Designed at Mach 4.00

The calculation of the off-design performance begins by determining the conditions at the entrance to the isolator, Station 2. This is done by using a tool that is in the HAP software package [20] called HAP(Air) for Oblique Shocks. As the inlet compression system geometry has already been designed, it is necessary to determine the flow parameters of the off-design Mach numbers after going through the series of oblique shocks. HAP(Air) for Oblique Shocks requires that p_0, V_0, T_0, M_0, and δ be entered as input for the determination of the flow parameters after the first oblique shock. Once the resulting flow parameters after the first shock have been determined, that information is then entered as input with the same value of δ, which was determined during the design of the compression system for Mach 4.00, to determine the flow parameter values after the second shock. This process is repeated until the values of the flow parameters after the fourth oblique shock wave have been determined. This point corresponds with the entrance to the isolator at Station 2. This procedure using HAP(Air) for Oblique Shocks is then repeated for each off-design Mach number. The results for the flow parameters at Station 2 at each of the off-design Mach numbers can be seen below in Table 5.4.

Table 5.4: Station 2 Flow Parameters for Each Off-Design Mach Number of 5, 6, 8, 10

M_0	M_2	T_2 (K)	V_2 (m/s)	p_2 (Pa)
5	1.78	808.23	999.48	171700
6	2.06	986.68	1271.16	198350
8	2.48	1403.04	1805.49	259150
10	2.79	1919.66	2351.96	322640

The next step in determining the off-design performance for the scramjet is to run the HAP(Burner) Design tool for each freestream Mach number to be tested using the corresponding off-design Station 2 parameters and the inlet-combustor geometry determined in Chapter 4 for the Mach 4.00 scramjet. The fuel-to-air ratio that was used for the on-design case (f=0.02) is used here as well, to be consistent, in addition to the use of the same constants displayed in Table 5.1. The influence that a variation of f with M_0 would have on off-design performance should be addressed in another project.

Once the results from HAP(Burner) have been determined, the data is transferred to the one-dimensional flow analysis spreadsheet where the burner results replace the corresponding one-dimensional analysis equations as described in Section 5.1, and the resulting performance parameters and Station 10 flow parameters can be determined. This process is repeated for each off-design Mach number. The results of this analysis can be found below in Table 5.5.

Table 5.5: Off-Design Performance Results for Mach Numbers of 5, 6, 8, 10 Including Mach 4.00 On-Design Data for Comparison

M	Isp (s)	F/m_0(N-s/kgA)	S (kg F/s-N)	η_o	η_{th}	η_p	T_0 (K)	T_3 (K)	T_4 (K)	T_{10} (K)	M_3	M_4	M_{10}	$(H_{10}-H_0)/H_{10}$	$(K_{10}-K_0)/K_{10}$
4	1440.73	282.67	7.08E-05	0.38	0.40	0.95	218.22	611.02	1135.88	631.81	1.58	1.16	3.02	75%	32%
5	1393.77	273.46	7.31E-05	0.46	0.47	0.98	221.09	808.23	1291.55	677.24	1.78	1.50	3.51	76%	26%
6	1301.42	255.34	7.83E-05	0.52	0.51	1.02	223.47	986.68	1443.51	709.57	2.06	1.82	3.99	77%	20%
8	1138.20	223.31	8.96E-05	0.61	0.57	1.09	227.26	1403.04	1798.69	793.93	2.48	2.33	4.86	79%	13%
10	992.98	194.82	1.03E-04	0.68	0.58	1.17	233.16	1919.66	2240.24	908.97	2.80	2.73	5.59	81%	8%

Figure 5.2 below displays the results of specific impulse and specific thrust across the trajectory; therefore, this trend includes both the on-design performance results for these values at M_0=4.00 as well as the off-design results for M_0=5, 6, 8, and 10.

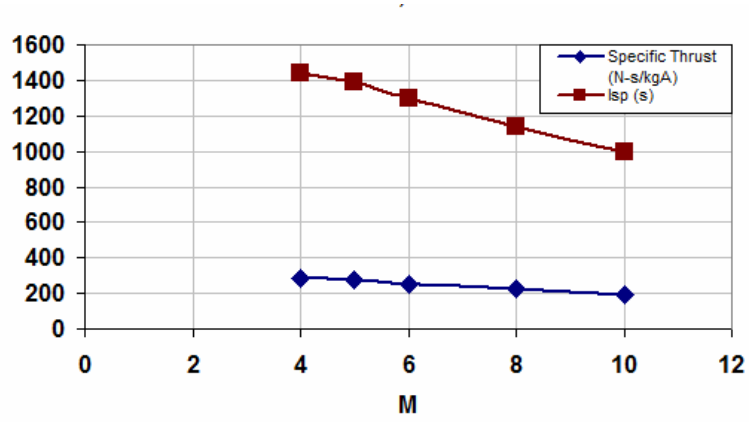

Figure 5.2: Scramjet Performance Results: I_{sp} and $F/\dot{m}_0$ Across Trajectory

As expected, the best performance for both I_{sp} and $F/\dot{m}_0$ occurs at M_0=4.00 and declines as the freestream Mach number increases, as the operation point is getting farther away from the on-design condition of the scramjet.

Figure 5.3 displays the results of the variation of the efficiency values across the trajectory.

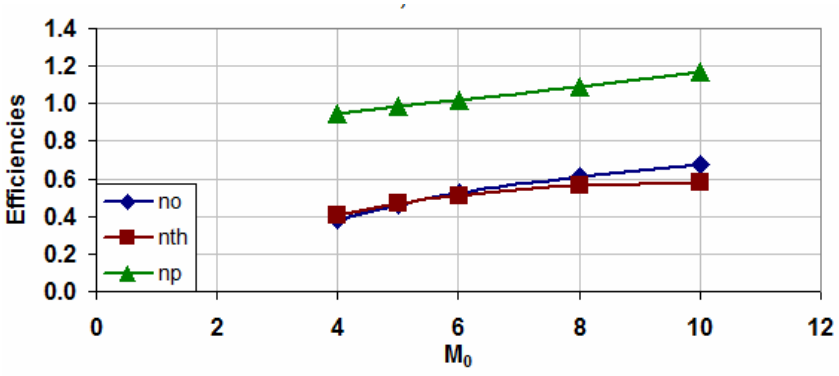

Figure 5.3: Scramjet Performance Results: η_0, η_{th}, and η_p Across Trajectory

Figure 5.4 below displays the difference from engine entrance to exit in H and K for each freestream Mach number that was analyzed across the trajectory. As the

figure shows, with increasing Mach number, the gain in H and K decreases; this is also a result of the engine design Mach number being 4.00.

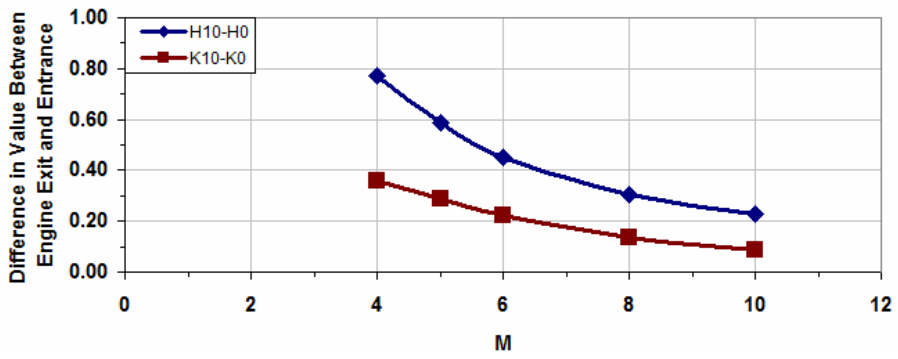

Figure 5.4: Scramjet Performance Results: Difference from Engine Entrance to Exit in H and K for Each Mach Number

Figure 5.5 displays the trend of specific fuel consumption across the trajectory, calculated for each freestream Mach number analyzed.

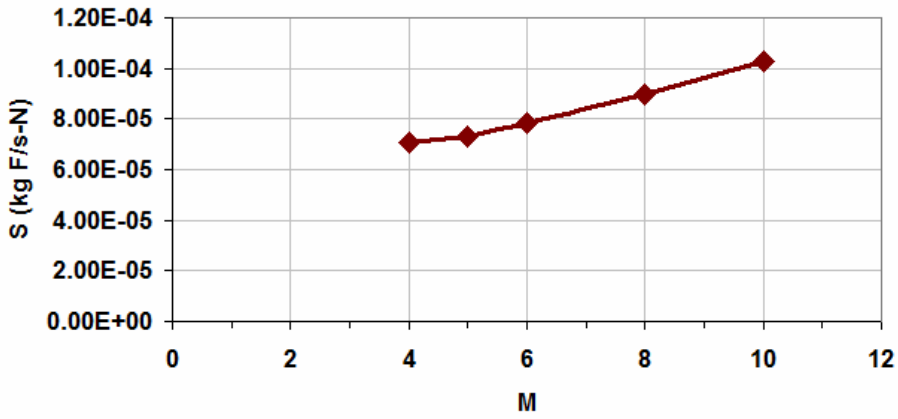

Figure 5.5: Scramjet Performance Results: Specific Fuel Consumption Across Trajectory

The next subsection will detail the process for the determination of the performance results for a scramjet designed for Mach 5.00, a more typical starting

Mach number for a scramjet. This will provide realistic values for comparison with the off-design performance for the Mach 4.00 engine.

5.2.2. Determination of On- and Off-Design Performance for Scramjet Designed at Mach 5.00

This section defines the procedure and results for designing a scramjet with a more typical starting Mach number of 5.00 and obtaining its on- and off-design performance results for comparison with the off-design performance of the Mach 4.00 scramjet. The procedure is defined in a series of steps below.

1. *Choose T_3/T_0 and f Values*

Evaluating Equations 3.2 through 3.22 with a range of T_3/T_0 and *f* values, the values for these terms can be chosen based on the best tradeoff of performance results—specifically, the best tradeoff between I_{sp} and $F/\dot{m}_0$. The range for *f* that was used is the same as the range shown in Table 3.14, as JP-7 fuel is used in these designs as well for comparison purposes. The range for T_3/T_0 is from 3.5 to 7.0; the higher values are used for the higher Mach numbers. The spreadsheet described previously containing Equations 3.2 through 3.22 is run for each T_3/T_0 across the series of *f* values discussed to determine the resulting performance values. The best values for *f* and T_3/T_0 can be determined by finding the pair that returns the best balance of I_{sp} and $F/\dot{m}_0$. (This was done by averaging the highest I_{sp} and $F/\dot{m}_0$ from the value of *f* nearest to the stoichiometric value and from the value of *f* that returned the highest specific impulse. The pair of *f* and T_3/T_0 that returned values closest to these averages was then chosen.)

The values of f and T_3/T_0 chosen for the Mach 5.00 engine are 0.04 and 3.75, respectively.

2. *Design Inlet Compression System*

The inlet compression system is the next step in the process, and should be designed according to the method described in Sections 4.1.1.1 and 4.2.1 for a starting Mach number of 5.00. The resulting values for the inlet compression system designed are shown below in Table 5.6.

Table 5.6: Inlet Compression System Parameters for On-Design Engine at M_0=5 for Scramjet Start at Mach 5.00

Input						
M_0	5					
T_3/T_0	3.75					
Number of OS	5					
γ_c	1.362					
Flow Properties to Determine Station 2 Values			**Resulting Compression System Properties**			
p_0	2736.0	Pa	delta	12.022	deg	
T_0	221.09	K	$p_{t3}/p_{t0}=\pi_c$	0.63		
C_{pc}	1090.0	J/kgK	n_c	0.95		
V_0	1490.40	m/s	n_{ke}	0.97		
Flow Properties After Each Oblique Shock						
O.S. Number	**M**	**T/T_0**	**p/p_0**	**A/A_0**	**p_t/p_{t0}**	**$(s-s_0)/C_p$**
1	3.8747	1.4862	3.587	0.439	0.8077	0.0568
2	3.1033	2.0141	10.0484	0.228	0.7211	0.0869
3	2.518	2.5726	23.6364	0.135	0.6754	0.1043
4	2.0393	3.1522	48.7781	0.089	0.649	0.1149
5	1.6171	3.75	91.3446	0.066	0.6323	0.1218
Flow Properties at Compression System Exit						
	p_2	249919	Pa			
	T_2	829.09	K			
	V_2	882.78	m/s			
	M_2	1.62				

3. *Design Combustion System*

The combustion system is the next step in the process, and should be designed according to the method described in Sections 4.1.2 and 4.2.2. The resulting values are shown below in Table 5.7.

Table 5.7: Combustion System Parameters for On-Design Engine at M_0=5, for Scramjet Start at Mach 5.00

Flow Properties of Burner		
M_3	1.62	
T_3	829.09	K
V_3	882.78	m/s
p_3	249843.85	kPa
M_4	1.096	
T_4	1870.42	K
V_4	897.79	m/s
p_4	241171.67	kPa
Isolator/Combustor Geometry		
x(2, 3, 3p, 4)	(0, 0.914, 0.914, 1.829)	m
A/A_2(2, 3, 3p, 4)	(1, 1, 1, 2.30)	
θ/H	0.03	
H	0.152	m
Axial Heat Addition Parameters		
θ	1	
x_i	0.914	m
$\eta_b f h_{PR}$	1580.517	kJ/kg
Isolator-Burner Interaction		
Shock-Free Isolator		

4. *Design Expansion System*

The expansion system is designed according to the method described in Section 4.1.3. An ideal nozzle assumption should be assumed in order to compare directly with the off-design performance obtained with the Mach 4.00 starting scramjet. A SERN nozzle is applied here as well. The results of the expansion system design can be found in the next step, where the height and length of each component is determined and the resulting dimensions and schematic are shown.

5. *Calculate Height and Length of Each Engine Component*

The height and length of each engine component for the engine designed here is calculated in the same manner as described in Section 4.3. The results and

corresponding engine schematic are displayed here in Table 5.8 and Figure 5.6, respectively.

Table 5.8: Scramjet Height and Length Values for On-Design Engine at M_0=5, for Scramjet Start at Mach 5.00

i	x (m)	A/A_2	h (m)	x(m) shifted to beginning of engine
0 (Freestream)	0.000	15.267	2.321	0.000
0a, after OS 1	6.117	6.696	1.018	6.117
0b, after OS 2	7.215	3.475	0.528	7.215
0c, after OS 3	7.511	2.056	0.313	7.511
0d, after OS 4	7.606	1.362	0.207	7.606
0e, after OS 5	7.637	1.000	0.152	7.637
Station 2 (Isolator)	0.000	1.000	0.152	7.637
Station 3 u (Combustor Entrance)	0.914	1.000	0.152	8.552
Station 3 d,s	0.915	1.001	0.152	8.552
3c	0.917	1.004	0.153	8.554
3d	0.948	1.048	0.159	8.585
3e	1.032	1.168	0.178	8.669
3f	1.143	1.325	0.201	8.780
3g	1.273	1.509	0.229	8.910
3h	1.412	1.707	0.259	9.049
3i	1.551	1.905	0.290	9.188
3j	1.690	2.102	0.320	9.327
Station 4 (Combustor Exit)	1.829	2.300	0.350	9.466
Station 10 (Engine Exit)	24.818	49.888	7.583	34.284

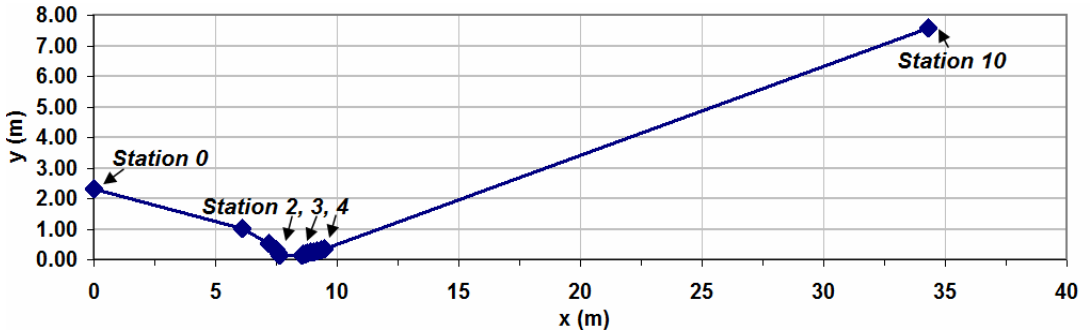

Figure 5.6: Two-Dimensional Schematic for Scramjet Designed at M_0=5, for Scramjet Start at Mach 5.00

6. *Input Combustor Data into Performance Spreadsheet*

The combustion system data obtained from HAP(Burner) is then entered into the Performance spreadsheet as described in Section 5.1.

7. *Obtain Performance Data for Comparison to Off-Design Performance for Mach 4.00 Designed Scramjet*

Equations 3.16 through 3.21 should be applied next to determine the on-design performance of the Mach 5.00 engine. The inputs required that have not already been discussed are the same as is found in Table 5.1.

The off-design performance for Mach numbers 6, 8, and 10 using the Mach 5.00 designed engine is calculated using the same procedure described in Section 5.2.1. Both the on- and off-design performance results are shown below in Table 5.9.

Table 5.9: On- and Off-Design Performance Results for Scramjet Designed for Mach 5.00

M	Isp (s)	F/m_0(N-s/kgA)	S (kg F/s-N)	η_o	η_{th}	η_p	T_0 (K)	T_3 (K)	T_4 (K)	T_{10} (K)	M_3	M_4	M_{10}	$(H_{10}-H_0)/H_{10}$	$(K_{10}-K_0)/K_{10}$
5	1323.63	519.39	7.70E-05	0.44	0.47	0.93	221.09	829.09	1870.42	900.72	1.62	1.10	3.40	82%	41%
6	1348.40	529.11	7.56E-05	0.54	0.56	0.96	223.47	1068.64	2048.58	938.54	1.87	1.45	3.86	83%	25%
8	1224.00	480.30	8.33E-05	0.66	0.63	1.04	227.26	1522.46	2413.10	993.11	2.28	1.96	4.67	83%	25%
10	1119.70	439.37	9.10E-05	0.77	0.69	1.12	233.16	2085.31	2867.30	1083.97	2.59	2.38	5.40	84%	17%

5.2.3. Determination of On-Design Performance for Scramjets Designed at Mach 6, 8, and 10 with Scramjet Start at Mach 5.00

This section will use the procedure outlined in Steps 1-7 in the previous section to design three scramjets that are designed for operation at Mach 6, 8, and 10, respectively, and determine their respective on-design performance values for comparison against the off-design performance of the Mach 4.00 and Mach 5.00 designed engines. Each of these engines will be designed to start at Mach 5.00, a value in the range of typical scramjet starting Mach numbers.

Only the titles of each of the steps outlined in the previous section are shown with the corresponding results for the three engines designed in this section, as the method is the same as in the previous section.

1. *Choose T_3/T_0 and f Values*

This process is completed for each engine to be designed: Mach 6, 8, and 10. Table 5.10 below displays the chosen *f* and T_3/T_0 for each freestream Mach number.

Table 5.10: Design *f* and T_3/T_0 for Each On-Design Engine at M_0= 6, 8, and 10

M	f	T_3/T_0
6	0.04	5.25
8	0.10	6.00
10	0.09	7.00

2. *Design Inlet Compression System*

The resulting inlet compression systems designed for each Mach number that also allow scramjet start at Mach 5.00 are shown below in Tables 5.11 through 5.13.

Table 5.11: Inlet Compression System Parameters for On-Design Engine at M_0=6 for Scramjet Start at Mach 5.00

Input						
M_0	6					
T_3/T_0	5.25					
Number of OS	6					
γ_c	1.362					
Flow Properties to Determine			**Resulting Compression System**			
p_0	1900.0	Pa	delta	11.630	deg	
T_0	223.47	K	$p_{t3}/p_{t0}=\pi_c$	0.52		
C_{pc}	1090.0	J/kgK	n_c	0.96		
V_0	1798.05	m/s	n_{ke}	0.97		
Flow Properties After Each Oblique Shock						
O.S. Number	M	T/T_0	p/p_0	A/A_0	p_t/p_{t0}	$(s-s_0)/C_p$
1	4.5327	1.5928	4.2434	0.3937	0.7363	0.0813
2	3.5977	2.2484	13.3065	0.1879	0.6312	0.1223
3	2.9217	2.9531	34.043	0.1037	0.5789	0.1453
4	2.3911	3.6936	75.0172	0.0643	0.5498	0.159
5	1.9462	4.4591	147.5039	0.0441	0.5322	0.1676
6	1.5442	5.2500	266.7485	0.0334	0.5207	0.1735
Flow Properties at Compression System Exit						
	p_2	506822.15	Pa			
	T_2	1173.2	K			
	V_2	998.25	m/s			
	M_2	1.54				

Table 5.12: Inlet Compression System Parameters for On-Design Engine at M_0=8, for Scramjet Start at Mach 5.00

Input						
M_0	8					
T_3/T_0	6					
Number of OS	4					
γ_c	1.362					
Flow Properties to Determine			**Resulting Compression System**			
p_0	1069.0	Pa	**delta**	13.037	deg	
T_0	227.26	K	$p_{t2}/p_{t0}=\pi_c$	0.28		
C_{pc}	1090.0	J/kgK	n_c	0.92		
V_0	2417.68	m/s	n_{ke}	0.97		
Flow Properties After Each Oblique Shock						
O.S. Number	**M**	**T/T_0**	**p/p_0**	**A/A_0**	**p_t/p_{t0}**	**$(s-s_0)/C_p$**
1	5.299	2.0689	7.2597	0.2991	0.4709	0.2002
2	3.9589	3.2799	30.4662	0.1201	0.3491	0.2797
3	3.0962	4.6009	93.9273	0.059	0.3012	0.3189
4	2.4622	6	235.274	0.0338	0.2779	0.3404
Flow Properties at Compression System Exit						
	p_2	251507.91	Pa			
	T_2	1363.56	K			
	V_2	1719.12	m/s			
	M_2	2.46				

Table 5.13: Inlet Compression System Parameters for On-Design Engine at M_0=10, for Scramjet Start at Mach 5.00

Input						
M_0	10					
T_3/T_0	7					
Number of OS	3					
γ_c	1.362					
Flow Properties to Determine			**Resulting Compression System**			
p_0	710.0	Pa	**delta**	14.175	deg	
T_0	233.16	K	$p_{t2}/p_{t0}=\pi_c$	0.14		
C_{pc}	1090.0	J/kgK	n_c	0.88		
V_0	3061.05	m/s	n_{ke}	0.96		
Flow Properties After Each Oblique Shock						
O.S. Number	**M**	**T/T_0**	**p/p_0**	**A/A_0**	**p_t/p_{t0}**	**$(s-s_0)/C_p$**
1	5.7137	2.7645	11.7485	0.2477	0.2561	0.362
2	4.0654	4.7852	60.0129	0.0897	0.166	0.4773
3	3.0903	7	206.7239	0.0414	0.1367	0.5289
Flow Properties at Compression System Exit						
	p_2	146773.97	Pa			
	T_2	1632.128	K			
	V_2	2362.49	m/s			
	M_2	3.09				

Tables 5.11 through 5.13 show a decrease in the number of oblique shock waves with each increasing Mach number design, which seems to be counterintuitive. However, it is logical as the compression efficiency also decreases with Mach number. Though it would have been beneficial for comparison purposes to keep the compression efficiency relatively constant, doing so would make the compression system

prohibitively long; therefore, a decrease in the number of oblique shock waves was employed.

3. *Design Combustion System*

The resulting combustion systems designed for each Mach number are shown below in Tables 5.14 through 5.16.

Table 5.14: Combustion System Parameters for On-Design Engine at M_0=6, for Scramjet Start at Mach 5.00

Flow Properties of Burner		
M_3	1.54	
T_3	1173.20	K
V_3	998.25	m/s
p_3	506720.79	kPa
M_4	1.16	
T_4	2202.10	K
V_4	1030.19	m/s
p_4	472611.65	kPa
Isolator/Combustor Geometry		
x(2, 3, 3p, 4)	(0, 0.914, 0.914, 1.829)	m
A/A_2(2, 3, 3p, 4)	(1, 1, 1, 1.95)	
θ/H	0.03	
H	0.152	m
Axial Heat Addition Parameters		
θ	1	
x_i	0.914	m
$\eta_b f h_{PR}$	1580.517	kJ/kg
Isolator-Burner Interaction		
Shock-Free Isolator		

Table 5.15: Combustion System Parameters for On-Design Engine at M_0=8, for Scramjet Start at Mach 5.00

Flow Properties of Burner		
M_3	2.46	
T_3	1363.56	K
V_3	1719.12	m/s
p_3	251382.15	kPa
M_4	1.453	
T_4	3973.41	K
V_4	1732.87	m/s
p_4	242378.17	kPa
Isolator/Combustor Geometry		
x(2, 3, 3p, 4)	(0, 0.914, 0.914, 1.829)	m
A/A_2(2, 3, 3p, 4)	(1, 1, 1, 3.00)	
θ/H	0.03	
H	0.152	m
Axial Heat Addition Parameters		
θ	1	
x_i	0.914	m
$\eta_b fh_{PR}$	3951.293	kJ/kg
Isolator-Burner Interaction		
Shock-Free Isolator		

Table 5.16: Combustion System Parameters for On-Design Engine at M_0=10, for Scramjet Start at Mach 5.00

Flow Properties of Burner		
M_3	3.09	
T_3	1632.13	K
V_3	2362.49	m/s
p_3	146715.26	kPa
M_4	2.004	
T_4	3957.91	K
V_4	2386.11	m/s
p_4	135560.44	kPa
Isolator/Combustor Geometry		
x(2, 3, 3p, 4)	(0, 0.914, 0.914, 1.829)	m
A/A_2(2, 3, 3p, 4)	(1, 1, 1, 2.60)	
θ/H	0.03	
H	0.152	m
Axial Heat Addition Parameters		
θ	1	
x_i	0.914	m
$\eta_b fh_{PR}$	3556.163	kJ/kg
Isolator-Burner Interaction		
Shock-Free Isolator		

4. *Design Expansion System*

As an ideal nozzle assumption applied to the scramjets designed for Mach 6, 8, and 10 would result in prohibitively long expansion systems [1], and as the expansion system does not have a direct bearing on the current project being evaluated, expansion systems have not been designed for these scramjet engines.

5. *Calculate Height and Length of Each Engine Component*

The height and length of each engine component for each engine designed here can be seen in Tables 5.17 through 5.19 below, and the corresponding engine schematic (containing the inlet compression system and combustion system only) are displayed in Figures 5.7 through 5.9, respectively.

Table 5.17: Scramjet Height and Length Values for On-Design Engine at M_0=6, for Scramjet Start at Mach 5.00

i	x (m)	A/A_2	h (m)	x(m) shifted to beginning of engine
0 (Freestream)	0.000	29.940	4.551	0.000
0a, after OS 1	13.406	11.787	1.792	13.406
0b, after OS 2	15.585	5.626	0.855	15.585
0c, after OS 3	16.134	3.105	0.472	16.134
0d, after OS 4	16.304	1.925	0.293	16.304
0e, after OS 5	16.362	1.320	0.201	16.362
0f, after OS 6	16.379	1.000	0.152	16.379
Station 2 (Isolator)	0.000	1.000	0.152	16.379
Station 3 u (Combustor Entrance)	0.914	1.000	0.152	17.294
Station 3 d,s	0.917	1.002	0.152	17.296
3c	0.919	1.004	0.153	17.298
3d	0.946	1.032	0.157	17.325
3e	1.059	1.150	0.175	17.438
3f	1.213	1.310	0.199	17.592
3g	1.367	1.470	0.223	17.746
3h	1.521	1.630	0.248	17.900
3i	1.675	1.790	0.272	18.054
Station 4 (Combustor Exit)	1.829	1.950	0.296	18.208

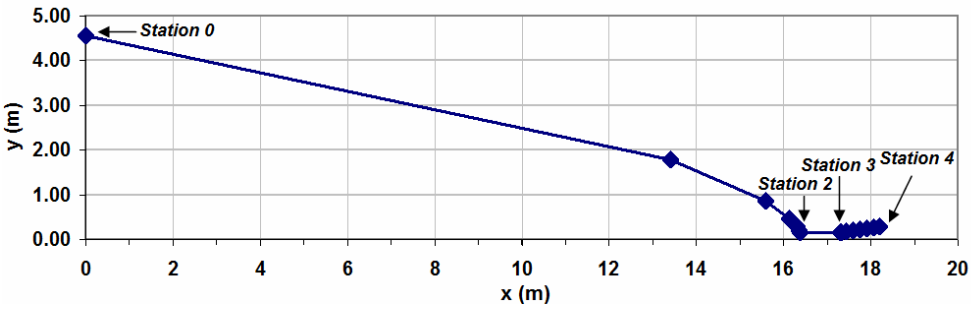

Figure 5.7: Two-Dimensional Schematic for Scramjet Designed at M_0=6, for Scramjet Start at Mach 5.00

Table 5.18: Scramjet Height and Length Values for On-Design Engine at M_0=8, for Scramjet Start at Mach 5.00

i	x (m)	A/A_2	h (m)	x(m) shifted to beginning of engine
0 (Freestream)	0.000	29.586	4.497	0.000
0a, after OS 1	13.613	8.849	1.345	13.613
0b, after OS 2	15.258	3.553	0.540	15.258
0c, after OS 3	15.596	1.746	0.265	15.596
0d, after OS 4	15.684	1.000	0.152	15.684
Station 2 (Isolator)	0.000	1.000	0.152	15.684
Station 3 u (Combustor Entrance)	0.914	1.000	0.152	16.598
Station 3 d,s	0.915	1.002	0.152	16.599
3c	0.919	1.009	0.153	16.602
3d	0.923	1.019	0.155	16.607
3e	0.964	1.108	0.168	16.648
3f	1.025	1.241	0.189	16.709
3g	1.096	1.398	0.212	16.780
3h	1.178	1.577	0.240	16.862
3i	1.271	1.779	0.270	16.955
3j	1.376	2.010	0.306	17.060
3k	1.489	2.257	0.343	17.173
3l	1.602	2.505	0.381	17.286
3m	1.716	2.752	0.418	17.400
Station 4 (Combustor Exit)	1.829	3.000	0.456	17.513

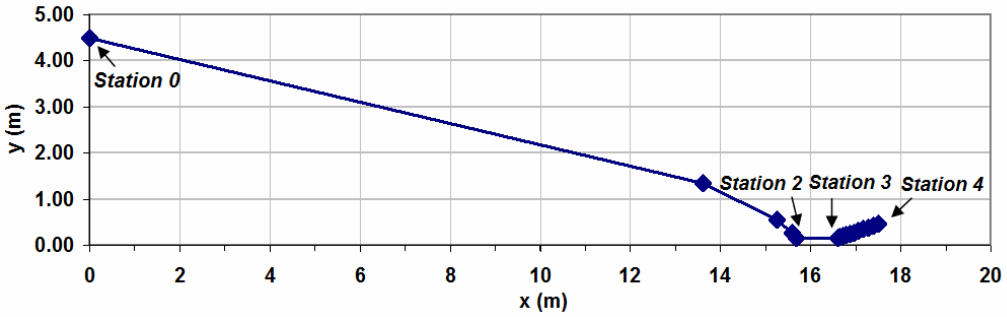

Figure 5.8: Two-Dimensional Schematic for Scramjet Designed at M_0=8, for Scramjet Start at Mach 5.00

Table 5.19: Scramjet Height and Length Values for On-Design Engine at M_0=10, for Scramjet Start at Mach 5.00

i	x (m)	A/A_2	h (m)	x(m) shifted to beginning of engine
0 (Freestream)	0.000	24.155	3.671	0.000
0a, after OS 1	10.935	5.983	0.909	10.935
0b, after OS 2	12.010	2.167	0.329	12.010
0c, after OS 3	12.203	1.000	0.152	12.203
Station 2 (Isolator)	0.000	1.000	0.152	12.203
Station 3 u (Combustor Entrance)	0.914	1.000	0.152	13.118
Station 3 d,s	0.915	1.002	0.152	13.119
3c	0.917	1.004	0.153	13.120
3d	0.930	1.028	0.156	13.134
3e	0.988	1.128	0.171	13.191
3f	1.071	1.273	0.193	13.274
3g	1.167	1.442	0.219	13.370
3h	1.276	1.633	0.248	13.479
3i	1.387	1.826	0.278	13.590
3j	1.497	2.020	0.307	13.700
3k	1.608	2.213	0.336	13.811
3l	1.718	2.407	0.366	13.921
Station 4 (Combustor Exit)	1.829	2.600	0.395	14.032

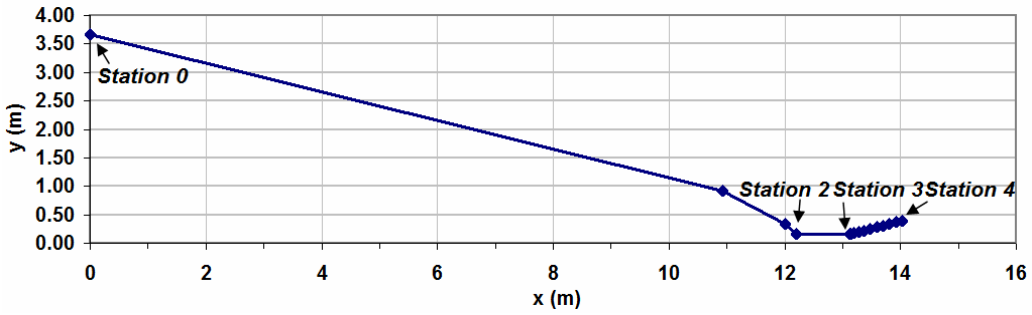

Figure 5.9: Two-Dimensional Schematic for Scramjet Designed at M_0=10, for Scramjet Start at Mach 5.00

6. *Input Combustor Data into Performance Spreadsheet*

The combustion system data obtained from HAP(Burner) is then entered into the Performance spreadsheet for each Mach number as described in Section 5.1.

7. *Obtain Performance Data for Comparison to Off-Design Performance of Mach 4.00 Designed Scramjet*

The overall performance of each engine is determined next. The inputs required that have not been discussed here are the same as is found in Table 5.1. Table 5.20

below displays the performance results that each of the scramjets designed for on-design operation at freestream Mach numbers 6, 8, and 10 generate.

Table 5.20: On-Design Performance Results for Scramjets Designed for M_0=6, 8, and 10, for Scramjet Start at Mach 5.00

M	Isp (s)	F/m_0(N-s/kgA)	S (kg F/s-N)	η_o	η_{th}	η_p	T_0 (K)	T_3 (K)	T_4 (K)	T_{10} (K)	M_3	M_4	M_{10}	$(H_{10}-H_0)/H_{10}$	$(K_{10}-K_0)/K_{10}$
6	1324.30	519.65	7.70E-05	0.53	0.55	0.97	223.47	1173.20	2202.10	908.99	1.54	1.16	3.91	82%	35%
8	1078.19	1057.71	9.45E-05	0.58	0.58	1.00	227.26	1363.56	3973.41	1662.41	2.46	1.45	4.09	90%	41%
10	900.98	795.48	1.13E-04	0.62	0.54	1.14	233.16	1632.13	3957.91	1698.11	3.09	2.00	4.54	90%	25%

5.2.4. Comparison of All Performance Values Obtained

Figures 5.10 through 5.14 compare all of the performance values obtained. These include: the on-design performance at Mach 4.00 and the off-design performance at Mach 5, 6, 8, and 10 in the Mach 4.00 scramjet; the on-design performance at Mach 5.00 and the off-design performance at Mach 6, 8, and 10 in the Mach 5.00 scramjet; and the on-design performance obtained for the scramjets designed for operation at each of the other respective Mach numbers (Mach 6, 8, and 10.)

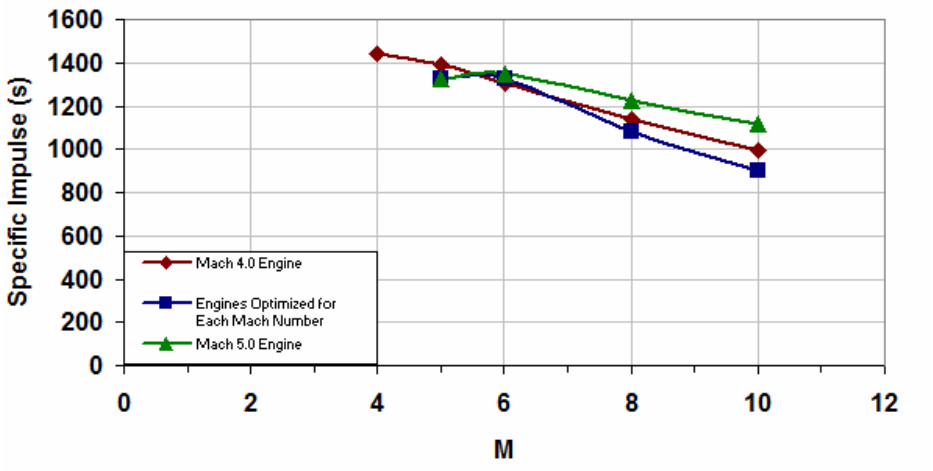

Figure 5.10: I_{sp} Values for On- and Off-Design Performance of Mach 4 and 5 Designed Engines and for On-Design Performance of Mach 6, 8, and 10 Engines

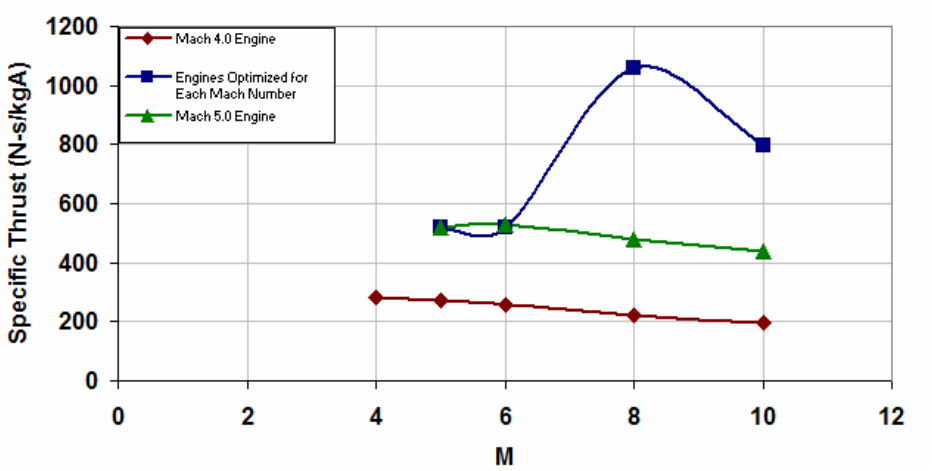

Figure 5.11: $F/\dot{m}_0$ **Values for On- and Off-Design Performance of Mach 4 and 5 Designed Engines and for On-Design Performance of Mach 6, 8, and 10 Engines**

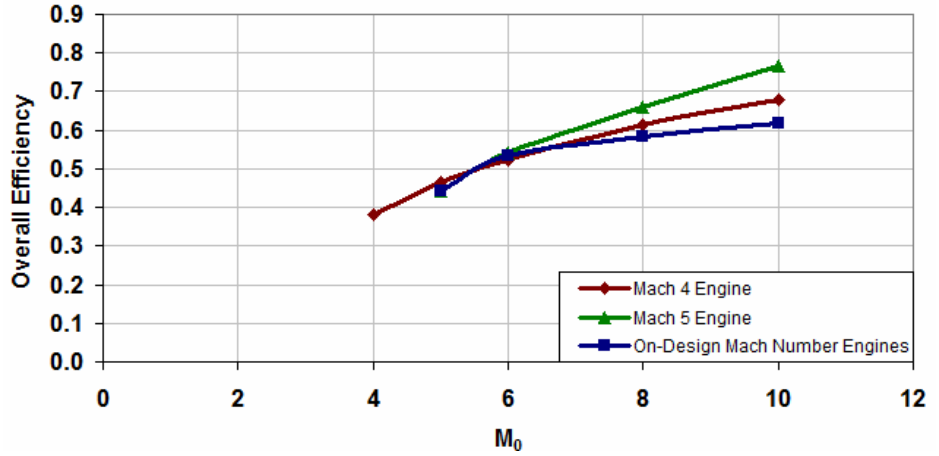

Figure 5.12: Overall Efficiency Values for On- and Off-Design Performance of Mach 4 and 5 Designed Engines and for On-Design Performance of Mach 6, 8, and 10 Engines

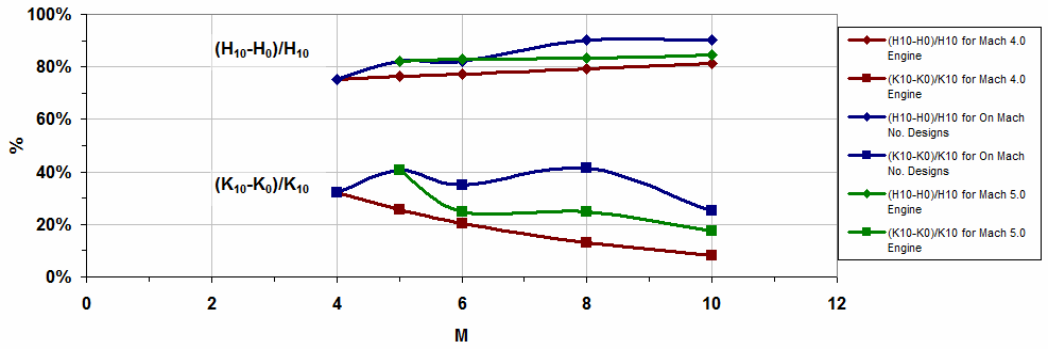

Figure 5.13: Values of $(K_{10}-K_0)/K_{10}$ and $(H_{10}-H_0)/H_{10}$ for Mach 4 and 5 Designed Engines and for On-Design Performance of Mach 6, 8, and 10 Engines

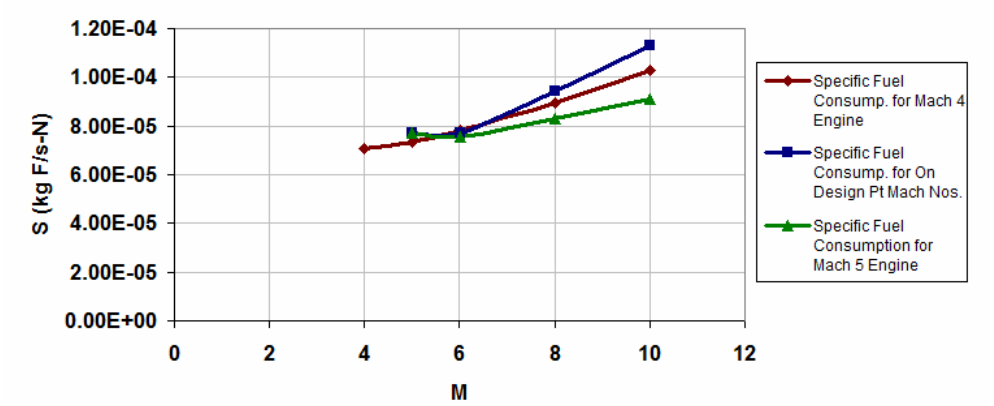

Figure 5.14: Specific Fuel Consumption for Mach 4 and 5 Designed Engines and for On-Design Performance of Mach 6, 8, and 10 Engines

5.3 Discussion and Summary of Results

The purpose of this chapter has been to calculate the resulting on- and off-design performance of the scramjet designed to start at Mach 4.00. This has been completed and presented.

The off-design performance results at Mach numbers 5, 6, 8, and 10 were compared to the performance results for scramjets that were designed in this chapter for on-design operation at each respective Mach number with a starting Mach number in

the typical range of design at Mach 5.00. Additionally, the off-design performance was compared to the off-design performance of the same Mach numbers in a Mach 5.00 designed engine, in order to have a comparison with a scramjet designed around a higher starting Mach number. Overall, the results in this chapter reveal consistent trends for on- and off-design performance. These are listed here and discussed in turn.

On-Design Performance

The on-design performance investigation (operation at Mach 4.00) resulted in performance values that are acceptable if a lowered starting Mach number is the desired goal. If the purpose of a scramjet to be designed is to achieve the highest efficiency and performance values possible, then this design is not the best choice. The specific impulse of the engine designed is respectable at 1440.73 s, especially when considering that the classical I_{sp} versus Mach number plot estimates that the scramjet maximum I_{sp} capability with hydrocarbon fuels is around 1500 s as shown below in Figure 5.15 and when considering that hydrocarbon scramjets have been estimated to be capable of a specific impulse of about 1000 seconds at Mach 6 [15, 24].

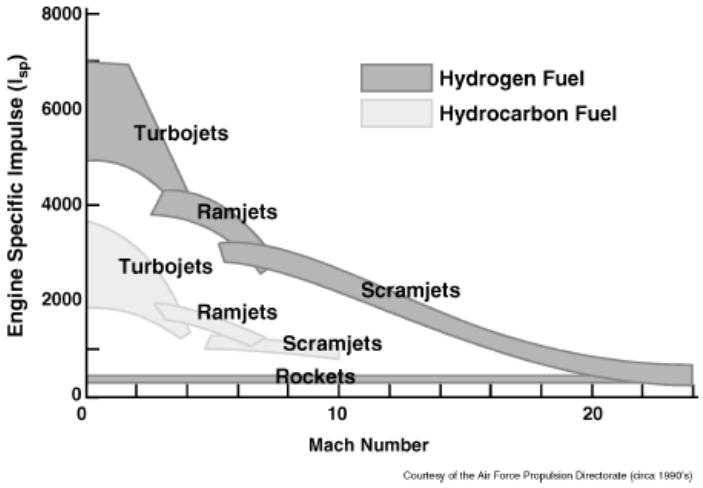

Figure 5.15: I_{sp} Versus Mach Number Plot for Various Engine Types [3]

However, the high performance for I_{sp} of the Mach 4.00 designed scramjet comes at a cost in specific thrust. As the fuel-to-air ratio is decreased, the specific thrust decreases and the specific impulse increases. As a very low fuel-to-air ratio, such as 0.02 for the case of the Mach 4.00 engine designed in this paper, is needed to start the engine at a low Mach number, specific thrust suffers. Though the specific thrust is not excellent, the H-K diagram generated and shown in Figure 5.1 for on-design performance of the Mach 4.00 engine displays that the engine still generates net thrust. This assures that a scramjet with a starting Mach number of 4.00 is possible.

Off-Design Performance

For the off-design performance generated in this chapter of the Mach 4.00 designed engine, the results are intuitive. As the Mach number increases, that is, as the Mach number gets farther and farther away from the design point of Mach 4.00, the specific thrust and specific impulse decrease in an almost linear fashion, with the specific impulse dropping off much more steeply with Mach number than the specific

thrust. This trend is also true for the performance comparison case of the Mach 5.00 designed engine at the same off-design Mach numbers. However, overall the Mach 5.00 designed engine returns higher performance values. This is primarily due to the fact that the engine starts at a Mach number closer to the off-design points evaluated.

Conversely, with an increase in Mach number, the overall efficiency increases as well, since it is related directly to velocity; the velocity increases at a faster rate than the specific fuel consumption increases. If the reverse were true, the overall efficiency would decrease steadily with increasing Mach number.

The specific fuel consumption increases with Mach number, as expected, due to the higher velocity (and thus, higher required thrust) of the flow that requires a higher overall quantity of fuel to keep the fuel-to-air ratio steady.

Comparing the relative increase of H and K for each of the cases tested shows that as Mach number increases, the value of H also increases while the value of K decreases. The overall gain in percentage is the highest in H and K for the on-design Mach number engine cases, with the off-design performance for the Mach 5.00 engine consistently being in second, and the gain in H and K of the off-design performance of the Mach 4.00 engine being the lowest of the three trends. This is primarily due to the increased velocity of the two cases with the highest overall gains.

A particularly revealing example of the opposite relationship specific thrust and specific impulse have in relation to the fuel-to-air ratio can be seen in Figures 5.10 and 5.11 for the on-design performance evaluation of the Mach 5, 6, 8, and 10 scramjets. As the design Mach number increases, in general the selected fuel-to-air ratio increases as

well, due to it providing the best tradeoff between specific impulse and specific thrust. However, as these figures show, the overall trend of specific impulse is decreasing with Mach number, while the overall trend of specific thrust increases. In fact, the trends for specific impulse and specific thrust are relative opposites of each other; as one increases, the other decreases. This is a visual example of the effect that the chosen fuel-to-air ratio has on the design of a scramjet. This insight is especially important when considering the design of a scramjet with a lowered starting Mach number, which therefore requires a lower fuel-to-air ratio to keep the flow supersonic throughout the combustor.

The performance parameters and comparisons generated in this chapter help provide the needed information for the determination of the impact that transitioning to scramjet power at a lower Mach number has on the overall performance.

CHAPTER 6

CONCLUSIONS AND RECOMMENDATIONS

6.1 Conclusions

The purpose of this paper has been to determine whether the freestream starting Mach number of a scramjet can be lowered to 3.50 while performance is maintained in the same flowpath at the higher, off-design Mach numbers and, if so, to define how it could be accomplished. If the goal is not possible, it is necessary to determine what the constraints are that prevent it and to define the lowest possible starting Mach number.

The purposes of this paper have been accomplished. By successively analyzing the driving parameters influencing the starting Mach number and applying the necessary theory and equations, it has been determined that obtaining a scramjet starting Mach number of 3.50, without fuel additives or another method of lowering the fuel ignition temperature, is not currently possible with any of the fuels analyzed.

This analysis has determined that in order for a scramjet to start at a Mach number of 3.50, a fuel with a lower heat of reaction and a lower ignition temperature (naturally or with the use of additives) than those analyzed here must be used; these are the key constraints on the ability of the scramjet to start at Mach 3.50. In Figure 6.1 below, obtained from applying the T_0 value at Mach 3.50 for a constant q trajectory of 47,880 N/m^2 to Figure 3.20, for a given ignition temperature of a given fuel, the fuel's

heat of reaction value must lay below the line or supersonic combustion will not be maintained.

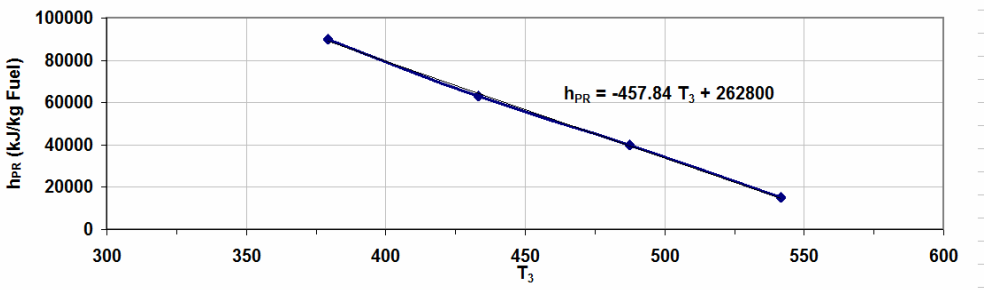

Figure 6.1: Maximum Heat of Reaction for Mach 3.50 Supersonic Combustion to be Maintained as a Function of Combustor Entrance Temperature (Same as Required Ignition Temperature) at *f*=0.02

With JP-7 fuel and no additives, it has been determined that a scramjet can start at a freestream Mach number of approximately 3.68. However, this leaves relatively no margin for error. The design of a scramjet with a starting Mach number of 4.00 has been shown instead to be a realistic and readily applicable case, and is at least a Mach number below the lower end of the average range of starting Mach number scramjet designs. Therefore, a scramjet with a starting Mach number of 4.00 has been designed in this paper. Performance results have been determined and demonstrate promise, as net thrust is shown to be produced and an impressive specific impulse has resulted.

As discussed previously, Fry states that a turbojet engine can provide for thrust from takeoff to a speed of Mach 3 or 4 [3]. Therefore, if the scramjet designed in this paper were applied to a hypersonic cruiser it could presumably allow for a reduction in total propulsion systems needed.

6.2 Recommendations

At the closing of this report, it is evident that there are important areas which call for future research and analysis. The first of these is that of the application of a fully designed expansion system employing the use of method of characteristics or computational fluid dynamics codes. This will enable more precise calculations of performance, as well as provide more realistic overall engine lengths to be obtained, as the nozzle does not have to be fully expanded to freestream conditions to gain a satisfactory amount of thrust.

Secondly, the maximum fuel-to-air ratio for JP-7 fuel of 0.03 should be applied to the design of a scramjet with a starting Mach number of 4.00 to determine whether the resulting increase in specific thrust outweighs the decrease in specific impulse. Additionally, the variation of the fuel-to-air ratio with freestream Mach number in the off-design cases can be explored if a higher specific thrust is needed, though at a cost in specific impulse.

In the pursuit of lowering the starting Mach number of the scramjet further than the Mach 4.00 engine designed here, the use of additives should be explored. (See References 2, 9, 16, 18, 19, and 31.)

As for the practical design of this scramjet, the use of cavity-based fuel injectors should be explored, as they have been demonstrated with JP-7 fuel [2]. (Also see Reference 27.) Additionally, items not addressed in this analysis that should be explored include: the method of fuel-air mixing [See References 1 and 26], combustion time required, and overall potential benefit of cooling scramjet with the JP-7 fuel.

For the next step in the design of this particular scramjet, higher fidelity analysis methods should be employed, to ensure that frictional effects, though not deemed significant in this analysis, are included. Additionally, the calculation of the resulting range and overall performance of the scramjet designed here by its application to an average hypersonic vehicle or missile would prove interesting and provide direction towards the application of this engine (References 3, 15, 25, and 28 are good resources towards this.)

APPENDIX A

ONE-DIMENSIONAL STREAM THRUST ANALYSIS SPREADSHEET

ONE DIMENSIONAL STREAM THRUST ANALYSIS		
<FUEL NAME INSERTED HERE>		
INPUT		
Mo		
Vo		m/s
To		K
T3/To		
f		
hpr		J/kg Fuel
fhpr		J/kg
Cpo		
Cpc		J/kgK
Tto		K
R		(m/s)^2/K
Vfx/V3		
Vf/V3		
Cf*Aw/A3		
Cpb		J/kgK
Cpe		J/kgK
nc		
nb		
ne		
hf		
To		K
p10/po		
go		m/s^2
gamma c		
gamma e		
gamma b		
po		Pa
OUTPUT		
Compression Component (0 to 3)		
Sao		
T3		K
V3		m/s
M3		
Sa3		
p3/po		
p3		Pa
p3		atm
A3/Ao		
Combustion Component (3 to 4)–Constant Pressure Combustion		
V4		m/s
M4		
T4		K
A4/A3		
Either Constant Pressure or Constant Area Combustion		
Sa4		
Expansion Component (4 to 10)		
p4/po		
T10		
V10		
M10		
Sa10		
A10/Ao		
ENGINE PERFORMANCE MEASURES		
F/mo		N-s/kgA
S		kg F/s-N
Isp		s
no		
nth		
np		
T3		
T4		
T10		
M3		
M4		
M10		

Figure A.1: Display of the Setup for the One-Dimensional Stream Thrust Equation Analysis Excel Spreadsheet

APPENDIX B

DESIGN SPACE PLOTS FOR OCTANE, METHANE, AND HYDROGEN FUELS AT LOWERED STARTING MACH NUMBERS

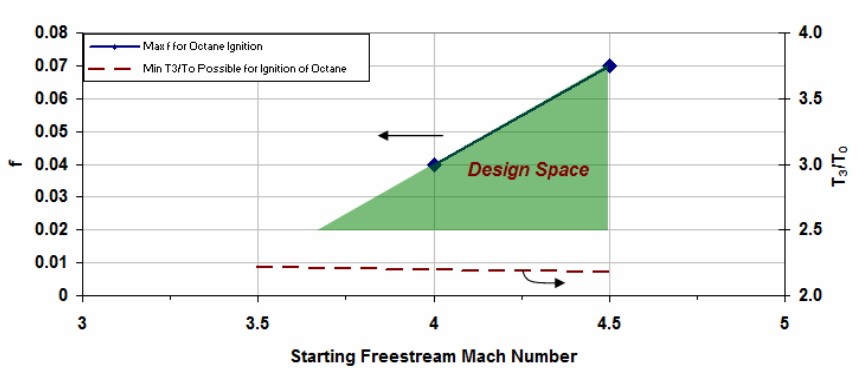

Figure B.1: Design Space Possible for Octane Ignition with Variation of Fuel-to-Air Ratio as a Function of Starting Mach Number

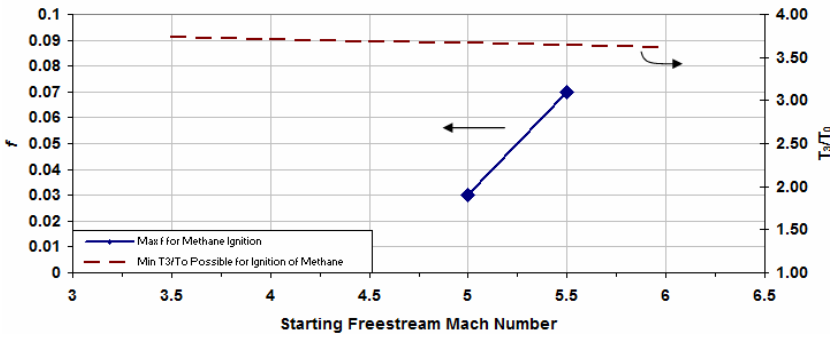

Figure B.2: Design Space Possible for Methane Ignition with Variation of Fuel-to-Air Ratio as a Function of Starting Mach Number; Methane Lacks Any Design Space for Lower Starting Mach Numbers

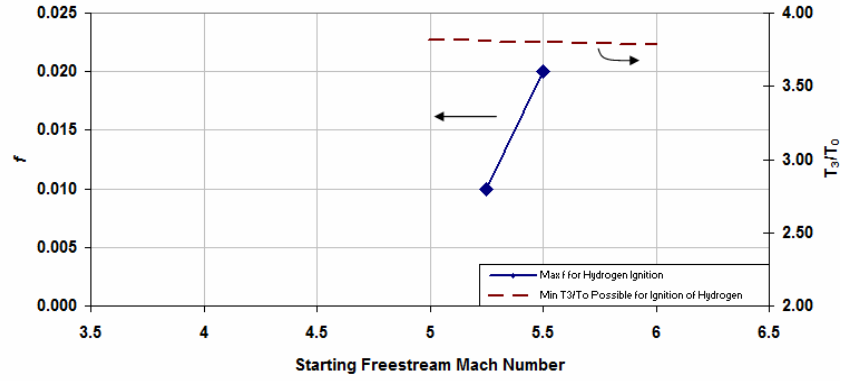

Figure B.3: Design Space Possible for Hydrogen Ignition with Variation of Fuel-to-Air Ratio as a Function of Starting Mach Number; Hydrogen Lacks Any Design Space for Lower Starting Mach Numbers

REFERENCES

[1] Heiser, William H., David T. Pratt, Daniel H. Daley, and Unmeel B. Mehta. Hypersonic Airbreathing Propulsion. Washington, D.C.: American Institute of Aeronautics and Astronautics, 1994.

[2] Curran, Edward T., "Scramjet Engines: The First Forty Years." Journal of Propulsion and Power, Volume 17, No. 6, November-December 2001.

[3] Fry, Ronald S. "A Century of Ramjet Propulsion Technology Evolution." Journal of Propulsion and Power, Volume 20, No. 1, January-February 2004: 27-58.

[4] Waltrup, Paul J., Michael E. White, Frederick Zarlingo, and Edward S. Gravlin. "History of Ramjet and Scramjet Propulsion Development for U.S. Navy Missiles." Johns Hopkins APL Technical Digest , Volume 18, 1997: 234-243.

[5] Thompson, Elvia, Keith Henry, and Leslie Williams. "Faster Than a Speeding Bullet: Guinness Recognizes NASA Scramjet." NASA. 20 June 2005. RELEASE : 05-156. <http://www.nasa.gov/home/hqnews/2005/jun/HQ_05_156_X43A_Guinness.html>.

[6] "HyShot Program Secures Place in Flight History." The University of Queensland in Australia. 16 Aug. 2002. <http://www.uq.edu.au/news/index.html?article=3469>.

[7] Waltrup, Paul J. "Upper Bounds on the Flight Speed of Hydrocarbon-Fueled Scramjet-Powered Vehicles." Journal of Propulsion and Power, Volume 17, No. 6, November-December 2001: 1199-1204.

[8] Townend, L.H. "Domain of the Scramjet." Journal of Propulsion and Power, Volume 17, No. 6, November-December 2001: 1205-1213.

[9] Powell, O.A., J.T. Edwards, R.B. Norris, K.E. Numbers, and J.A. Pearce. "Development of Hydrocarbon-Fueled Scramjet Engines: the Hypersonic Technology (HyTech) Program." Journal of Propulsion and Power, Volume 17, No. 6, November-December 2001: 1170-1176.

[10] McClinton, C.R., E.H. Andrews, and J.L. Hunt, "Engine Development for Space Access: Past, Present, and Future." International Symposium on Air Breathing Engines, January 2001. ISABE Paper 2001-1074.

[11] "SBIR AF073-058 (AirForce)." Department of Defense SBIR. 1 Sept. 2007 <http://www.dodsbir.net/sitis/archives_display_topic.asp?Bookmark=31383>.

[12] "World's First Flight-Weight, Hydrocarbon-Fueled Scramjet Completes Mach 4.5 Testing, Running At Mach 6.5." Pratt & Whitney. 20 June 2003. <http://www.pw.utc.com/vgn-ext-templating/v/index.jsp?vgnextoid=2e35288d1c83c010VgnVCM1000000881000aRCRD&prid=28f2e3776af3c010VgnVCM1000000881000a>.

[13] Builder, C.H. "On the Thermodynamic Spectrum of Airbreathing Propulsion." AIAA 1st Annual Meeting, Washington, D.C., June 1964. AIAA Paper 64-243.

[14] Edwards, Tim. " 'Kerosene' Fuels for Aerospace Propulsion – Composition and Properties." 38th AIAA/ASME/SAE/ASEE Joint Propulsion Conference & Exhibit, Indianapolis, Indiana, 7 July 2002. AIAA Paper 2002-3874.

[15] Lewis, Mark J. "Significance of Fuel Selection for Hypersonic Vehicle Range." Journal of Propulsion and Power, Volume 17, No. 6, November-December 2001: 1214-1221.

[16] Yu, G., J.G. Li, X.Y. Chang, L.H. Chen, and C.J. Sung. "Investigation of Kerosene Combustion Characteristics with Pilot Hydrogen in Model Supersonic Combustors." Journal of Propulsion and Power, Volume 17, No. 6, November-December 2001: 1263-1272.

[17] National Research Council, Committee on the National Aerospace Initiative, Air Force Science and Technology Board, Division on Engineering and Physical Sciences. Evaluation of the National Aerospace Initiative. Washington, DC: The National Academies Press, 2004.

[18] Wickham, D.T., J.R. Engel, B.D. Hitch, and M.E. Karpuk. "Initiators for Endothermic Fuels." Journal of Propulsion and Power, Volume 17, No. 6, November-December 2001: 1253-1257.

[19] SR-71 Flight Manual. 2 June 2008 <http://www.sr-71.org/blackbird/manual/>.

[20] Heiser, William H., David T. Pratt, Daniel H. Daley, and Unmeel B. Mehta. Brief Description of the HAP Software Package. “ReadMe” File for Hypersonic Airbreathing Propulsion Software Package. Washington, D.C.: American Institute of Aeronautics and Astronautics, 1994.

[21] Weber, R.J., and J.S. McKay. “Analysis of Ramjet Engines Using Supersonic Combustion." 1958. NACA Paper TN-4386.

[22] Shapiro, A.H. The Dynamics and Thermodynamics of Compressible Fluid Flow, Volume I. New York: Ronald Press, 1953.

[23] Aerodynamics Research Center. The University of Texas at Arlington. 10 July 2008 <http://arc.uta.edu/research/pde.htm>.

[24] Kerrebrock, Jack L. "Some Readily Quantifiable Aspects of Scramjet Engine Performance." Journal of Propulsion and Power, Volume 8, No. 5, September-October 1992.

[25] Bowcutt, Kevin G. "Multidisciplinary Optimization of Airbreathing Hypersonic Vehicles." Journal of Propulsion and Power, Volume 17, No. 6, November-December 2001: 1184-1190.

[26] Seiner, John M., S.M. Dash, and D.C. Kenzakowski. "Historical Survey on Enhanced Mixing in Scramjet Engines." Journal of Propulsion and Power, Volume 17, No. 6, November-December 2001: 1273-1286.

[27] Mathur, Tarun, Mark Gruber, Kevin Jackson, Jeff Donbar, Wayne Donaldson, Thomas Jackson, and Fred Billig. "Supersonic Combustion Experiments with a Cavity-Based Fuel Injector." Journal of Propulsion and Power, Volume 17, No. 6, November-December 2001: 1305-1312.

[28] Czysz, Paul A., and Claudio Bruno. Future Spacecraft Propulsion Systems: Enabling Technologies for Space Exploration. Chichester, UK: Praxis, 2006.

[29] Zucrow, Maurice J., and Joe D. Hoffman. Gas Dynamics. Vol. 1. New York: John Wiley & Sons, Inc., 1976.

[30] Anderson, Jr., John D. Modern Compressible Flow with Historical Perspective. 2nd Ed. New York: McGraw-Hill Company, 1990.

[31] Curran, E.T., and S.N.B. Murthy. Scramjet Propulsion. Vol. 189: Progress in Astronautics and Aeronautics. Reston, Virginia: American Institute of Aeronautics and Astronautics, Inc., 2000.

[32] Ciccarelli, G., and J. Card. "Detonation in Mixtures of JP-10 Vapor and Air." AIAA Journal, Volume 44, No. 2, February 2006.

[33] Handbook of Chemistry and Physics, 88th Edition, 2007 – 2008, CRC Press, LLC, URL: http://www.hbcpnetbase.com/; Section 2: Definitions of Scientific Terms; Section 16: Flammability of Chemical Substances.

[34] Handbook of Aviation Fuel Properties, CRC Report No. 635, 3rd edition, Coordinating Research Council, Inc (CRC), Alpharetta, GA, 2004.

[35] Kuchta, J. M., Investigation of Fire and Explosion Accidents in the Chemical, Mining, and Fuel-Related Industries – a Manual, Bulletin 680, U.S. Bureau of Mines, 1985, Appendix A.

[36] Canan, James W. "Breathing New Hope Into Hypersonics." Aerospace America, November 2007: 26-31.

[37] Wilson, J.R. "High Hopes for HiFire Scramjet." Aerospace America, November 2007: 33-37.

[38] Hill, Philip, and Carl Peterson. Mechanics and Thermodynamics of Propulsion. 2nd ed. Reading, Mass.: Addison-Wesley, 1992.

BIOGRAPHICAL INFORMATION

KRISTEN ROBERTS was born in Oklahoma in 1982. Kristen earned her diploma from Mustang High School in 2001, graduating as Valedictorian. Inheriting her father's love of learning and Sooner pride, Kristen attended the University of Oklahoma immediately after high school. There she earned her Bachelor of Science in Aerospace Engineering degree with Magna Cum Laude honors in 2005, beginning her lifelong dream of chasing the stars. During the Junior and Senior years of her undergraduate education, Kristen worked as an Engineering Trainee at the Federal Aviation Administration in Oklahoma City, OK, assisting a team of engineers in the maintenance of the federal flight inspection aircraft fleet.

Kristen then moved to Texas to pursue her Master of Science in Aerospace Engineering degree at the University of Texas at Arlington. During her education at UTA, Kristen was involved in various research projects which culminated in four AIAA conference publications at the AIAA Annual Aerospace Sciences Meeting and Exhibit in 2006 and 2007. These projects were with the Aerospace Vehicle Design Lab at UTA and focused on the conceptual design stage of hypersonic and supersonic vehicles as well as knowledge based systems.

This thesis details the results of Kristen's work towards extending the operability range of scramjets, which is a key area in the development of future

hypersonic transportation systems. Kristen plans to continue pursuing her goals of being a designer for the next generation of hypersonic aerospace vehicles.